RECOMBINANT LYSINE:N^6-HYDROXYLASE: STRUCTURE-FUNCTION RELATIONSHIP

by

Laura Marrone

A thesis
presented to the University of Waterloo
in fulfilment of the
thesis requirement for the degree of
Doctor of Philosophy
in
Chemistry

Waterloo, Ontario, Canada, 1996

The University of Waterloo requires the signatures of all the persons using or photocopying this thesis. Please sign below, and give address and date.

ABSTRACT

Recombinant lysine:N^6-hydroxylase catalyses the conversion of L-lysine to its N^6-hydroxy derivative upon supplementation with cofactors NADPH and FAD. The catalytic function of the protein is adversely affected at higher concentrations of Cl^- ions, with total loss of activity being observed at concentrations ≥600 mM of these ions. In contrast, under similar ionic strength conditions, both phosphate and sulfate ions have no such deleterious effects on the enzyme.

Of the five cysteine residues present in the protein, three are accessible to titration with 5,5'-dithiobis (2-nitrobenzoic acid), DTNB, in the native conformation of the protein. In contrast, under similar experimental conditions only two functions are alkylatable by iodoacetate and these have been identified as Cys51 and Cys158 residues present in the protein. Modification of thiol groups either by DTNB or iodoacetate results in a complete loss of the protein's catalytic function. *r*IucD can form either a covalent or noncovalent complex with 2,6-dichlorophenol indophenol (DPIP), the former process being dependent on the presence of unmodified thiol functions in the protein. Both the covalent and the noncovalent complexes of *r*IucD and DPIP are capable of mediating NADPH oxidation by a mechanism involving an exchange of reducing equivalents between the protein bound dye and that free in the environment. However, only the latter type of complex which is formed in the absence of thiol groups in *r*IucD is capable of functioning as a diaphorase in the presence of FAD.

The replacement of Cys51 and Cys158 of *r*IucD with alanine residues, by site directed mutagenesis of iucD, does not lead to a loss in the catalytic function(s) of the protein. Studies with *r*IucD muteins have shown that Cys51 plays an important role in the protein's covalent interaction with DPIP. Replacement of Cys51 and Cys158, either individually or in combination, with alanine is accompanied by an enhancement in the ability of *r*IucD to promote NADPH oxidation in the absence of its hydroxylatable substrate.

*r*IucD is stringently specific with respect to its hydroxylatable substrate. This feature has formed the basis for a novel proposal which envisages the participation of an activated lactam intermediate of the substrate in the catalytic mechanism of the protein.

ACKNOWLEDGMENTS

I would like to express my deepest appreciation to Dr. T. Viswanatha for always having confidence in me and my work, for his inimitable guidance throughout the course of my research, and for his dear friendship. I would also like to express my gratitude to Dr. L. J. Brubacher, Dr. R.A.B. Keates, and Dr. B. Greenberg for their valuable time and advice throughout this study.

I would like to thank Doug Socha, Mike Beecroft, Joe Gaspar, Janice Lim, Bob Papalombropoulos, Stefan Siemann, Scott Houliston, Scott Dick and Vicky Wang for their friendships, for all their valuable discussions shared and for their assistance during the course of this work; Dr. A. Thariath for advising us on the site directed mutagenesis method; Dr. G. Guillemette for his advice on designing mutagenic primers and for the use of his PCR equipment; Lorne Taylor for the ESMS analyses; Dr. N.L. Benoiton from the Department of Biochemistry at the University of Ottawa, for providing us with the compound, α-N-methyllysine; Dr. B. Martin, for his advice and for the amino acid analysis on the CDP-Y experiments; Dr. G. Murray for his advice and encouragement; and Lynda Steele, for all her help and availability during my stay at $(GWC)^2$.

I would like to express my sincere thanks to my friends here at the University of Waterloo, Souzan, Peter, John, and Henry for making my time in and outside of ESC 336A more enjoyable; the Viswanatha family, T.V. (already mentioned above) Sundra, Anjana and Patrick for all their encouragement, for their welcoming friendship, and of course, for keeping me well fed.

Financial assistance from the University of Waterloo, and for the research assistantships furnished by the NSERC grant to Dr. Viswanatha, is greatly acknowledged

I will always be grateful to my parents and sister, Paola, for being understanding and for their unconditional support.

Finally, I would like to express my sincere appreciation to Neil Rao for encouraging me to do my best and for his constant understanding and devotion.

TABLE OF CONTENTS

		Page
ABSTRACT		(iv)
ACKNOWLEDGMENTS		(v)
LIST OF FIGURES		(ix)
LIST OF SCHEMES		(xi)
LIST OF TABLES		(xii)
ABBREVIATIONS USED		(xiii)
1.0	INTRODUCTION	1
	1.1 Aerobactin	2
	1.2 Lysine:N^6-hydroxylase	6
	1.3 *Para*-hydroxybenzoate hydroxylase	9
	1.4 Objective	30
2.0	MATERIALS	31
3.0	METHODS	35
	3.1 Molecular biology techniques	35
	3.1.1 Preparation of competent cells	35
	3.1.2 Transformation protocol	35
	3.1.3 Isolation and purification of plasmids	36
	3.1.4 Digestive and plasmid DNA with restriction endonucleases	37
	3.1.5 Electrophoretic analysis of DNA fragments	38
	3.2 Growth of *Escherichia coli* and transformants	39
	3.2.1 *Escherichia coli* DH5α	39
	3.2.2 Growth of organisms	39
	3.3 Isolation and purification of *r*IucD and its muteins	39
	3.3.1 Preparation of cell free extract	39
	3.3.2 Purification of Lysine:N^6-hydroxylase	40
	3.4 Site directed mutagenesis of iucD	41
	3.4.1 Designing primers	43
	3.4.2 Conditions for Quick Change® mutagenesis	43
	3.5 Analytical Methods	45
	3.5.1 Determination of the homogeneity and molecular weight of the protein preparations	45

3.5.2 Determination of protein concentration 46
3.5.3 Determination of DNA concentration 46
3.5.4 Determination of lysine:N^6-hydroxylase activity 46
3.5.5 Determination of NADPH oxidation 47
3.5.6 Determination of H_2O_2 47
3.5.7 Reaction of *r*IucD with DPIP 48
3.5.8 Isolation of DPIP-*r*IucD complex 48
3.5.9 Measurement of diaphorase activity 48
3.5.10 Estimation of cysteine residues present in *r*IucD and its muteins 49
3.6 Location of cysteine residues alkylatable in the native conformation of *r*IucD 51
3.6.1 Fragmentation of the S-[^{14}C]carboxymethylated *r*IucD 51
3.6.2 Isolation of the radiolabelled peptides 52
3.7 Treatment of *r*IucD with proteases 52
3.7.1 Proteolysis using TPCK-trypsin 52
3.7.2 Treatment with TLCK-chymotrypsin 53
3.7.3 Reaction with carboxypeptidase Y 53
3.8 Miscellaneous procedures 54
3.8.1 Preparation of TLCK-chymotrypsin 54
3.8.2 Influence of FAD on TPCK-trypsin 54
3.8.3 Influence of L-norleucine on CPD-Y mediated hydrolysis of furylacryloyl-L-Phe-LAla 55
3.8.4 Stability of IucD at low temperatures 55
3.8.5 Effects of various ions on lysine:N^6-hydroxylase activity 55
4.0 RESULTS 57
4.1 Characteristics of *r*IucD preparations 57
4.1.1 Primary structure 57
4.1.2 Physico-chemical properties 58
4.1.3 Influence of FAD on the rate of *r*IucD mediated NADPH oxidation and lysine:N^6-hydroxylase 61
4.1.4 Influence of cofactor analogs 63
4.1.5 Proteolysis of *r*IucD 63
4.1.6 Attempts to produce truncated *r*IucD preparations 70
4.1.7 Influence of anions 72
4.2 Specificity of *r*IucD 74
4.3 Cysteine residues in *r*IucD 82

4.3.1 Location of exposed thiol functions of *r*IucD 85
4.4 Reaction of *r*IucD with artificial electron acceptor 90
4.4.1 Reaction with DPIP 90
4.4.2 Catalytic properties of DPIP-*r*IucD conjugate 91
4.4.3 Influence of FAD on the interaction between DPIP and *r*IucD 95
4.5 Site directed mutagenesis of *r*IucD 97
4.5.1 Characterisation of iucD and its variants 97
4.5.2 Characterisation of *r*IucD muteins 98
4.5.3 Reactivity of cysteine residues in *r*IucD muteins 103
4.5.4 Reaction of *r*IucD muteins with DPIP 103
5.0 DISCUSSION 109
6.0 APPENDIX 130
7.0 REFERENCES 148

LIST OF FIGURES

1.	Chemical structures of siderophores	3
2.	Structure of aerobactin and ferric aerobactin	4
3.	Genes in the aerobacin operon, the enzymes and the reaction they catalyse for the biosynthesis of aerobactin	5
4.	Details of the pUC19-iucD gene fusion	7
5.	A ribbon diagram of the overall structure of the polypeptide chain of PHBH	12
6.	An illustration of the influence of tyrosine residues, in the active site of PHBH, on the activation of the substrate, *p*-hydroxybenzoate	17
7.	The active site of wild type PHBH (FAD)	18
8.	The structural differences between the wild type PHBH and its muteins: A. Tyr201Phe and B. Tyr385Phe	20
9.	The structural differences between the wild type PHBH and PHBH mutein, Asn300Asp	23
10.	The comparison of the structural differences between the wild type PHBH and its mutein Tyr222Phe	26
11.	Active site of PHBH interacting with 2,4-dihydroxybenzoate Molecular modeling experiments showing the active site of *p*-hydroxybenzoate hydroxylase	27
12.	Molecular modeling experiments showing the active site of *p*-hydroxybenzoate hydroxylase	29
13.	An outline of Statagene's Quick Change® procedure	42
14.	SDS-PAGE profile of *r*IucD preparations of the fractions recovered from the affinity matrix Orange A	59
15.	ESMS analysis of *r*IucD439	60
16	Production of N^6-hydroxylysine and H_2O_2 by *r*IucD	62
17	Effects of analogs of FAD and NADPH on the lysine:N-hydroxylase activity of *r*IucD	64
18.	A. SDS PAGE profile of *r*IucD following treatment with TPCK-trypsin B. Vertical bar graph representation of lysine:N^6-hydroxylase activity of *r*IucD following treatment with TPCK-trypsin:	66 66

19.	SDS profile illustrating the effects of FAD on the proteolytic treatment of *r*IucD with TLCK-chymotrypsin	67
20.	The effect of carboxypeptidase Y on the lysine:N^6-hydroxylase activity of *r*IucD	69
21.	Restriction enzyme analysis of Arg400stop *r*iucD mutation	71
22.	Effects of ionic strength on the activity of lysine:N^6-hydroxylase	73
23.	Effects of freezing on the lysine:N^6-hydroxylase activity of *r*IucD	75
24.	Effects of freezing on the lysine:N^6-hydroxylase activity of *wt*IucD	76
25.	Structural features inherent in L-lysine	77
26.	Chemical structures of L-lysine and various substrate analogs of *r*IucD:	79
27.	Reaction of *r*IucD with DTNB	84
28.	Chromatographic profile of the peptides produced upon CNBr treatment of the insoluble fraction of tryptic digest of S-carboxymethyl *r*IucD	88
29.	Chromatographic profile of the soluble component of the tryptic digest of [^{14}C]-S-carboxymethyl *r*IucD	89
30.	Spectral and catalytic properties of DPIP-*r*IucD complex	92
31.	Reaction of DPIP-*r*IucD complex catalysing NADPH dependent reduction of exogenous DPIP	94
32.	Influence of FAD on the NADPH oxidase activity of *r*IucD in the presence of DPIP	96
33.	Restriction enzyme analysis of Cys51Ala *r*iucD mutation	99
34.	Restriction enzyme analysis of Cys158Ala *r*iucD mutation	100
35.	Restriction enzyme analysis of Cys51Ala/Cys158Ala *r*iucD mutation	101
36.	SDS-PAGE profile of *r*IucD and *r*IucD mutein preparations recovered from the affinity matrex Orange A	102
37.	NADPH oxidtion by *r*IucD and its muteins in the presence and in the absence of lysine	104
38.	Reaction of *r*IucD or its muteins with DTNB	105
39.	Reaction of *r*IucD and its muteins with DPIP	108
40	Similarities in the structural features of DPIP and the isoalloxazine segment of FAD	124

LIST OF SCHEMES

1.	Mechanism of hydroxylation by FAD containing monooxygenases	10
2.	The "BI Uni Uni Bi" ordered mechanism as proposed for *p*-hydroxybenzoate hydroxylase	13
3.	A general mechanism for *r*IucD mediated N-hydroxylation of lysine	110
4.	Proposed mechanism for *r*IucD mediated lysine:N^6-hydroxylase	117
5.	Mechanism for NADPH-dependent reduction of exogenous DPIP by covalent *r*IucD-DPIP complex	121
6.	Mechanism for NADPH-dependent reduction of exogenous DPIP by noncovalent complex of *r*IucD and DPIP: (A) Reducing equivalent exchange (B) Diaphorase activity	122

LIST OF TABLES

1.	Steady state kinetic parameters for *p*-hydroxybenzoate hydroxylase with *p*-hydroxybenzoate, NADPH and oxygen as the substrates	15
2.	Some kinetic properties of wild type and mutant *p*-hydroxybenzoate hydroxylase	21
3.	Details of the site directed mutagenesis of iucD	44
4.	Carboxypeptidase Y-catalysed proteolysis of *r*IucD	68
5.	Influence of various effectors on the enzymatic activity of *r*IucD	80
6.	Influence of norleucine analogs on the catalytic function of *r*IucD	83
7.	Reactivity of thiol functions of IucD	86

ABBREVIATIONS USED

ADP	adenosine diphosphate
2'-P-ADP	adenosine 2',5'-diphosphate
ADPR	5'-adenosine diphosphate ribose
AMP	adenosine monophosphate
Arg400stop *r*IucD	recombinant lysine:N^6-hydroxylase mutein with a truncation of 27 amino acid residues from its C-terminus
BSA	bovine serum albumin
BTEE	benzoyl tyrosine ethylester
C51A *r*IucD	Cys51Ala recombinant lysine:N^6-hydroxylase mutein
C158A *r*IucD	Cys158Ala recombinant lysine:N^6-hydroxylase mutein
C51A/C158A *r*IucD	Cys51Ala/Cys158Ala recombinant lysine:N^6-hydroxylase mutein
CCCP	carbonylcyanide-*m*-chlorophenylhydrazone
CPD-Y	carboxypeptidase Y
DNA	deoxyribonucleic acid
DNase	deoxyribonuclease I
dNTP	deoxynucleotide triphosphate
DPIP	2,6-dichlorophenol indophenol
DTNB	5,5'-dithiobis(2-nitrobenzoic acid)
DTT	DL-dithiothreitol
EDTA	ethylenediamine tetraacetic acid
ESMS	electrospray mass spectrometry
ϵ_M	molar extinction coefficient
FAD	flavin adenine dinucleotide (oxidized form)
$FADH_2$	flavin adenine dinucleotide (reduced form)
FCCP	carbonylcyanide-*p*-trifluoromethoxyphenylhydrazone
G-6-P	glucose-6-phosphate
HEPES	N-(2-hydroxyethyl) piperazine-N'-(2-ethanesulphonic acid)
HPLC	high performance liquid chromatography
iucA and iucC	genes encoding for proteins catalysing the terminal steps in aerobactin biosynthesis
iucB	gene encoding for acetyl transferase
iucD	gene encoding for lysine:N^6-hydroxylase
IucD	lysine:N^6-hydroxylase, iucD gene product
K_d	dissociation constant
Ksp	solubility constant
lacZ	gene encoding for β-galactosidase
mutein	protein containing amino acid replacement
NAD^+	nicotinamide adenine dinucleotide (oxidized form)
NADH	nicotinamide adenine dinucleotide (reduced form)
$NADP^+$	nicotinamide adenine dinucleotide phosphate (oxidized form)
NADPH	nicotinamide adenine dinucleotide phosphate (reduced form)

NSERC	Natural Sciences and Engineering Research Council
NTCB	2-nitro-5-thiocyanobenzoic acid
pABN5	plasmid bearing the genes in the aerobactin operon
pAT5	plasmid bearing *r*iucD
PHBH	*para*-hydroxybenzoate hydroxylase
PMSF	phenylmethane sulphonyl fluoride
*p*OHB	*para*-hydroxybenzoate
R.E.	restriction endonuclease
RNAase	ribonuclease A
*r*iucD	recombinant gene encoding for lysine:N^6-hydroxylase
*r*IucD	recombinant cytoplasmic lysine:N^6-hydroxylase
*r*IucD439	a recombinant form of lysine:N^6-hydroxylase
SBTI	soyabean trypsin inhibitor
SDS-PAGE	sodium dodecyl sulfate - polyacrylamide gel electrophoresis
TAE	Tris/acetic acid/EDTA buffer
TCA	trichloroacetic acid
TFA	trifluoroacetic acid
TLCK	N-tosyl-L- lysyl chloromethyl ketone
TPCK	N-tosyl-L-phenylalanine chloromethyl ketone
Tris (Trizma base)	Tris(hydroxymethyl) aminomethane
*wt*IucD	wild type (membrane associated) lysine:N^6-hydroxylase

diaphorase: The term diaphorase refers to the enzyme mediated electron transfer between NAD(P)H and an artificial electron acceptor such as DPIP or $K_3Fe(CN)_6$ and the process generally involves the intermediacy of a flavin cofactor. Although such processes occurring in the absence of flavin are also currently referred to as diaphorases (D.M. Glick, Glossary of Biochemistry and Molecular Biology, 1990, Raven Press, New York), the former definition is used in the current investigations.

1.0

INTRODUCTION

Iron is an indispensable element for all forms of life, the exception being certain strains of lactobacilli which have evolved to survive in an environment devoid of this metal (1). The absolute necessity of this metal in the case of all other organisms is due to its participation in a number of fundamental processes such as the reduction of molecular oxygen (respiration), of carbon dioxide (photosynthesis), of dinitrogen (nitrogen fixation) as well as DNA replication, transport and storage of oxygen, detoxification of H_2O_2 and other vital biological phenomena.

Although iron is the fourth most abundant element in this planet, its bioavailability is restricted in view of its occurrence predominantly in the ferric oxidation state, which is virtually insoluble ($K_{sp} = 10^{-38}$ M^4) under physiological conditions. Consequently, the equilibrium concentrations of Fe^{3-} in solution at pH 7.4 is approximately 10^{-18} M, a level 10^{11} times too low to support growth of even the simplest microorganisms (2-4). Hence, it is no wonder that living systems have developed novel methods not only to sequester iron from the environment but also to prevent its loss following its acquisition. The current presentation will focus attention on such mechanisms encountered in the microbial systems.

Many microorganisms have been found to respond to the conditions of iron deprivation by the production of a novel class of compounds, referred to as siderophores. These are generally low molecular weight compounds (molecular weight less than 1000 Da)

and have phenomenal affinity for ferric iron. Their sole function is to sequester iron from the environment and deliver it to the parent organism. Since the initial discovery of ferrichrome by J. B. Neilands in 1952 (5), several hundreds of these siderophores have been isolated and their structures identified. As a consequence of the diversity in their structural features these compounds have been classified into three distinct groups (3,6). These are the hydroxamates, the catecholates and the mixed function siderophores. Structures of some of these are shown in Figure 1.

1.1 Aerobactin

Of particular interest is the siderophore, aerobactin, originally isolated from the culture fluids of *Enterobacter aerogenes* (7). It comprises two molecules of N^6-acetyl N^6-hydroxylysine which are condensed to the distal carboxyl groups of citric acid. In addition to its two hydroxamate functions, an α-hydroxy carboxylate group participates in the formation of the hexadentate, octahedral complex (Figure 2). Elegant investigations by Neilands and associates (8,9) and Braun and his coworkers (10,11) have led to the mapping of the genes in the aerobactin operon. Concurrent biochemical investigations resulted in the identification of the sequence of events in the biosynthesis of aerobactin (12,13). The genetic map of the aerobactin operon and the reactions catalysed by the enzymes encoded by the various genes in the operon are shown in Figure 3. The initial step in the biosynthesis of aerobactin, the N^6-hydroxylation of L-lysine catalysed by the iucD gene product (IucD) is followed by the conversion of N-hydroxylysine to its hydroxamate derivative, the process being mediated by the iucB gene product. The terminal steps in the biosynthesis involve the peptide bond formation reactions which are catalysed by enzymes encoded by iucA and

Figure 1. **Chemical structures of siderophores**:

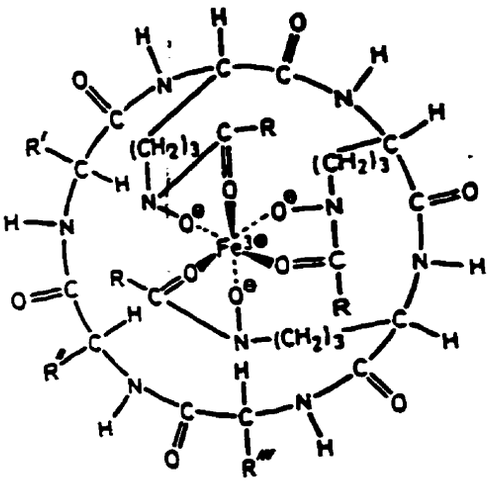

Ferrichrome

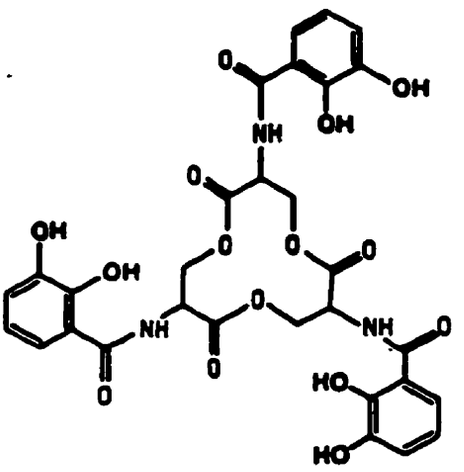

Enterobactin

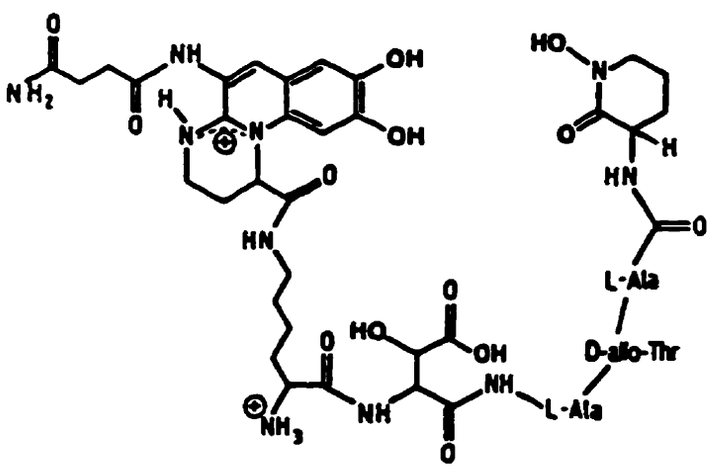

Pseudobactin

Figure 2. **Structure of aerobactin and ferric aerobactin:**

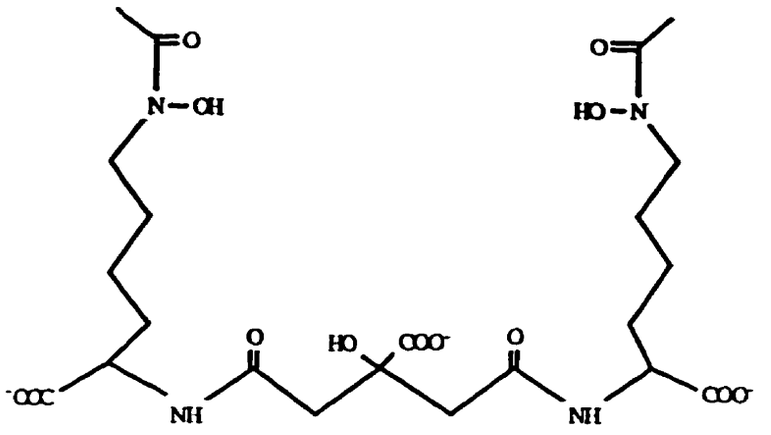

Aerobactin

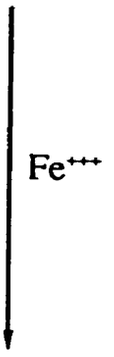

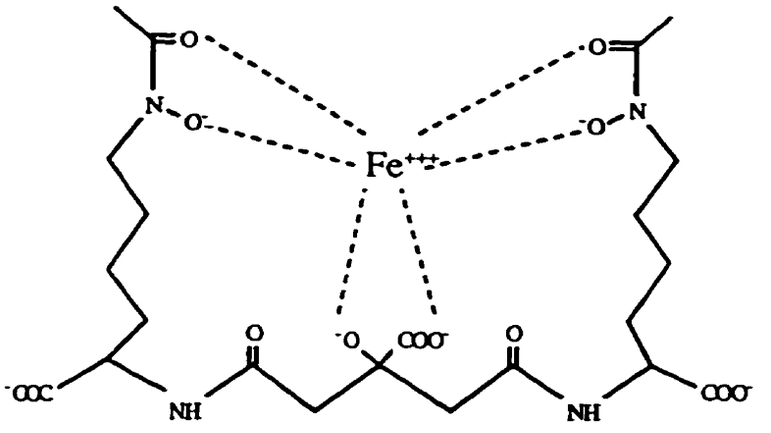

Ferric-aerobactin

Figure 3. **Genes in the aerobactin operon and the enzyme catalysed reactions in the biosynthesis of aerobactin:**

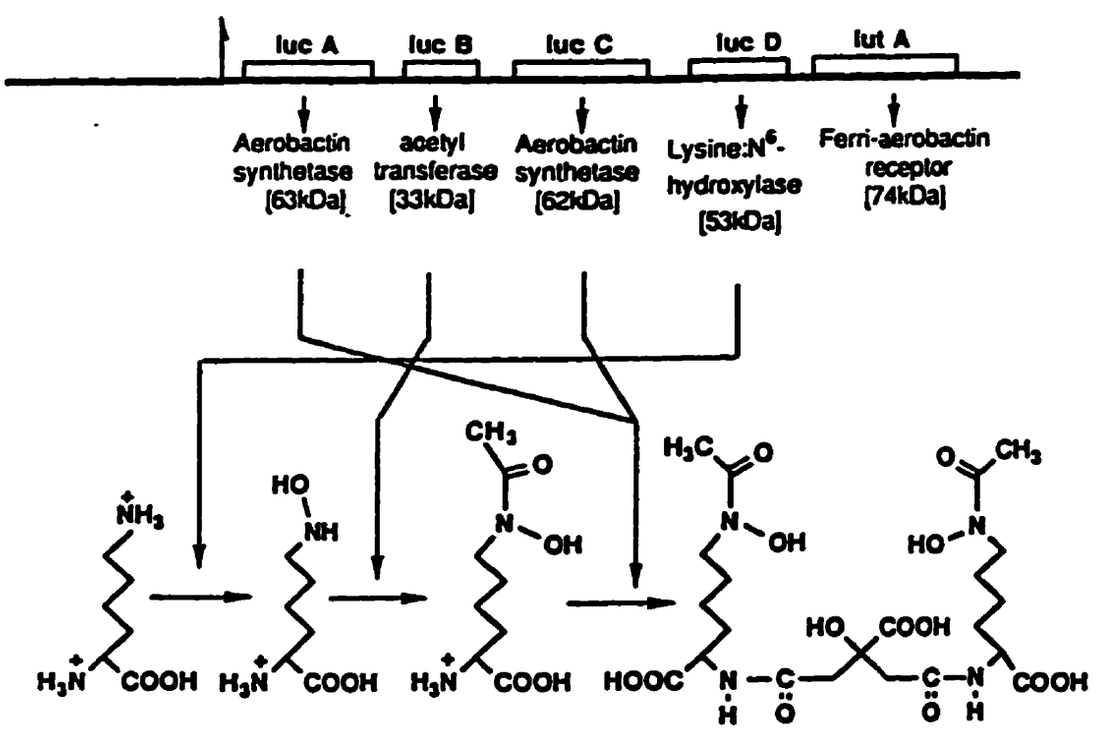
iuc A
iuc B
iuc C
iuc D
iut A
Aerobactin synthetase [63kDa]
acetyl transferase [33kDa]
Aerobactin synthetase [62kDa]
Lysine:N6-hydroxylase [53kDa]
Ferri-aerobactin receptor [74kDa]

iucC. This latter aspect of the biosynthesis has been partially characterized (13).

1.2 Lysine:N^6-hydroxylase (IucD)

Of special interest to the current investigation is the enzyme (IucD) that catalyzes the novel process of N-hydroxylation of lysine. This protein is normally membrane bound and consequently much of the early work was achieved with vesicular preparations of the protein. The salient features of membrane-bound IucD are: (i) L-lysine is the preferred substrate while L-glutamate and L-glutamine serve as positive effectors by their ability to stabilize as well as to activate the enzyme (14,15); (ii) pyruvate which stimulates the IucD mediated lysine:N-hydroxylation serves both as the source of reducing equivalents as well as of the acetyl moiety required for the formation of the hydroxamate (14,16,17); and (iii) the enzyme is inhibited by thiol modifying agents, protonophores (CCCP and FCCP), cinnamylidine and gramicidin (18). The cofactor requirements of wild type IucD (*wt*IucD) could not be established.

The inability to obtain a membrane-free, catalytically functional preparation of IucD prompted exploration of approaches based on recombinant DNA technology to achieve cytoplasmic form(s) of the protein. To this end, an in frame gene fusion of iucD with a segment of lacZ coding for the amino terminal portion of the cytoplasmic protein, β-galactosidase was performed (19). The genetic construct and the resulting fusion product, *r*IucD439 is shown in Figure 4. Thus, *r*IucD439 comprises a leader sequence of 13 amino acid residues derived from β-galactosidase and the remaining residues are those of *wt*IucD. The in frame gene fusion approach resulted in the production of three cytoplasmic forms of IucD (*r*IucD) and two of these have been isolated in a homogenous state (19,20). These

Figure 4. **Details of the pUC19-iucD gene fusion:** Fusion endpoints on pAT5 was deduced from the reported sequence of pUC19 and iucD, respectively. Shadowed amino acids indicate the portion of the recombinant polypeptide segment contributed by the β-galactosidase α-peptide encoded by pUC19. Double underlined amino acids denote the IucD sequence. (19)

pAT5 (*iuc*D439)

***iuc*D**

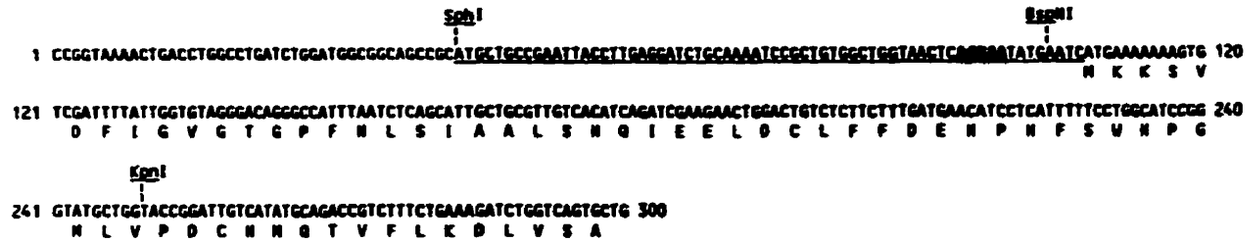

recombinant cytoplasmic preparations are apoproteins which require maintenance in buffer(s) of ionic strength > 0.25 for the preservation of the protein in its native conformation (19). Under these conditions, the protein exists as a tetramer and exhibits lysine:N^6-hydroxylase activity upon supplementation with cofactors FAD and NADPH (19). Pyruvate has no stimulatory effect on the reaction catalysed by these *r*IucD preparations. Like *wt*IucD, the recombinant forms are inhibited by thiol modifying agents, protonophores (FCCP and CCCP) and cinnamylidine, and are specific with L-lysine serving as the hydroxylatable substrate.

The finding that *r*IucD requires a flavin cofactor (FAD) for its function is in keeping with the need for the activation of molecular oxygen, an obligatory step in the catalytic mechanism of the protein. To elaborate further on this point, molecular oxygen exists as a ground state triplet which can not react with singlet molecules to yield singlet products. This is because the direct reaction of a triplet molecule with a singlet to give singlet products, is a spin-forbidden process. Hence, oxygen is usually activated by anyone of the two mechanisms: (i) Complexing with a transition metal to allow some overlap of metal ion orbitals with those of O_2 such that the unpaired electrons are no longer identifiable with either metal ion or oxygen. Under these conditions, oxygen can react with singlet molecules to form singlet products provided the number of unpaired electrons in the complex remain constant; and (ii) The reaction between ground state oxygen and substrate (or cosubstrate) occurs via a free radical mechanism yielding free radical intermediates which can recombine to give singlet products. This reaction is endothermic for most organic compounds but if the radical is part of the conjugated system, the structure may be stabilized by resonance

delocalization and the reaction will occur. This latter mechanism is implicated in flavin dependent oxygenation reactions.

The IucD mediated lysine:N-hydroxylation does not involve the participation of a metal since the process is not inhibited by such reagents as CO, metyrapone and EDTA (17). Hence, the requirement for the participation of a flavin cofactor (FAD) is to be expected. Although several proposals have been advanced concerning the nature of the oxygenating agent (21-24), studies with model flavin analogs have identified 4a-peroxyflavin as the probable oxygenating species (25,26). Furthermore, the 4a-peroxyflavin has been shown to be the oxygenating species in a number of flavin dependent monooxygenases. These include such diverse systems as *p*-hydroxybenzoate hydroxylase (PHBH) (27,28), phenol hydroxylase (29-32), melilotate hydroxylase (33), bacterial luciferase (34), 2-methyl-3-hydroxy pyridine-5-carboxylate oxygenase (35), *p*-hydroxyphenylacetate hydroxylase (36,37) and cyclohexanone monooxygenase (38). Depending on the nature of the substrate, 4a-peroxy flavin can function either as an electrophile or as a nucleophile in facilitating the transfer of distal oxygen to the substrate. These mechanisms are illustrated in Scheme 1.

Approaches based on X-ray crystallographic analysis and site directed mutagenesis have been successfully exploited to gain an understanding of the various events in the catalytic mechanism of PHBH which, at the present time, serves as a prototype for flavin dependent monooxygenases. An overview of the currently available information on this enzyme is provided below.

1.3 *Para*-hydroxybenzoate hydroxylase

This enzyme has been crystallised as a homodimer of subunits 44,000 Da in size (39-

Scheme 1. **Mechanism of hydroxylation by FAD containing monooxygenases:**
A: FAD-4a-OOH as an electrophile in the hydroxylation of *p*-hydroxybenzoate mediated by *p*-hydroxybenzoate hydroxylase.
B: FAD-4a-OOH as a nucleophile in the oxygenation of ketones by ketone mono-oxygenases.

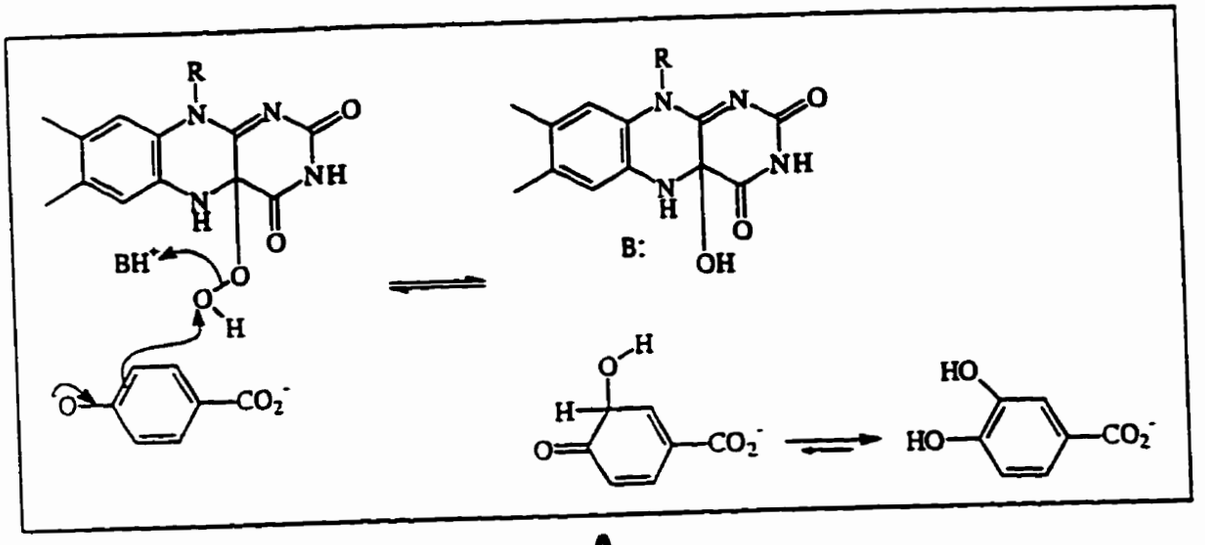

A

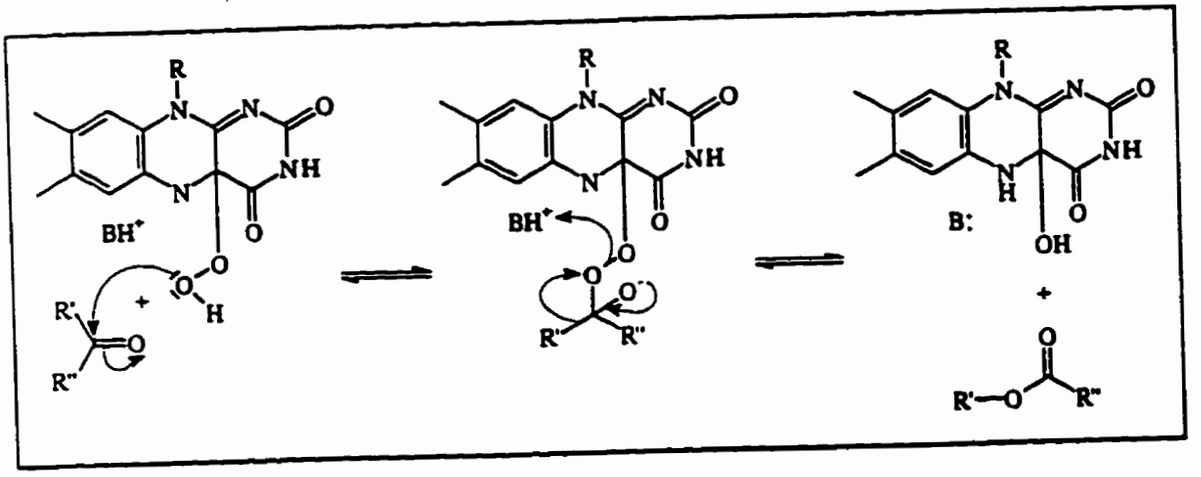

B

42). X-ray crystallographic studies have revealed considerable information regarding the interactions that prevail within the holoenzyme. The three dimensional structure is characterized by the presence of three distinct domains which encompass the active site of the protein. These are: (i) the FAD binding domain; (ii) the substrate binding domain; and (iii) the interface domain (41, 43). Figure 5 illustrates the overall structure of PHBH.

The FAD binding domain comprises the first 175 residues of the primary structure of PHBH. This segment accommodates the conserved amino acid residues that contribute to the βαβ fold motif, a feature typically observed in nucleoside diphosphate binding proteins (44). The βαβ fold is believed to interact with the ADP moiety of the flavin cofactor (FAD). Although NADPH is an obligatory cofactor, a distinct domain for its interaction has yet to be identified. Attempts to crystallise the enzyme in the presence of excess NADPH (400 mM) have been futile since the cofactor was found to displace FAD from its binding region (42).

Located between residues 176 and 290, the substrate binding domain consists of a wall of β strands lining one side of the catalytic site (43). In addition, the interface domain comprising residue 291 to 394, which is in intimate contact with the neighbouring subunit, also contributes to the make up of the active centre of the enzyme (43). Despite the absence of intersubunit disulfide bond, the strength of subunit interaction is such that the dimeric structure prevails even in a medium containing 8 M urea or 6 M guanidine hydrochloride (45).

As outlined below in Scheme 2A, PHBH uses three substrates during the course of its catalytic cycle, *p*-hydroxybenzoate (*p*-OHB), NADPH, and O_2. The order of the

Figure 5. **A ribbon diagram representing the overall structure of the polypeptide chain of PHBH.** (41,43)

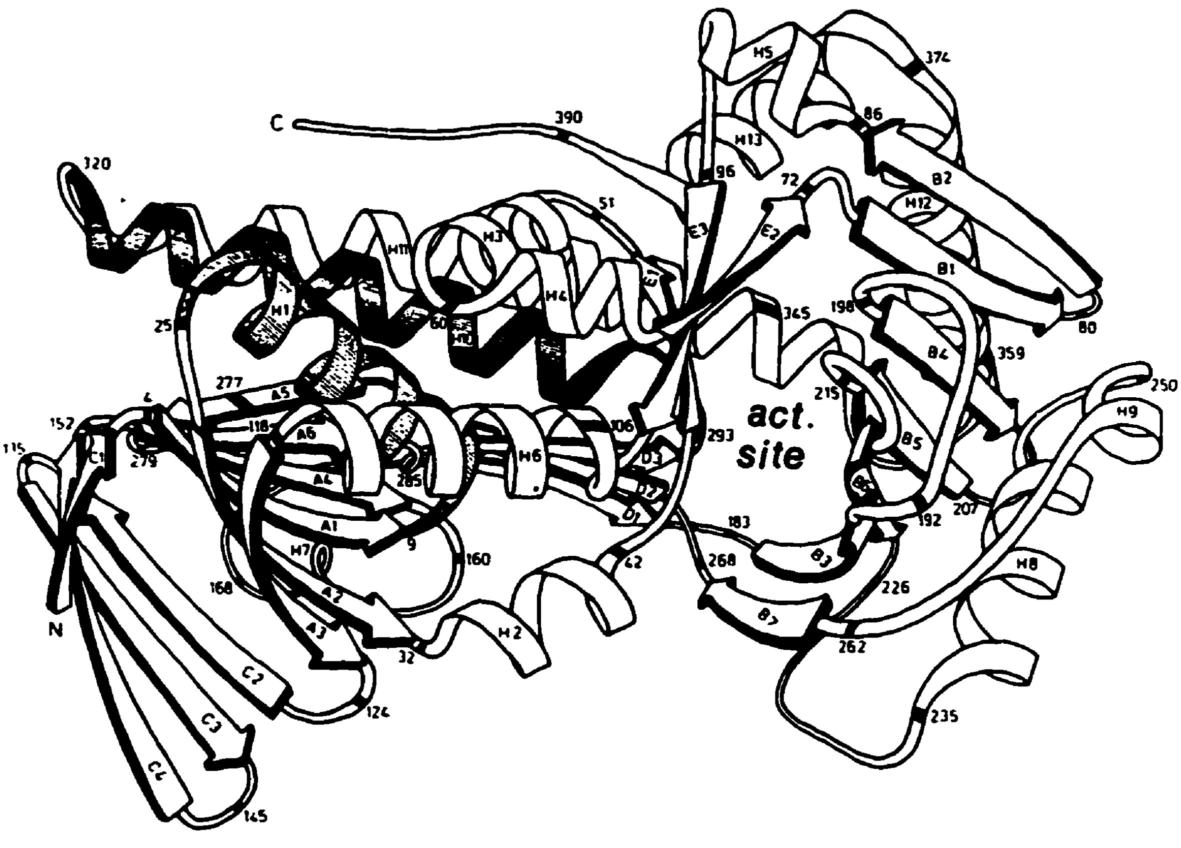
C
390
320
N
act.
site
H1
H2
H3
H4
H5
H6
H7
H8
H9
H10
H11
H12
H13
A1
A2
A3
A4
A5
A6
B1
B2
B3
B4
B5
B6
B7
C1
C2
C3
C4
D1
D2
D3
E1
E2
E3
4
9
25
32
42
51
60
72
80
86
96
106
115
118
124
145
152
160
168
183
192
198
207
215
226
235
250
262
268
277
279
285
293
345
359
374

Scheme 2. **The "Bi Uni Uni Bi" ordered mechanism as proposed for *p*-hydroxybenzoate hydroxylase**:
A: Order of substrate binding and product release. The ternary complex between the enzyme, *p*-hydroxybenzoate, and NADPH may be formed by the random addition of substrates or by a compulsory sequence of substrate addition (46).
B: Sequence of hydroxylation catalysed by PHBH. Reaction with rate constant, k_5, represents the wasteful production of H_2O_2 in the absence of substrate or in the presence of a non-hydroxylatable substrate.

A.

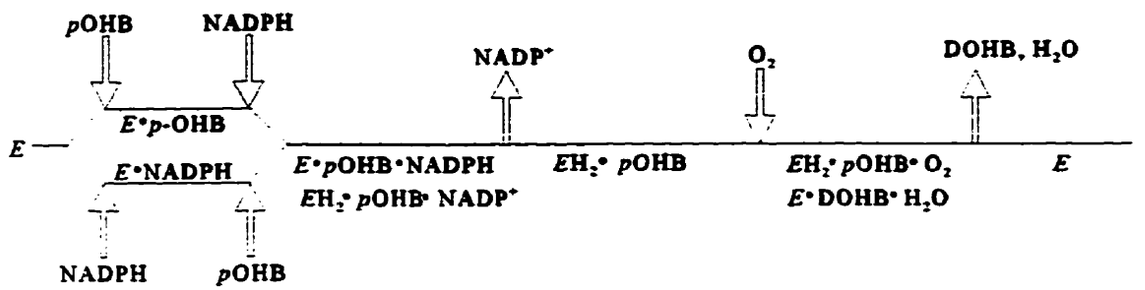
pOHB
NADPH
E
E•p-OHB
E•NADPH
NADPH
pOHB
NADP+
O2
DOHB, H2O
E•pOHB•NADPH
EH2• pOHB• NADP+
EH2• pOHB
EH2• pOHB• O2
E• DOHB• H2O
E

B.

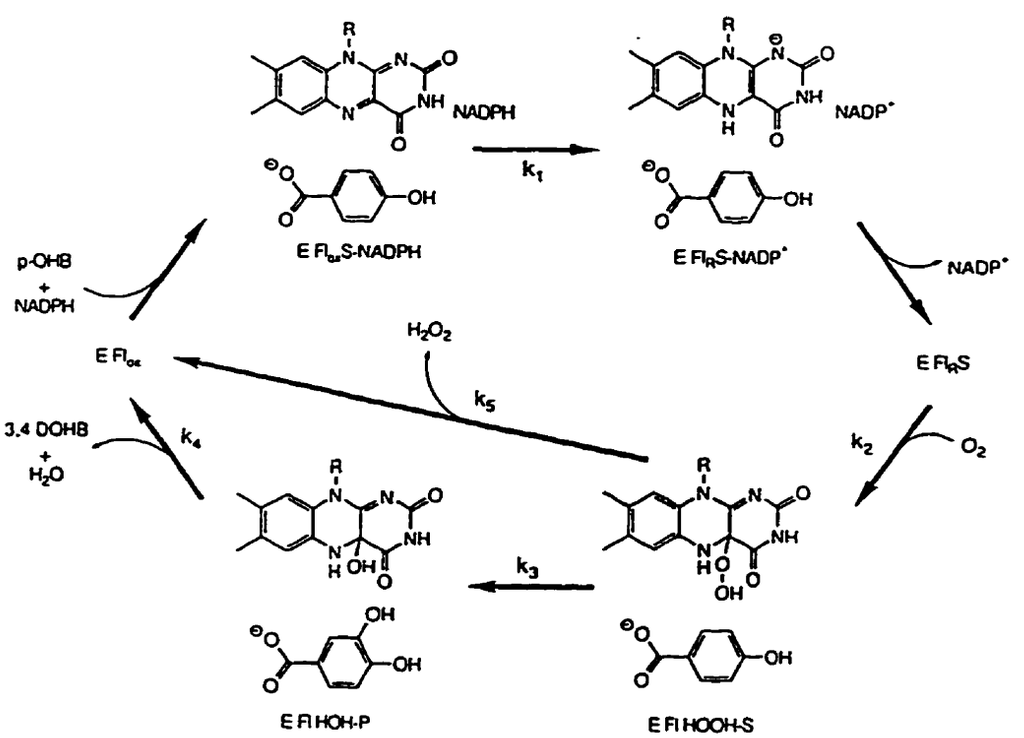
NADPH
NADP+
k1
E FlOxS-NADPH
E FlRS-NADP+
p-OHB
+
NADPH
E FlOx
NADP+
E FlRS
H2O2
k5
3.4 DOHB
+
H2O
k4
k2
O2
k3
E FlHOH-P
E FlHOOH-S

reaction proceeds with the first ternary complex formed by the random binding of *p*-OHB and NADPH to the enzyme (K_d for NADPH and *p*-OHB are reported in Table 1). Reduction of the enzyme-FAD by NADPH is followed by the release of the first product, $NADP^+$. The reduced enzyme-$FADH_2$-*p*-OHB complex reacts rapidly with the third substrate O_2, to form the second ternary complex. The enzyme bound *p*-OHB reacts with the activated oxygen to give 3,4-dihydroxybenzoate which is released at the same time that the enzyme is regenerated to its oxidized form (PHBH-FAD). Thus a Bi Uni Uni Bi PING PONG type mechanism appears to be operative in the PHBH catalytic reaction (46).

The catalysis of PHBH can be visualized to occur in two stages. The first is the reductive half reaction where *p*-OHB and NADPH bind and reduce the enzyme bound FAD. The second stage of the reaction is the oxidative half reaction where *p*-OHB bound enzyme-$FADH_2$ complex reacts with O_2 to form 4a-peroxyflavin required for the hydroxylation of the substrate followed by the release of the dihydroxy product (46). A more detailed reaction scheme is presented in Scheme 2B. As seen in many other external flavin monooxygenases (37,47), there is an important biological control feature seen in the reductive half reaction. The reduction of enzyme-FAD by NADPH oxidase activity, is minimal in the absence of substrate, *p*-OHB (k_1=0.02 min^{-1}). However, this activity is greatly stimulated (140,000 times) upon substrate binding (46). This effector role played by *p*-OHB appears to be explained by interactions between itself and the enzyme-FAD-NADPH complex. Non-hydroxylatable substrates for example, 5-hydroxypicolinate or the product, 3,4-dihydroxybenzoate, can also play this type of effector function (48). In these cases, the non-hydroxylatable substrate enhances NADPH oxidase activity causing reduction of the

Table 1. **Steady state kinetic parameters for *p*-hydroxybenzoate hydroxylase with *p*-hydroxybenzoate, NADPH and oxygen as the substrates (46):**

Kinetic parameters	Substrate		
	p-OHB	NADPH	O_2
Michaelis constant (M)	5.5×10^{-6}	2.1×10^{-5}	3.1×10^{-5}
Dissociation constant (M)	4.16×10^{-5}	1.2×10^{-4}	n.a.

enzyme-FAD. The reduced enzyme-$FADH_2$ complex rapidly reacts with oxygen, however instead of substrate hydroxylation, the activated oxygen species is eliminated as H_2O_2.

In order for the hydroxylation to proceed, the phenolic function of the *p*-OHB has to be deprotonated. In solution, *p*-hydroxybenzoate has a pKa value of 9.3, however, in the active site, the pKa of the function is lowered to 7.4 (49,50). Hence, the phenolic function of the substrate is deprotonated at the pH optimum of the catalysed reaction, i.e. between 7.5 and 8.5 (51). This observation of a decrease in pKa value is a result of a hydrogen bond network in the active site of the protein. X-ray crystallography has revealed the presence of two important tyrosine residues, Tyr201 and Tyr385, that are involved in polarizing the 4-OH of the substrate and hence, causing deprotonation at a lower pH (49,52) as shown in Figure 6.

Significant interactions in the active site of PHBH (40, 53) that contribute to the hydroxylation of *p*-OHB is illustrated in Figure 7. It is important to note that PHBH binds the substrate, *p*-OHB, in a large, solvent inaccessible hydrophobic pocket. The carboxylate function of *p*-OHB is involved in a salt bridge with Arg214 and a hydrogen bond with the Tyr222 and Ser212. The 4-OH function of the substrate hydrogen bonds to Tyr201, which in turn hydrogen bonds to Tyr385. This relay system has been mentioned previously as the hydrogen bond network that is responsible for the deprotonation of the substrate. Lastly, Asn300 hydrogen bonds with the C2 oxygen (O2) of the isoalloxazine ring of the FAD molecule.

Site directed mutagenesis of the triplets encoding for tyrosine residues 201 and 385 in the PHBH gene, has been achieved in separate experiments and the structures and

Figure 6. **An illustration of the influence of tyrosine residues, in the active site of PHBH, on the activation of the substrate, *p*-hydroxybenzoate:** The influence of hydrogen bonding on the formation of the phenolate form of *p*-hydroxybenzoate in the active site of the protein (49,53).

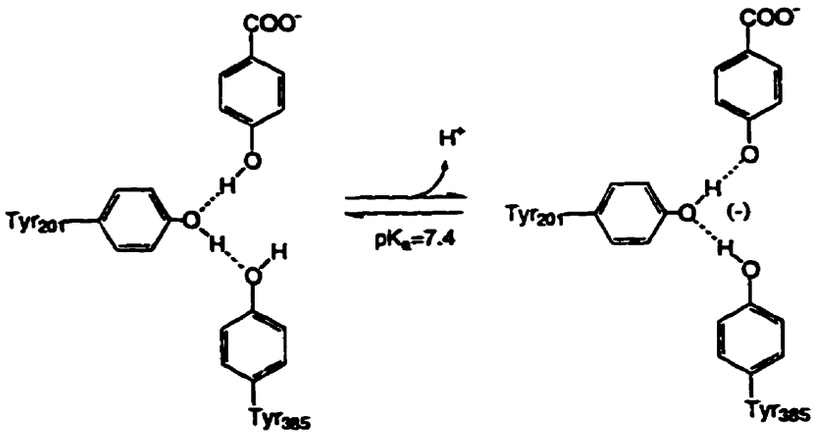
COO⁻
Tyr201
Tyr385
H⁺
pKa=7.4
(-)

Figure 7. **The active site of wild type PHBH (FAD):**
The substrate, *p*-hydroxybenzoate is shown with thick outlined bonds. Enzyme is from *P. fluorescens.* (40,53)

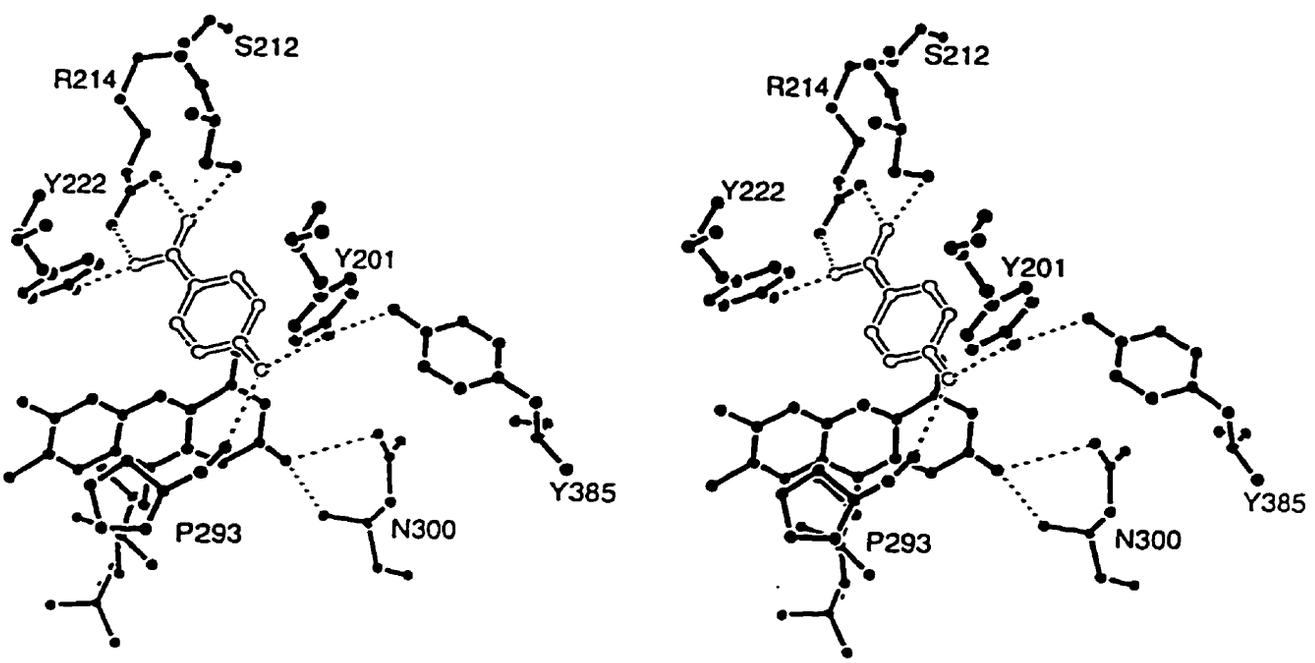
S212
R214
Y222
Y201
Y385
P293
N300
S212
R214
Y222
Y201
Y385
P293
N300

kinetics of their reactions have been investigated. In the case where Tyr201 is replaced with a Phe residue, crystallographic studies reveal that the hydrogen bond network involved in the activation of the substrate is abolished (Figure 8A), (53). As a result, Tyr385 is tilted upwards and appears to be in a hydrogen bond with a solvent molecule. Kinetic studies have revealed a significant decrease in the turnover rate. This would appear to be due to the inability of the substrate to deprotonate, with the pKa of the phenol function remaining above 9 in the active site. As a result, the rate of substrate hydroxylation (k_3 in Table 2) becomes limiting in the reaction. Also, there is a significant decrease in the amount of NADPH oxidation channelled towards hydroxylation. Approximately 94% of the NADPH oxidized is diverted to the production of H_2O_2 (49,53). Thus, the NADPH oxidation would become significantly uncoupled from substrate hydroxylation when Tyr201 is replaced by Phe. This is demonstrated by the finding that the rate constant for the decay of the C(4a)-peroxy-FAD to H_2O_2 formation, 0.72 s^{-1}, exceeds the rate of substrate hydroxylation (k_3=0.04s^{-1}, Table 2). When Tyr385 is replaced by phenylalanine, minimal changes are observed in the orientation of the residue in the active site (Figure 8B). Tyr201 would appear to still participate in a hydrogen bond with the substrate's phenol function, however, Phe385 is now incapable of hydrogen bonding with Tyr201. The consequence of the inability of Phe385 to participate in the hydrogen bond with Tyr201 is not notably apparent until the kinetics of the reaction are analysed. Although 75% of NADPH oxidation is still being used for hydroxylation of substrate, the rate of hydroxylation is found to decrease. Pre-steady state analyses have revealed that although the rate of substrate hydroxylation decreased, the first step in the reaction, i.e., the reduction of FAD by NADPH oxidation

Figure 8. **The structural differences between the wild type PHBH and its muteins: A. Tyr201Phe and B. Tyr385Phe** :
A superimposition of the active site centres of the wild type PHBH and the muteins, as indicated with solid lined bonds and thick outlined bonds, respectively (53).

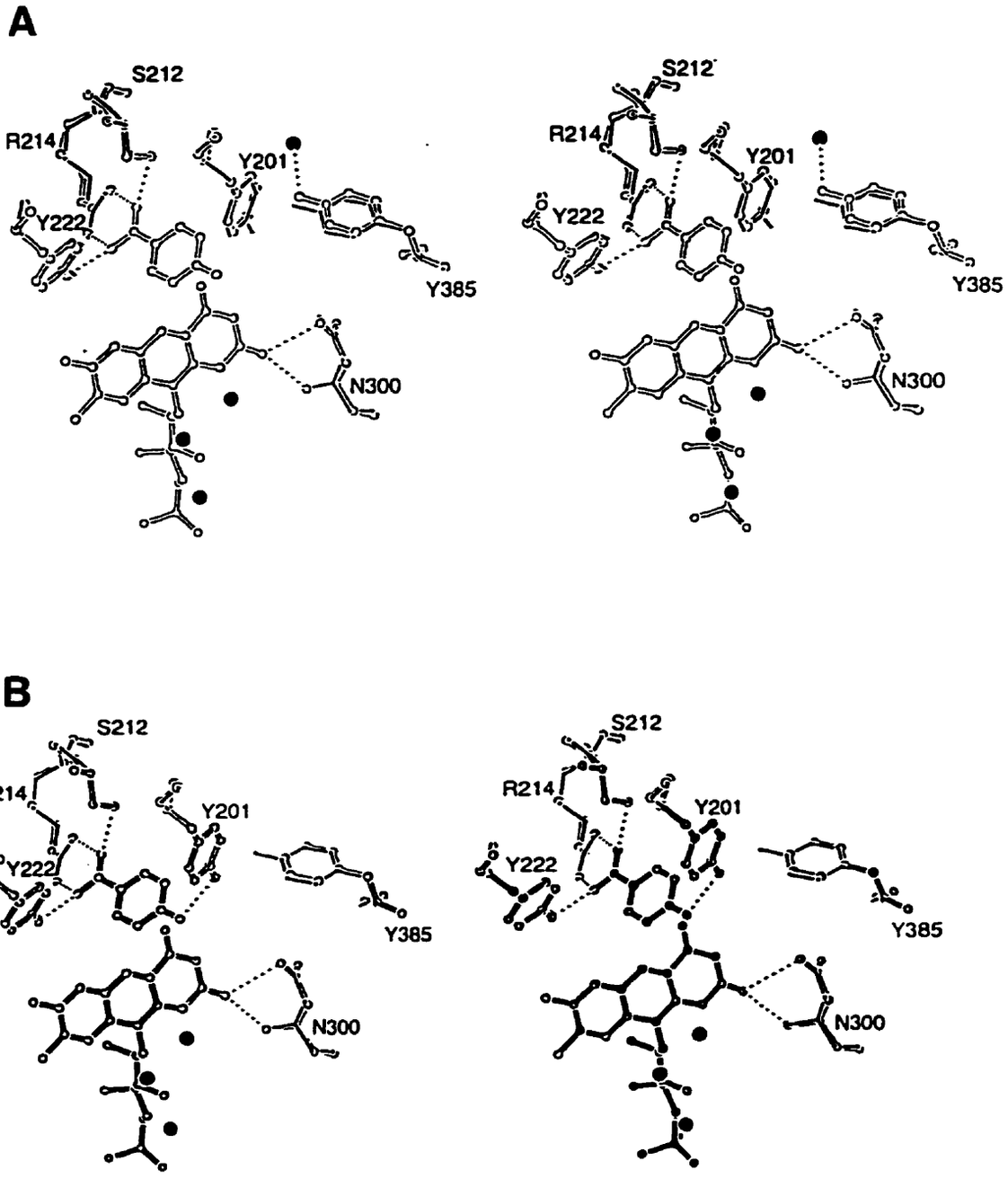
A
S212
R214
Y201
Y222
Y385
N300
S212
R214
Y201
Y222
Y385
N300
B
S212
R214
Y201
Y222
Y385
N300
S212
R214
Y201
Y222
Y385
N300

Table 2. **Some kinetic properties of wild type and mutant *p*-hydroxybenzoate hydroxylase:**
Rate constants for the reactions illustrated in Scheme 2. $*k_5$ = 0.72 s^{-1} (49,50,53)

Enzyme	Turn-over (s^{-1})	%NADPH used for...		k_1 (s^{-1})		k_2 ($M^{-1}s^{-1}$)	k_3 (s^{-1})	k_4 (s^{-1})	E_o' (mV)
		diOHB	H_2O_2	- pOHB	+ pOHB				
w.t.	5.7	100	n.a.	4×10^{-4}	50	2.8×10^5	47	14	-165
Y201F	0.42	5.9	94*	7×10^{-4}	5	3.0×10^5	0.04	n.d.	-156
Y385F	0.36	75	n.a.	8×10^{-4}	0.5	3.2×10^5	1.7	>15	-154
N300D	0.06	100	n.a.	1×10^{-3}	0.15	3.9×10^5	1.1	0.12	-205

appears to be rate limiting. X-ray crystallographic analysis has not provided a basis for this phenomenon, but it is believed to be a consequence of a change in the initial orientation of the cofactors, FAD and NADPH (52,53).

In addition to the tyrosine contribution within the active site, the asparagine residue, Asn300, is believed to be of importance in the reduction of FAD. X-ray crystallographic studies reveal FAD to be in an extended conformation within the enzyme, practically spanning half the length of the enzyme protomer (1mol FAD/ mol of PHBH protomer), (41,43). As previously mentioned, the ADP moiety of the flavin cofactor interacts mainly with the βαβ fold of the first 32 residues in the primary sequence of PHBH. In contrast, the isoalloxazine ring system of the flavin molecule interacts in the active site cleft. It is believed to be held in place exclusively by the interaction with main chain atoms except for the amide hydrogen of Asn300 which is found to hydrogen bond with the C2 oxygen of the flavin ring system (O2). Asn300, is located at the start of the α-helix, H10, and it is believed that this residue produces an electron withdrawing effect on the flavin ring system via the helix dipole, thereby altering the flavin's reactivity (49,53).

By site directed mutagenesis, Palfey *et al.* have produced an Asn300Asp PHBH mutein. X-ray diffraction studies of this PHBH mutein have revealed significant structural changes in the vicinity of the mutation (Figure 9). In the Asn300Asp PHBH , the side chain of the Asp300 is moved away from the isoalloxazine ring. This movement eliminates the hydrogen bond between the -NH of Asn300 with the O2 of the flavin ring. Instead this hydrogen bond is replaced with a weaker hydrogen bond (0.5- 0.6 Å longer) between a water molecule and the O2 of the flavin ring (50). In addition, there is a significant shift in

Figure 9. **The structural differences between the wild type PHBH and PHBH mutein, Asn300Asp:**
A superimposition of the active site centres of the wild type PHBH and the mutein, as indicated with solid lined bonds and thick outlined bonds, respectively (53).

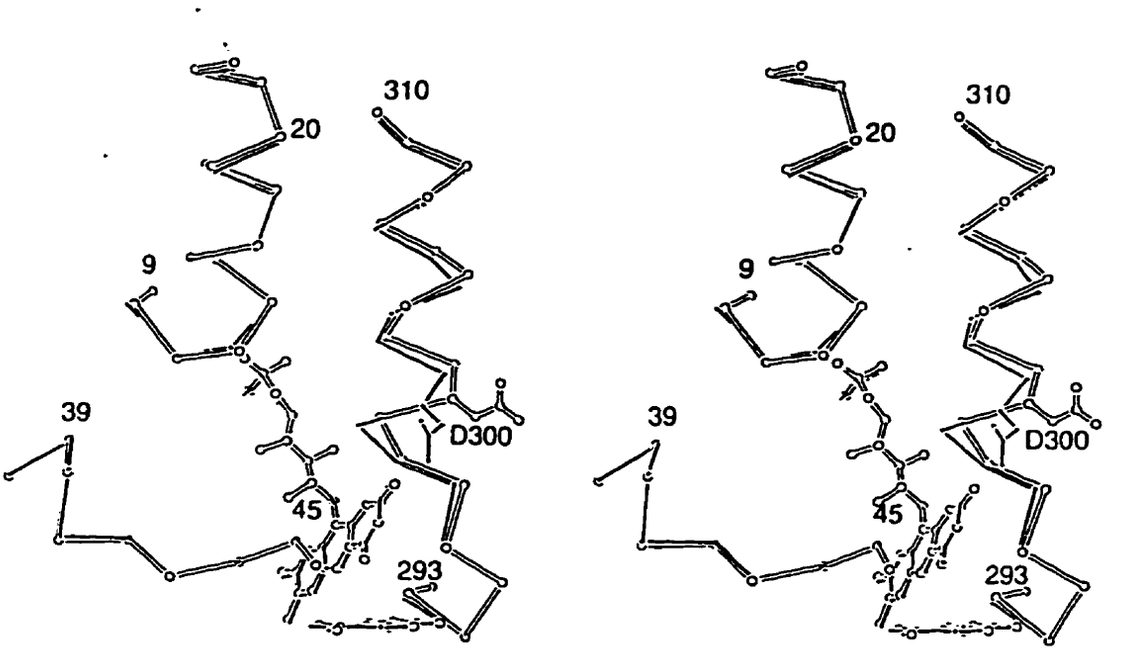
310
20
9
39
D300
45
293
310
20
9
39
D300
45
293

the backbone of the α-helix, H10, that minimizes the local dipole interactions of the backbone peptides and the flavin ring system. Kinetic investigations have revealed modifications in the rates of catalysis as tabulated in Table 2. The limiting reduction rate of the enzyme bound flavin was recorded as k_1 of 0.15 s^{-1}. This is 330 times lower than that in the wild type enzyme (50 s^{-1}). The decrease in k_1 can be explained by a change in the 2 electron reduction potential of the enzyme flavin, from a value of -165 to -205 mV. The observable rate decrease in the hydroxylation of the substrate (represented by the rate constant k_3) may be explained by the electronic perturbations exerted by the presence of a carboxyl anion in the active site. Although 12Å away, this foreign functional group causes a lengthening in the hydrogen bond between *p*-OHB and Tyr201 (from 2.67 to 2.88 Å). Lengthening of the hydrogen bond is believed to be due to an increase in the pKa of the substrate's phenolic function by about one unit, but, apparently not enough to explain the observed increase in pKa from 7.4 to above 9 (50). The decreased rate of dehydration of the C(4a)-hydroxy-FAD, as well as, the release of the product (represented by the rate constant, k_4) is due to the change in the flavin reactivity, that is probably due to a change in conformation. This factor is also thought to explain the 10^5 increase in k_2, the second order rate constant, for oxygen activation by the reduced enzyme-$FADH_2$ (50,53).

The preceding PHBH structures have shown the isoalloxazine ring of the FAD cofactor as being predominantly static within the active site of the enzyme. Recently however, the flavin in PHBH has been proven to having the ability of adopting either of two positions in the active site (54,55). The two orientations of the flavin were first noticed in X-ray studies of the crystals of Tyr222Phe PHBH. Examination of the electron density at

the active site have revealed the FAD as being in a mixture of an "in" and an "out" orientations in a ratio of 3:7, respectively. In this connection, the "out" orientation of the flavin ring is more pronounced when the wild type PHBH is crystallised in the presence of 2,4-dihydroxybenzoate, a poor hydroxylatable substrate. In the Tyr222Phe PHBH, the "out" conformation of the FAD is observed to be stabilized by an interaction between the O4 of the isoalloxazine ring and the guanidinium function of the Arg220 (The orientation of the Arg220-side chain apparently shifts in the mutated form of the enzyme). This is illustrated in Figure 10. In the presence of 2,4-dihydroxybenzoate, the conformation of the "out" position is observed to be stabilized by a hydrogen bond interaction between the N3 of the isoalloxazine and the 2'-OH of the 2,4-dihydroxybenzoate (Figure 11).

It is important to note the environment of the flavin ring system in both the "in" and the "out" orientations. In the "in" position, the reactive atoms in the isoalloxazine ring, that is the C-4a and the N5, are shielded from solvent molecules and hence, when the C(4a)-peroxy-FAD is formed, it is in perfect position to hydroxylate the substrate. However, when the flavin adopts the "out" orientation, the C-4a and the N5 of the flavin ring are exposed to the solvent. Therefore, when the C(4a)-peroxy-FAD is formed it is exposed to solvent and as a result rapidly decays to H_2O_2 before reacting with the substrate (54). It has been postulated that the PHBH in the absence of substrate exists primarily with the FAD cofactor in the "in" orientation. Once the substrate binds PHBH, the FAD opens up the active site by moving to its "out" position and allows the entrance of the substrate into the binding pocket. Binding of the substrate is followed by the FAD moving back into its "in" position. This suggested sequence of events has been reinforced by crosslinking experiments where 6-

Figure 10. **A. The comparison of the structural differences between the wild type PHBH and its mutein Tyr222Phe:**
A superimposition of the active site centres of the wild type PHBH and the mutein, as indicated with solid lined bonds and thick shaded outlined bonds, respectively (54).

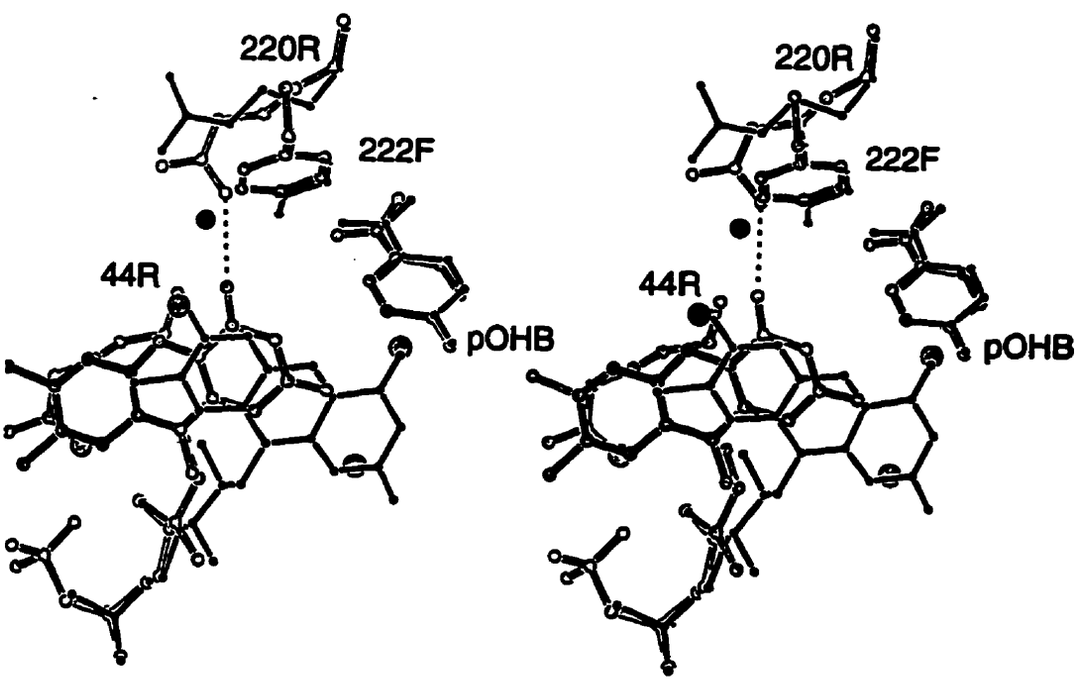
220R
222F
44R
pOHB
220R
222F
44R
pOHB

Figure 11. **Active site of PHBH interacting with 2,4-dihydroxybenzoate**
Wild type PHBH bound to 2,4-dihydroxybenzoate in the presence of Br^-. The "in" and "out" positions of the flavin are as indicated. (54).

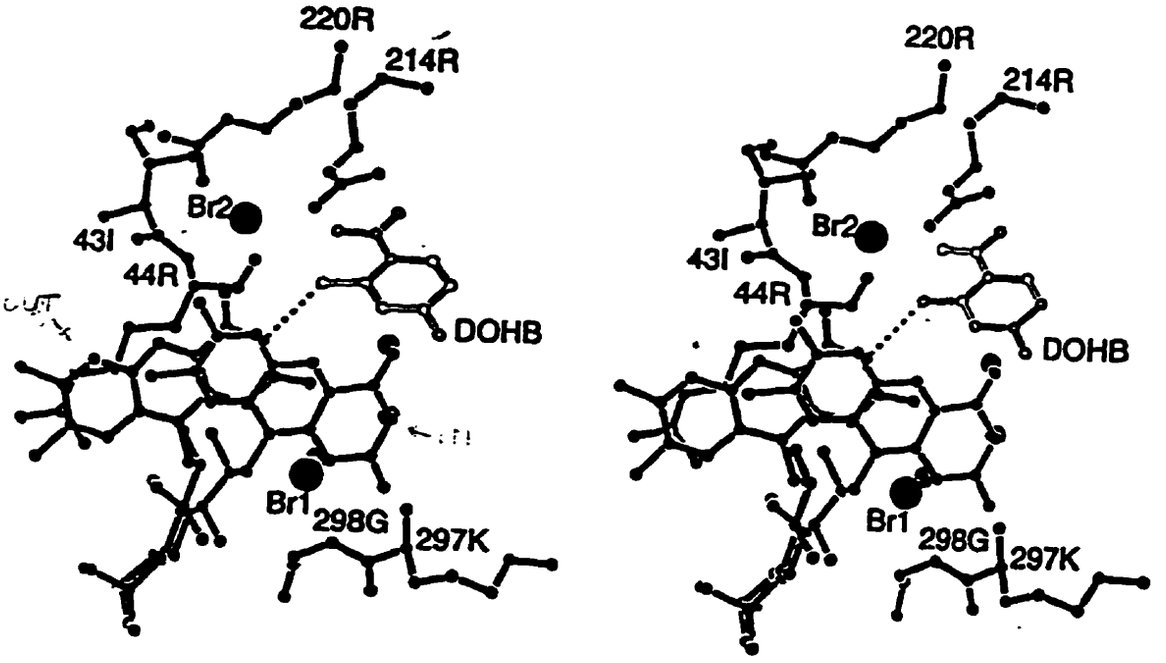
220R
214R
Br2
43I
44R
DOHB
Br1
298G
297K
220R
214R
Br2
43I
44R
DOHB
Br1
298G
297K

azido-FAD (a flavin analog carrying a photo reactive azido function) was used to monitor the orientation of the flavin. When the FAD analog is irradiated with visible light, the azido function is converted to a highly reactive nitrene. Therefore, if the 6-azido-FAD is in the "in" position when irradiated, the nitrene should cross link to the enzyme. If the FAD analog is in the "out" position when irradiated, the nitrene is assumed to react with the solvent and consequently results in no observable cross linking. Hence, the observed 80% and 66% cross linking in the absence and presence of substrate, respectively, and 17% in the presence of 2,4-dihydroxybenzoate, suggests that the FAD normally is in the "in" position and is moved to its "out" position , transiently, to enable the substrate to enter the active site. This finding vividly demonstrates the important biological control feature in PHBH for minimizing the wasteful NADPH oxidase activity in the absence of substrate (54).

In addition, it has been suggested that this type of swinging motion of the flavin allows it to function as a gate that controls the route into and out of the active site. Modelling experiments have indicated that when the flavin is in the "out " orientation, there is an open channel from the solvent to the substrate binding pocket. Upon closing the gate, when the flavin returns back to the "in" conformation, the active site is sealed away from the aqueous solvent, allowing efficient and specific hydroxylation of the substrate (Figure 12). This structure related functional role for the flavin to act as an instrument for the enzyme's use, in addition to its chemically reactive role, represents a novel alternative role for the flavins in biological systems.

Figure 12. **Molecular modeling experiments showing the active site of *p*-hydroxybenzoate hydroxylase:**
A. The active site in the closed conformation where FAD is in the "in" position (central structure). Volumes not occupied by the protein are contoured in white. (54)
B. The active site in the open conformation where FAD is in the "out" position. (54)

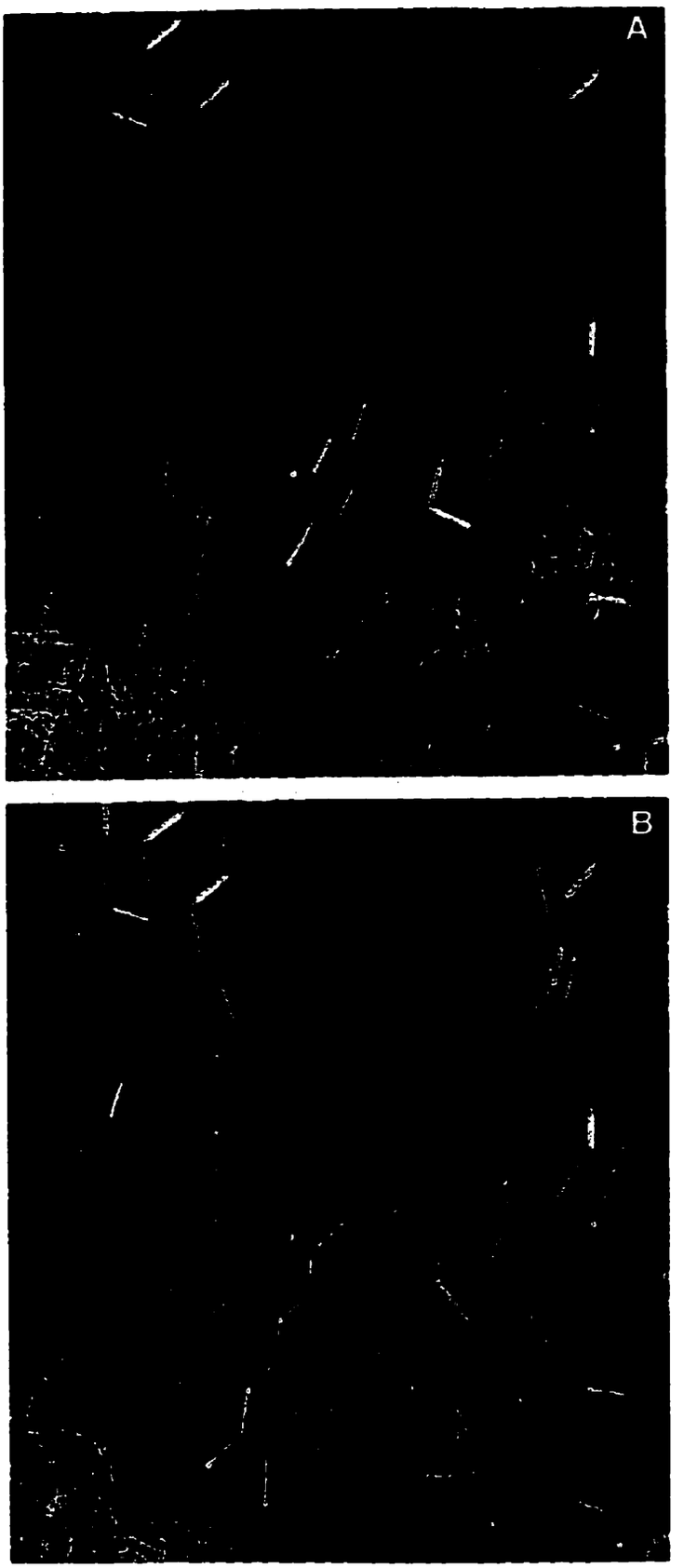
A
B

1.4 Objective:

Aerobactin is a virulence determinant in many septicaemic organisms. Lysine:N^6-hydroxylase which catalyses the initial step in the biosynthesis of this siderophore serves as an excellent target for the development of a new class of antimicrobial agents since this enzyme is only found in the microbial kingdom. Current studies were undertaken to elucidate the structure-function relationship inherent in this enzyme so as to gain information to develop potent inhibitors of its function. Consequently, current investigations focused attention on the following aspects: (1) factors contributing to the stability and structural integrity of the protein; (2) examination of the specificity of the protein with respect to its hydroxylatable substrate; and (3) analysis of the cysteine residues of the protein and their contribution to the various catalytic functions by approaches based on their chemical modification as well as their replacement with alanine by site directed mutagenesis.

2.0

MATERIALS

Chemical	Supplier
Dyematrex Orange A gel	Amicon Corporation Beverly, MA
L-α-aminobutyric acid ϵ-*N*-methyllysine L-norleucine DL-norleucine L-norvaline	Aldrich Chemical Company Milwaukee, WI
ampicillin [2-^{14}C]ICH$_2$COOH	Amersham Life Sciences Arlington Heights, IL
Calcium chloride dihydrate DPIP Guanidine hydrochloride, ultrapure bioreagent HEPES, ultrapure bioreagent Hydrochloric acid Magnesium sulphate heptahydrate ($MgSO_4 \cdot 7H_2O$) Potassium phosphate, dibasic (K_2HPO_4) Potassium phosphate, monobasic (KH_2PO_4) Sodium acetate, trihydrate Sodium citrate	J.T. Baker Chemical Company Phillipsburg, NJ
trans 4,5-dehydro-L-lysine Furylacryloyl-L-Phe-Ala L-lysineamide L-lysinemethylester	Bachem, Biosciences Inc. King of Prussia, PA
Acetic acid Acetonitrile, HPLC grade	BDH Chemical Company Toronto, Ontario

Formic acid Sodium chloride Sodium hydroxide Sodium sulphate Trichloroacetic acid Trifluoroacetic acid	
ammonium persulfate acrylamide and bisacrylamide BioGel-P10 (200-400 mesh) SDS Dowex 50W-X8 and X16 (200-400 mesh, H^+ form)	Bio-Rad Laboratories Richmond CA
Carboxypeptidase B	Boehringer Mannheim W. Germany
α-ϵ-diaminopimelic acid	Calbiochem San Diago CA
Carboxypeptidase Y	Carlbiotech Copenhagen, Denmark
Bacteriological agar Casamino acids Tryptone Yeast extract	Difco Laboratories Detroit, MI
Iodine Sulfanilic acid	Fisher Scientific Toronto, Ontario
Carboxypeptidase A Glucose dehydrogenase α-naphthylamine	Fluka Biochemika Switzerland
Ammonium sulphate, ultrapure PMSF	ICN Biochemicals Cleveland, OH

Oligonucleotide primers	MOBIX
DNA sequencing	McMaster University, Hamilton, ON
Dra III, *Dpn* I and *Nde* I restriction endonulease (and buffer)	New England Biolabs
BSA molecular biology grade	Mississauga, Ontario
SDS-PAGE molecular weight standards	Pharmacia
(94 kDa, 67 kDa, 43 kDa, 30 kDa, 20.1 kDa)	Baie d'Urfe, Quebec
TPCK trypsin	Pierce Chemical Company
	Rockford, IL
*Eco*R I restriction endonuclease (and buffer)	Promega
Kpn I restriction endonuclease (and buffer)	Madison, WI
BSA, molecular biology grade	
dNTPs, Ultrapure	Pharmacia LKB Biotechnology
	Uppsala, Sweden
Qiagen plasmid starter kit	Qiagen Inc.
	Chatsworth, CA
ADP	Sigma Chemical Company
ADPR	St. Louis, MO
2'P-ADP	
AMP	
BAEE	
BSA	
BTEE	
Chymotrypsinogen A, type II	
Cyanogen bromide (CNBr)	
DNase	
DTNB	
DTT	
EDTA	
Ethidium Bromide	

Ferrous ammonium sulphate	Sigma Chemical Company
FAD	St. Louis, MO
D-glucose	
Glucose-6-phosphate	
Glucose-6-phosphate dehydrogenase	
L-glutamine	
Iodoacetate (ICH_2COOH)	
LB media (powder mix)	
L-lysine	
$NADP^+$	
NADPH	
NTCB	
Plasmid mini-prep kit	
Potassium thiocyanate	
RNAase	
SBTI	
Sodium sulphate, anhydrous granular (Na_2SO_4)	
Trizma base (Tris)	
Vydac, C4 reverse phase column (300 Å)	

and other substrate analogs used in this study

3.0

METHODS

3.1 Molecular biology techniques

3.1.1 Preparation of competent cells (56, 57):

The desired bacterial culture was grown overnight at 37 °C in 5 ml of LB or 2xYT medium (Appendix A) with constant shaking. This starter culture was used to inoculate 100 ml of the same medium and allowed to grow until it reached an optical density of 0.3 at 600 nm (≈ 3 hours). The cells were chilled to 4 °C in an ice water bath for 15 minutes, transferred to sterile centrifuge tubes and centrifuged (2,000 xg) for 5 minutes. The cell pellet was resuspended in 100 ml of sterile, ice cold transformation buffer (Appendix A) and incubated in an ice water bath for 30 minutes . Following centrifugation (2,000 xg) for 5 minutes, the cells were resuspended in 8 ml of sterile, ice cold transformation buffer containing 15% glycerol (v/v). Aliquots of the suspension (200 µl) were transferred to sterile microfuge tubes and either used immediately or frozen and stored at -80 °C until ready to use.

3.1.2 Transformation protocol (56,57):

The desired plasmid preparation, approximately 1 µg (and this included the Quick Change® products) was added to a suspension of competent cells (200 µl) and incubated in an ice water bath. After 45 minutes, the cells were heat shocked by immersion in a 42 °C water bath for 2 minutes. LB or 2xYT medium (500 µl) was added and the culture was

allowed to grow for 1-2 hours at 37 °C (with no shaking). The suspension was streaked on 2xYT or LB agar plates (Appendix A) containing ampicillin (100 mg/l) and incubated for approximately 24 hours at 37 °C for the selection of the ampicillin resistant colonies.

3.1.3 Isolation and purification of plasmids:

(a) *mini-scale preparation:* The plasmid mini-prep kits were obtained from Sigma Chemical Co. (St. Louis, MO) and used according to the procedure recommended by the supplier. *E.coli* DH5α transformed with the plasmid of interest, was grown in 5 ml of LB medium (supplemented with ampicillin, 100 mg/l), with constant shaking at 37 °C. After 14-16 hours, the culture was centrifuged (6,000 xg) for 30-60 seconds. The supernatant was removed and the cells were suspended in Solution A (250 µl). Next, Solution B (250 µl) was added to the suspension and gently mixed. After 2-3 minutes, Solution C (250 µl) was added slowly with constant mild agitation. The precipitated proteins and chromosomal DNA were removed by centrifugation (12,000 xg) for 15 minutes and the clear supernatant was applied onto a Sigma-miniprep filter. The filter was placed in a microfuge tube and centrifuged (12,000 xg) for 30-60 seconds. It was washed twice with 500 µl of Solution D (1X) and the wash collected by centrifugation and the microfuge tube was discarded. The DNA was eluted by the addition of Solution E (50 µl) to the filter and centrifugation (12,000 xg) for 30-60 seconds and then stored at -20 °C until used.

(b) *large-scale preparation:* The preparation of pAT5 on a large scale was performed using the Qiagen plasmid kit (refer to Appendix B for the buffer solutions used). *E.coli* DH5α, transformed with pAT5 was grown in LB medium (100 ml) supplemented with ampicillin (100 mg/l), overnight at 37 °C, to achieve an absorbance of 1.4 at 600 nm.

The cells were harvested by centrifugation (600 xg) for 15 minutes and the supernatant was decanted. The cell pellet was thoroughly resuspended in Buffer P1 (10 ml). After 5 minutes, Buffer P2 (10 ml) was added and mixed by gentle inversion of the centrifuge tube. Once the solution became clear and viscous (<5 minutes), Buffer P3 (10 ml) was added and immediately mixed by gentle repeated inversions of the centrifuge tube. The mixture was allowed to incubate at 4 °C for 20 minutes. The precipitated proteins and chromosomal DNA was removed by centrifugation (35,000 xg for 30 minutes) and the supernatant was further filtered through glass wool. The clear filtrate was applied onto a Qiagen Tip 500 equilibrated with Buffer QBT and allowed to enter the column by gravity flow. The Qiagen Tip was washed with Buffer QC followed by elution of the plasmid DNA with Buffer QF (15 ml). The DNA was precipitated with 0.7 volumes of isopropanol and the stored at -20 °C until needed.

3.1.4 Digestion of plasmid DNA with restriction endonucleases:

The plasmid DNA was digested with the appropriate restriction endonuclease (R.E.) using the conditions recommended by the manufacturer. Plasmid DNA (approximately 0.5-1.0 µg) was used for each reaction. A typical reaction mixture is described below:

H_2O	4.5 µl
buffer, 10X (appropriate for the R.E.)	1 µl
BSA, 10X (1mg/ml)	1 µl
plasmid (2-4 µg/10 µl)	2.5 µl
R.E.	1 µl

The restriction endonucleases used were as follows: (i) the plasmid with the iucD variant

encoding for C51A *r*IucD was digested with *Kpn* I (18 units) for 6 hours at 37 °C; (ii) the plasmid containing the iucD variant encoding for C158A *r*IucD was digested with *Dra* III (3 units) for 6 hours at 37 °C; (iii) the plasmid containing the iucD variant encoding for *r*IucD with the C-terminal deletion was digested with *Eco*R I (14 units) for approximately 12 hours at 37 °C; (iv) the plasmid with the iucD variant encoding for C51A/C158A *r*IucD was digested with both *Kpn* I (18 units) and *Dra* III (3 units), separately, for 6 hours at 37 °C; and (v) the parent plasmid, pAT5, was digested with each of the three restriction endonucleases under similar conditions. Assay mixtures with the restriction endonuclease replaced by an equal aliquot of water served as control.

3.1.5 Electrophoretic analysis of DNA fragments (58):

The plasmids or the DNA fragments were separated and analysed by electrophoresis on agarose gel (1 %). A solution containing agarose (1 %) in TAE buffer was prepared. The suspension was heated to get a clear solution and then cooled to luke warm temperature prior to the addition of ethidium bromide (1 µl of 0.5 mg/ml). After mixing thoroughly, the agarose was poured into a horizontal chamber to generate a gel, approximately 5 mm thickness. Prior to setting of the gel, a comb was placed on one end of the gel to form wells that were needed for the application of the samples. Once the TAE buffer was added to the electrophoresis chamber until the gel surface was covered, the samples (12 µl, prepared in loading buffer) were added to the wells and the electrophoresis was conducted at constant voltage of 85 volts for 1-2 hours at room temperature. The DNA bands were visualized under ultra-violet light and the profile was recorded with the aid of a Polaroid photographic transilluminator system purchased from Bio/Can Scientific, Mississauga, ON.

3.2 Growth of *Escherichia coli* and transformants

3.2.1 *Escherichia coli* DH5α:

E. Coli DH5α [F⁻ϕ80dlacZΔM15 Δ(argF-lacZYA)U169 *deo*R *rec*A1 *end*A1 *hsd*R17 (rk^- mk^-)*sup*E44 λ^- thi-1 *gyr*A96 *rel*A1] was obtained from Gibco BRL, Gaithesburg, MD. The cells were grown and maintained on LB agar slants at 4°C. A typical starter culture was prepared by inoculating the bacterial cells from the agar slants into the LB medium (5 ml) and grown for 10-12 hours by incubating at 37 °C with continuous shaking.

3.2.2 Growth of organisms:

E. Coli DH5α was transformed with the plasmid pAT5 or its variants. The starter culture was usually grown in LB medium and then transferred to minimal medium (Monod M9) with yeast extract (1 g/L) and casamino acids (1 g/L) (see Appendix A). The medium was supplemented with ampicillin (100 mg/l) in all cases. The cultures were grown to late log phase (14-16 hours) prior to harvesting.

3.3 Isolation and purification of *r*lucD and its muteins

3.3.1 Preparation of cell free extract:

Cell free extracts were obtained by rupturing the cells under high pressure (French press) similar to that described by Goh *et al.* (18). The cells were harvested by centrifugation (6,000 x g) for 15 minutes and washed in a saline solution (0.85% NaCl). They were suspended in a 50 ml solution of potassium phosphate buffer (10 mM, pH 7.0) containing L-glutamine (1 mM) and DTT (1 mM), and ruptured by a single passage through a prechilled (4 °C) French press chamber under constant pressure of approximately 10,000 psi. The resulting slurry was incubated for 15 minutes (at room temperature) in the presence

of DNase (1 mg) and RNase (1 mg) prior to centrifugation (140,000 xg) for 1 hour to remove the insoluble material comprising unbroken cells and cell debris.

3.3.2 Purification of lysine:N^6-hydroxylase:

The cell free extract was treated with solid ammonium sulfate to achieve 40% saturation, with respect to the salt. The suspension after standing at 4 °C overnight, was centrifuged (35,000 xg) for 15 minutes and the precipitate (which contained most of the lysine:N^6-hydroxylase activity) was collected..

At this stage, the original procedure (19) was modified as follows: The above material, consisting of the proteins precipitated with ammonium sulfate at 40% saturation, was dissolved in 20 ml of potassium phosphate buffer (10 mM, pH 8.0) containing NaCl (300 mM), and DTT (1 mM) and dialysed against the same buffer for 12-16 hours at 4 °C. The dialysed material was treated with solid ammonium sulphate to 30% saturation and after 2-3 hours at 4 °C, the suspension was centrifuged (35,000 xg) for 15 minutes. The precipitate (which contained most of the lysine hydroxylase activity) was collected, dissolved in 10 ml of potassium phosphate buffer (10 mM, pH 7.0) containing NaCl (250 mM), and DTT (1mM) and dialysed against the same buffer for 12-16 hours. This procedure was essential not only for the removal of the ammonium sulfate but also that of the free flavin cofactor present in the protein preparation. The solution was then dialysed for two hours against potassium phosphate buffer (10 mM, pH 7.0) containing DTT (1 mM) prior to application on the Orange A Dye mätrex column equilibrated with the same buffer. The protein(s) were recovered by elution with potassium phosphate buffer (10 mM, pH 7.0) with stepwise increases in NaCl concentration (250 mM, 500 mM, 750 mM, and 1000 mM).

Fractions (25 ml) were collected and examined for the presence of lysine:N^6-hydroxylase activity. The enzymatic activity was usually found in the fractions eluted with buffer medium containing 750 mM NaCl. However, this property was found to depend on the quality of the commercial preparation of the Orange A and the extent of its previous use for achieving the purification of the protein. Thus, with Orange A preparations, after repeated use, the lysine:N^6-hydroxylase activity was found to elute at concentrations of NaCl $\leq$ 750 mM.

Finally, it is pertinent to note that the second ammonium sulfate precipitation step (with 30% ammonium sulfate, at pH 8.0) is a modification of the earlier method (19) and facilitates the purification of the enzyme by removal of considerable amounts of extraneous proteins at this stage.

3.4 Site directed mutagenesis of iucD (59)

The replacement of cysteine residues 51 and 158, either, individually or in combination was achieved with the aid of Quick Change® mutagenesis kit obtained from Stratagene Cloning Systems, (LaJolla, California) employing the protocols recommended by the supplier (Instruction Manual, Catalog #200518, Revision #125001). The procedure which involves the use of complementary mutagenic primers (30-45 bases in length), both carrying the desired mutation, utilizes the relatively high fidelity *Pfu* DNA polymerase for the simultaneous replication of both strands of the plasmid. The use of complementary mutagenic primers restricts the replication by DNA polymerase, during temperature cycling, to the parent plasmid template, thereby minimizing the possibility of amplifying errors in the replication process (59). An outline of the procedure used is illustrated in Figure 13.

Figure 13. **An outline of Statagene's Quick Change® procedure (59):**
For the site directed mutagenesis of *r*lucD

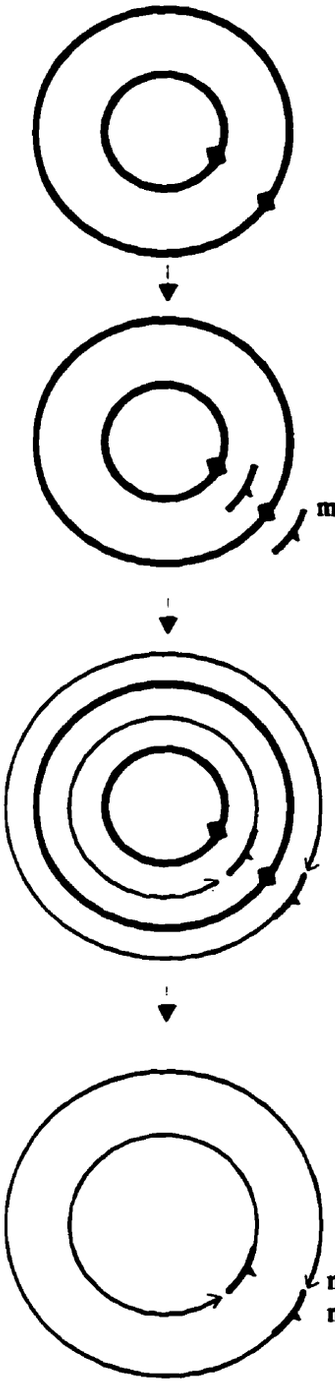

I. Plasmid Preparation: Gene in plasmid with target site (■) for mutation.

II. Temperature cycling: The plasmid was denatured and the oligonucleotide primers (⟵▼⟶) containing the desired mutation (▼) was annealed.

Using the non-strand-displacing action of Pfu DNA polymerase,the mutagenic primers were extended and incorporated, resulting in nicked circular strands.

III. Digestion: The methylated, non-mutated parental DNA template was digested with Dpn I.

IV. Transformation: The circular nicked double stranded DNA were transformed into *E.coli* competent cells.

3.4.1 Designing primers:

For the replacement of cysteine 51 of *r*IucD by alanine, the complementary primers were synthesised with: (i) a change of the triplet TGT, coding for cysteine to GCT, the triplet for alanine; and (ii) a silent mutation in the triplet coding for valine 48 from GTA to GTT. The latter mutation leads to elimination of one of the two *Kpn* I restriction enzyme sites in the parent plasmid. For the replacement of cysteine 158 of *r*IucD by alanine, the complementary primers were designed with: (i) a change in the cysteine triplet TGT to GCT, the triplet coding for alanine; and (ii) a silent mutation, CAT to CAC, in the triplet coding for histidine 161. The first of these mutations results in the elimination of the unique *Dra* III and the latter leads to the deletion of one of the *Nde* I restriction enzyme sites. The above set of complementary primers were also used to introduce the second cysteine to alanine mutation, starting with the appropriate plasmid preparation harboring the single mutation.

For the deletion of 27 amino acid residues at the carboxy terminus of *r*IucD, the complementary primers were synthesized with a change in the triplet CGT, coding for Arg 400, to the triplet TGA, a stop codon. This mutation results in an insertion of a second *Eco*R I site in the plasmid preparation. The details with respect to the mutagenic primers employed and the effects of the mutation(s) are presented in Table 3.

3.4.2 Conditions for Quick Change® mutagenesis:

The plasmid, pAT5, containing the iucD gene and the ampicillin resistant gene, served as the template for the *Pfu* DNA polymerase. The following reagents in the amounts indicated were introduced in the order shown: *Pfu* reaction buffer (10X), 5 µl; homogeneous pAT5 (5 ng/µl), 10 µl; primer1 (125 ng/µl), 10 µl; primer2 (125 ng/µl),

Table 3. **Details of the site directed mutagenesis of iucD:** In pAT5, the recombinant DNA technique involves an inframe gene fusion of iucD with a lacZ segment that encodes for the N-terminal 13 amino acid residues of β-galactosidase (19).

The incorporation of the desired site specific mutation(s) was achieved by the use of complementary primers containing the mutation of interest (underlined codon). The incorporation of the desired mutation(s) was confirmed both on the basis of the profile of the product(s) generated upon treatment with restriction enzyme(s) as well as by the determination of the nucleotide sequence.

[1] pAT5 with iucD encoding for C51A *r*IucD was used to effect the second mutation.

[2] pAT5 with iucD encoding for C158A *r*IucD was employed to effect the second desired mutation.

PCR experiments were performed with the aid of Amplitron® II thermocycler manufactured by Thermolyne coorporation.

Plasmid	**Complementary primers used (5′→3′)**	**Mutation in *r*lucD**	**Change in restriction enzyme site**
pAT5	none	none	none
pAT5	GGGTATGCTGGTTCCGGAT GCTCATATGCAGACCGTC GACGGTCTGCATATGAGCA TCCGGAACCAGCATACCC	C51A	loss of one of two Kpn I sites
pAT5	CCTTATTTACCACCCGCTGT GAAGCACATGACACAATCC GGATTGTGTCATGTGCTTCA CAGCGGGTGGTAAATAAGG	C158A	loss of a unique Dra III site and an Nde I site
C51A-pAT5[1]	CCTTATTTACCACCCGCTGT GAAGCACATGACACAATCC GGATTGTGTCATGTGCTTCA CAGCGGGTGGTAAATAAGG	C51A/C158A	loss of a unique Dra III site and an Nde I site
C158A-pAT5[2]	GGGTATGCTGGTTCCGGAT GCTCATATGCAGACCGTC GACGGTCTGCATATGAGCA TCCGGAACCAGCATACCC	C51A/C158A	loss of one of two Kpn I sites
pAT5	GGAGATCTGCATGAATTC TTAATCGCGTAATGGG CCCATTACGCGATTAAGA ATTCATGCAGATCTCC	R400stop	insertion of a second EcoR I site

10 µl; dNTP mixture of all four (10 mM), 1 µl; H_20 (sterile), 13 µl; and *Pfu* DNA polymerase (2.5 U/µl), 1 µl. The reaction mixture was kept at 4°C until ready for thermocycling. The temperature cycling was programmed as follows:

jumpstart	85 °C, 2 minutes
	95 °C, 30 seconds
	55 °C, 1 minute
	68 °C, 10 minutes

The cycle, excluding the jumpstart period, was repeated 15 times followed by a dwelling period of 15 minutes at 68 °C to allow for the extension of any incomplete replications.

Following the temperature cycling, the reaction mixture was treated with 20 units of *Dpn* I for one hour at 37 °C to degrade the parent plasmid. The mutation-containing synthesized DNA product was used to transform the competent cells of *E. coli* (DH5α) or *Epicurium coli*® XL-1 Blue and the transformants were selected from nutrient agar plates on the basis of ampicillin resistance.

3.5 Analytical methods

3.5.1 Determination of the homogeneity and molecular weight of the protein preparations:

Sodium dodecyl sulfate-polyacrylamide gel electrophoresis, SDS-PAGE (60), was used to assess the homogeneity as well as to obtain an estimate of the molecular weight of the purified lysine:N^6-hydroxylase preparations. The stacking and separating gel were made with a 3% and a 10% acrylamide content, respectively. After the electrophoresis was achieved under constant current of 17.5 mA, the gel was stained with coomassie blue and destained with a solution of methanol:acetic acid:water (30:10:60).

An accurate estimate of the molecular weight of the purified enzyme preparations was further achieved by the use of electrospray mass spectrometry, ESMS (61). Protein samples were rendered free of salt by dialysis against distilled, deionized water prior to analysis by ESMS.

3.5.2 Determination of protein concentration:

The absorbance of a homogenous preparation of lysine:N^6-hydroxylase (or its muteins) was measured at 280 nm and the protein concentration of the solution was estimated by using an ϵ_{280} value of 67,500 M^{-1} cm^{-1} (62).

3.5.3 Determination of DNA concentration:

The concentration of the DNA (plasmid or primer) preparations was determined by measuring the absorbance of the solution at 260 nm. One absorbance unit corresponds to 50 μg/ml and 38 μg/ml for double strand (plasmid) and single strand (mutagenic primers) DNA, respectively (58).

3.5.4 Lysine:N^6-hydroxylase activity:

The ability of *r*IucD and its muteins to effect N-hydroxylation of lysine was accomplished by a protocol similar to that reported previously (19). A typical assay, in a final volume of 5 ml, included potassium phosphate (100 mM, pH 7.2), L-lysine (1 mM), FAD (30 μM), $NADP^+$ (160 μM), G-6-P (800 μM), G-6-P dehydrogenase (1.25 U) and *r*IucD (80-100 nM). After incubation at 37°C, with constant shaking for 15 minutes, the reaction was stopped by the addition of a slurry of Dowex 50W-X8 (200-400 mesh, H^+ form) resin in distilled water. The entire mixture was transferred to a 1.2 x 25 cm column and washed with 0.2 N HCl (40 mL) prior to elution with 6N HCl (25 mL). The effluent

was taken to dryness under reduced pressure. The residue was dissolved in water (5 ml) and an aliquot (4.5 ml) used for the determination of N^6-hydroxylysine by the iodine oxidation procedure (63).

For the determination of the K_M value for FAD, the experimental conditions were similar to that described above except for the flavin concentration that varied over a range of 0 to 100 μM. In the experiments designed to determine the K_M for NADPH, G-6-P, G-6-P dehydrogenase and $NADP^+$ were replaced by NADPH over a range of 0 - 700 μM. The K_M values were determined from the double reciprocal plots of the data (64).

3.5.5 Determination of NADPH oxidation:

The assay mixture, in a volume of 3 ml, consisted of potassium phosphate (100 mM, pH 7.0), FAD (40 μM), NADPH (200 μM), L-lysine (1 mM), and *r*IucD (300-500 nM). In these experiments, the baseline was initially established by the introduction of FAD and buffer prior to the addition of the NADPH followed by the enzyme. After monitoring the decrease in absorbance at 340 nm for 1-2 minutes, lysine was introduced and the decline in absorbance was monitored as a function of time. The decrease in the absorbance at 340 nm in the absence of substrate reflects the NADPH oxidation that is not coupled to the N-hydroxylation process.

3.5.6 Determination of H_2O_2:

The qualitative assessment of H_2O_2 production was performed by the procedure of Hildebrandt et al (65). In a typical experiment, the assay mixture, in a final volume of 5 ml, consisting of potassium phosphate (100 mM, pH 7.2), FAD (30 μM), $NADP^+$ (160 μM), G-6-P (800 μM), G-6-P dehydrogenase (1.25 U) and *r*IucD (80-100 nM), was incubated at

37°C (shaking). At desired time intervals, an aliquot of 1 ml was removed and treated with an equal volume of trichloroacetic acid (3%). To the mixture, 0.5 ml of ferrous ammonium sulfate (10 mM) was added followed by the addition of 0.2 ml of potassium thiocyanate (2.5 M). After standing for 10 minutes at room temperature, the absorbance at 480 nm was recorded.

3.5.7 Reaction of *r*lucD with DPIP:

To a solution of DPIP (100 μM) in potassium phosphate buffer (100 mM, pH 7.0), an aliquot of a solution containing *r*lucD was added. The absorbance at 600 nm was found to decline steadily, reaching a constant value after approximately 5 minutes. The magnitude of this deacrease in absorbance was recorded. The amount of DPIP bound to *r*lucD was calculated by using an ϵ_{M} value of $2x10^4$ $M^{-1}cm^{-1}$ for the dye (62).

3.5.8 Isolation of DPIP-*r*lucD complex:

*r*lucD or its muteins (≈10 μM) in 200 mM potassium phosphate, pH 7.0 was treated with DPIP to achieve a final concentration of 100 μM. After 15 minutes at 25 °C, the reaction mixture was subjected to chromatography on a 10x1 cm column of BioGel P4 with 200 mM potassium phosphate, pH 7.0, serving as equilibration and elution medium. The absorbance of the recovered protein was recorded at 280 nm and 600 nm. Calculations based on the ϵ_{M} values of 6.75×10^4 $M^{-1}cm^{-1}$ and 2×10^4 $M^{-1}cm^{-1}$ for the protein and the dye respectively, were used to determine the stoichiometry of the interaction (62).

3.5.9 Measurement of diaphorase activity:

DPIP was used to monitor the diaphorase activity of *r*lucD and its muteins. In a typical experiment, the initial absorbance at 600 nm of DPIP (100 μM), in potassium

phosphate, (200 mM, pH 7.0) was recorded prior to the introduction of the desired *r*lucD preparation. After the addition of the protein, the reaction between the DPIP and the enzyme was allowed to proceed and monitored for the specific periods of time as indicated. An aliquot of the solution of NADPH was added to obtain a final concentration of 200 μM and the change in absorbance at 600 nm was recorded. After 40 seconds, FAD was added to a final concentration of 100μM and the decline in the absorbance of 600 nm was monitored as a function of time.

3.5.10 Estimation of cysteine residues present in *r*lucD and its muteins:

(a) *Titration with DTNB (or NTCB):* The thiol content in the native state of *r*lucD and its muteins was determined by reaction with DTNB (66). In a typical experiment, *r*lucD (5-12 μM), in one ml of potassium phosphate (200 mM, pH 8.0), was treated with an aliquot (100 μl) of DTNB (5 mM) and the increase in absorbance at 412 nm was recorded. Similar experiments performed in the absence of the protein served as controls and allowed for making the correction for the contribution arising from the spontaneous hydrolysis of DTNB. An ϵ_M value of 14,150 M^{-1} cm^{-1} (67) was used to determine the number of thiol groups present in the protein. Experiments performed in the presence of guanidine hydrochloride (4.0 M) provided an estimate of the thiol functions accessible to modification upon denaturation of the protein. It is important to emphasize that denaturation of the protein should be achieved in the presence of DTNB in order to ensure the modification of all of its available thiol functions.

(b) *Alkylation of rlucD* (68): The alkylation of *r*lucD was achieved using [2-^{14}C]ICH_2COOH. Prior to use, the commercial preparation of the radioactive iodoacetate

(50 μCi) was mixed with non-radioactive ICH_2COOH (102 mg) dissolved in 10 ml of H_2O, to achieve a final concentration of 55 mM with respect to the reagent.

The specific activity of the preparation was assessed by the determination of radioactivity associated with aliquots (10-50 μl) of samples prepared after dilution (1:100) of the stock solution. For the assessment of the purity of the commercial preparation of [^{14}C]iodoacetate, an aliquot (50 μl) of the stock solution (55 mM) was treated with 1 ml of cysteine (100 mM) , 500 μl of potassium phosphate (1.0 M, pH 7.0) and 550 μl of H_2O. After 20 minutes of reaction, the mixture was treated with 5 ml slurry of Dowex 50W X8 (H^- form) resin and the entire mixture was transferred to a 10x1 cm glass column. The resin was washed with distilled, deionized water until the pH of the effluent turned neutral, prior to elution with 40 ml of 6 N HCl. The effluent was taken to dryness and the residue made up to 100 ml. Aliquots (100 μl) were used to assess the radioactivity in the recovered material. Calculations based on the specific activity and the amount of iodoacetate used to label cysteine indicated the commercial preparation to be 98% pure.

The reaction of *r*IucD with [^{14}C]iodoacetate was performed both under nondenaturing and denaturing conditions. In the former case, the native preparation of *r*IucD (containing 1 to 2 mM DTT) in a medium of potassium phosphate (200 mM, pH 7.0), was treated with a 20 fold molar excess of [^{14}C] iodoacetate over that of the thiol functions (contributed by both the protein and DTT). After 20 minutes at 25°C, the reaction was terminated by the addition of DTT to achieve a final concentration equal to that of the alkylating agent. The reaction mixture was dialysed extensively against water to remove the extraneous radiolabelled materials. The protein which was precipitated under these conditions, was

recovered by centrifugation, and dissolved in guanidine hydrochloride (4.0 M) prior to determination of the radioactive label with the aid of Beckman Model 5000 TD Liquid Scintillation Counter. To achieve alkylation of the protein under denaturing conditions, experimental procedures were similar to those mentioned above except for the inclusion of guanidine hydrochloride (4.0 M) in the reaction mixture.

3.6 Location of cysteine residues alkylatable in the native conformation of *r*IucD

3.6.1 Fragmentation of the S-[^{14}C]carboxymethylated *r*IucD

(a) *CNBr cleavage* (69)*:* The alkylated *r*IucD preparations were treated with CNBr to generate peptide fragments of the protein. The *r*IucD preparation in a medium of 70% formic acid, was treated with CNBr to achieve 100 fold molar excess of the reagent over that of the methionine residues present in the protein. After 24 hours, the reaction mixture was taken to dryness under reduced pressure and the residue served as the source for the isolation of the peptide fragments of *r*IucD.

(b) *Trypsin cleavage:* In the proteolytic degradation of *r*IucD (or its S-carboxymethyl derivative) trypsin was employed. The enzyme obtained from Pierce Chemical Company was a preparation pretreated with TPCK in order to inhibit chymotryptic activity associated with the protein. Prior to use, the activity of TPCK-trypsin was assessed by using BAEE (70) as a substrate. The *r*IucD preparation, after alkylation under nondenaturing conditions, was dialysed extensively against a medium of potassium phosphate (200 mM, pH 8.0) prior to treatment with TPCK-trypsin (the enzyme to substrate ratio, 1:10). The digestion was allowed to proceed for 18 hours at 37°C. The digest was centrifuged (13,000 xg, 10 minutes). Both the soluble and the insoluble materials served as

the sources for the isolation of the labelled peptide fragments. The former component was subjected to chromatography for the recovery of the labelled peptide. The latter component was subjected to CNBr cleavage prior to its use for the isolation of the labelled peptide.

3.6.2 Isolation of the labelled peptide fragments

The isolation of the peptide fragments containing the radioactively labelled cysteine residue from either the CNBr of the tryptic digest was achieved by HPLC using a Beckman System Gold instrument. Peptides were separated on a Vydac 300Å reverse phase C4 column (5μ, 250 mm x 4.6 mm) employing a solvent system consisting of water (0.1% TFA) and acetonitrile (0.1% TFA) with a linear gradient over a period of 45 or 100 minutes. The experimental conditions were: flow rate, 0.8 ml/min, temperature, ambient and detection, absorbance at 220 nm and 280 nm. Fractions were collected using a ISCO fraction collector. Those containing the radioactivity were pooled, concentrated and purified by re-chromatography on the same matrix. The identification of the fragments bearing the radioactive label was achieved by ESMS analysis (61).

3.7 Treatment of *r*lucD with Proteases

The susceptibility of *r*lucD to proteolysis was investigated both in the presence as well as in the absence of its cofactors (NADPH and FAD) and substrate (L-lysine). The effect of three different proteolytic enzymes, TPCK-trypsin, TLCK-chymotrypsin and carboxypeptidase Y on the integrity and the catalytic function of *r*lucD was investigated by monitoring the change in the SDS-PAGE profile and lysine:N^6-hydroxylase activity.

3.7.1 Proteolysis using TPCK-trypsin

A mixture consisting of *r*lucD (14 µM) and TPCK-trypsin (7 µM) was incubated at

room temperature. FAD and L-lysine, when used in the incubation mixture was present at a final concentration of 0.5-1 mM and 5 mM, respectively, while NADPH was used at a final concentration of 1 mM. At the desired time interval, aliquots of the reaction mixture were removed and the proteolysis stopped by the addition of 2 fold molar excess of SBTI over that of trypsin. These aliquots were used for the determination of lysine:N^6-hydroxylase activity and the extent of proteolysis by SDS-PAGE.

3.7.2 Treatment with TLCK-chymotrypsin

The effect of chymotrypsin on the catalytic activity of *r*IucD was examined by a procedure similar to that employed with trypsin. At desired time intervals, aliquots of the incubation mixture were treated with PMSF to stop further proteolysis. These were used to monitor the extent of degradation and enzymatic activity of *r*IucD.

3.7.3 Reaction with carboxypeptidase Y (71)

The importance of the C-terminus of *r*IucD, for its catalytic activity, was assessed by treatment with CPD-Y. A typical reaction mixture, in a final volume of 1 ml contained the following: potassium phosphate buffer (100 mM, pH 6.0); *r*IucD (10 μM); and CPD-Y (0.3 μM). FAD, L-lysine and L-norleucine when included in the assay were used at a final concentration of 1 mM, 5 mM, 5 mM, respectively. Aliquots drawn at desired intervals were either diluted with phosphate buffer, pH 7.0 or with Tris-glycine, pH 8.8. The former samples were used for the estimation of lysine:N-hydroxylase activity and the latter for SDS-PAGE analysis.

3.8 Miscellaneous procedures

3.8.1 Preparation of TLCK-chymotrypsin

The commercial preparation of the chymotrypsinogen A was converted to chymotrypsin by treatment with trypsin under conditions documented in literature (72). The enzyme was subsequently treated with TLCK (73) to render it free of trypsin activity. Prior to use, the activity of the TLCK-chymotrypsin was assessed by using BTEE (74) as a substrate.

3.8.2 Influence of FAD on TPCK-trypsin

The ability of TPCK-trypsin to digest casein was assessed in the presence and in the absence of FAD. A solution of casein (1%) in potassium phosphate buffer (100 mM, pH 8.0) was treated with TPCK-trypsin (50 µg/ml) either in the presence or absence of FAD (1 mM) for 20 minutes at room temperature. The reaction was terminated by the addition of an equal volume of TCA (10%). After approximately 16 hours at 4°C, the suspension was centrifuged (13,000 xg, 4 °C) for 20 minutes. The supernatant was decanted and the wet weight of the pellet determined.

It is pertinent to mention that proteins which are normally insoluble in TCA become soluble upon proteolysis by endopeptidases like trypsin and chymotrypsin. The usual procedure employed for assessing the extent of proteolysis is to monitor the increase in the absorbance at 280 nm of TCA soluble material accompanying the reaction. However, this procedure could not be employed in the current study in view of the high UV-visible absorbance spectra of FAD. Hence, the degree of proteolysis was assessed on the basis of the TCA insoluble precipitate remaining after exposure to the proteolytic enzyme. Thus,

inhibition of proteolysis by effectors such as FAD would result in a larger amount of TCA insoluble precipitate relative to that found in their absence.

3.8.3 Influence of L-norleucine on CPD-Y mediated hydrolysis of furylacryloyl-L-Phe-L-Ala

The activity of CPD-Y was assessed by using the substrate, furylacryloyl-L-Phe-L-Ala (FA-Phe-Ala) (75) in the presence and absence of L-norleucine. The reaction mixture, 1 ml in volume, consisted potassium phosphate buffer (100 mM, pH 6.0), FA-Phe-Ala (1mM), and CPD-Y (50 μg/ml). The assay was initiated with the addition of CPD-Y and the reaction was followed by monitoring the decrease in the absorbance at 340 nm. L-norleucine when included in the assay was used at a final concentration of 5 mM.

3.8.4 Stability of IucD preparations at low temperatures

The stability of the *wt*IucD and *r*IucD preparations at subzero temperatures was examined by an assessment of lysine:N^6-hydroxylase activity both after 20 minutes as well as 2 weeks of storage at -80°C following its exposure to liquid nitrogen. In the case of *wt*IucD, the effect of gylcerol as a cryoprotectant was examined by its inclusion over a range of 0-43.75 % (V/V) in the medium. In the case of *r*IucD, the protein was either in 10 mM potassium phosphate, pH 7.0 containing NaCl (750 mM) or in 200 mM potassium phosphate, pH 7.0. Both these preparations were treated with gylcerol over a range of 0-37% (V/V) prior to freezing. Frozen samples were thawed at 4 °C at the desired times and aliquots were used to determine lysine:N^6-hydroxylase activity.

3.8.5 Effects of various ions on lysine:N-hydroxylase activity

A medium of ionic strength≥ 0.25 is necessary for protecting the native conformation of *r*IucD (19). Hence, an investigation of the effects of various anions (HPO_4^{2-}, SO_4^{2-} or Cl^-)

on the catalytic activity of *r*IucD was undertaken. For these experiments an aliquot (50 µl) of the enzyme solution, rendered free of chloride ions by dialysing against potassium phosphate (200 mM), was added to a typical assay medium (as described in E.4) containing the desired buffer. Thus, in the reactions used for examining the effects HPO_4^{2-}, the assay mixtures included potassium phosphate (pH 7.0) over a concentration range 100 mM to 300 mM. The reactions used for studying the influence of SO_4^{2-} ions consisted of HEPES buffer (25 mM, pH 7.0) with concentrations of Na_2SO_4 ranging from 65 mM to 260 mM. Finally, in order to study the influence of Cl^- ions, the reaction mixtures included HEPES buffer (25 mM) containing Na_2SO_4 (65 mM) and NaCl over the range of 0 mM to 600 mM. The N-hydroxylase activity of the enzyme preparation was analysed as a function of ionic strength.

4.0

RESULTS

4.1 Characteristics of *r*IucD preparation

4.1.1 Primary Structure:

The recombinant lysine:N^6-hydroxylase preparation, *r*IucD439, is expected to contain 439 amino acid residues, 13 of which arise from the N-terminal β-galactosidase segment and the rest from the iucD gene product (19). Hence, the protein is expected to have a molecular weight of 50397 Da. The above value was calculated by using a molecular weight of 48968 Da for the iucD gene product (76) and 1429 Da for the β-galactosidase peptide segment. However, a determination of the nucleotide sequence of iucD and its variants performed in connection with the studies involving site directed mutagenesis (discussed in a later section) has uncovered a few discrepancies in the data published earlier (76). These include:

(i) the triplet AGT encoding for Ser172 should be ATG, the triplet for Met;

(ii) the triplet GAT, encoding for Asp237 should actually be GAG the triplet for Glu; and (iii) the segment of nucleotide sequence 772-807, (ACTGACATCGGATGGCATCA CTGCCCGATTCTTTTA) encoding for the sequence of amino acids, TDIGWHHCPILL, should actually be (ATGACATCGGATGGCATCACTGCCGATTCTTTA) encoding for the amino acid sequence, MTSDGITADSL.

The consequences of these differences between the previously published nucleotide sequence

(76) and that determined in the current investigations are as follows:

(i) the total number of amino acid residues in the iucD gene product is 425 instead of 426 as previously recorded;

(ii) a loss in a cysteine residue resulting in only 5 cysteine residues instead of six such residues per mole of protein;

(iii) the loss of a tryptophan, two histidines, a proline, an isoleucine and a leucine residue with a concomitant gain of methionine, threonine, two serine, aspartic acid and alanine residues in the primary structure of the protein; and

(iv) a change in the molecular weight of the recombinant protein since it now contains 438 amino acid residues. Thus the molecular weight of *r*IucD preparations used in this study is expected to be 50151 Da.

The nucleotide sequence of iucD, both the one documented in the literature (76), as well as that revised on the basis of the observations in the current investigations, are presented in the Appendix C.

4.1.2 Physico-chemical properties:

SDS-PAGE analysis revealed *r*IucD preparations to be homogeneous (Figure 14). ESMS analysis indicated a molecular weight of 48810 ±5 Da (Figure 15), a value lower than the predicted value mentioned above. This observation would suggest that the protein preparation has been processed by a post-translational processing mechanism. Removal of the first twelve amino acid residues from the N-terminus of *r*IucD by a post-translational processing event would appear to be compatible with the observed molecular weight of the protein. The occurrence of such a phenomenon which leads to the deletion of the β-

Figure 14. **SDS-PAGE profile of *r*IucD preparations of the fractions recovered from the affinity matrix Orange A:**
The protein was eluted using 10 mM potassium phosphate buffer, pH 7.0, containing NaCl as indicated:
Lanes 1. 500 mM NaCl (second fraction); 2. Molecular weight standards (94 kDa, 67 kDa, 43 kDa, 30 kDa, 20.1 kDa); 3. 750 mM NaCl (first fraction); and 4. 750 mM NaCl (second fraction).

1 2 3 4

Figure 15. **ESMS analysis of *r*lucD439**

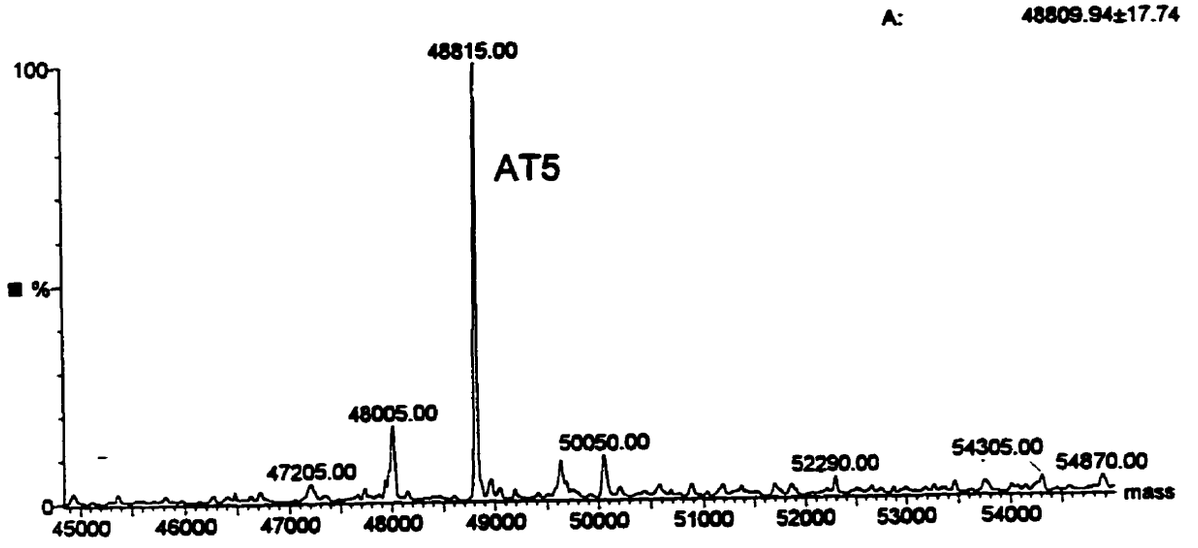
A:
48809.94±17.74
48815.00
AT5
100
%
0
48005.00
47205.00
50050.00
52290.00
54305.00
54870.00
mass
45000
46000
47000
48000
49000
50000
51000
52000
53000
54000

galactosidase peptide segment from *r*IucD has been established by the analysis of the N-terminal amino acid sequence of the protein (77).

The pH optimum of the enzyme was determined by performing assays in 25 mM HEPES containing Na_2SO_4 (150 mM) with pH values between 7 and 8. These studies indicate that the enzyme is maximally active at pH values between 7.5 and 7.8. It is pertinent to note that a high concentration of HEPES (200 mM) inhibits the enzymatic activity of *r*IucD.

4.1.3 Influence of FAD on the rate of *r*IucD mediated NADPH oxidation and lysine:N^6-hydroxylation:

Previous studies have shown that the rate of the *r*IucD catalyzed lysine:N^6-hydroxylation, which is coupled to that of NADPH oxidation, is maximal at FAD concentrations of 30-40 μM in the assay and it declines progressively with further increases in the concentration of the flavin cofactor (20). Experiments were undertaken to determine if the observed decrease in the rate of lysine:N^6-hydroxylation at elevated levels of FAD in the assay is a consequence of the process being uncoupled from that of NADPH oxidation. Hence, the rate of *r*IucD catalyzed NADPH oxidation was determined, both in the presence as well as in the absence of lysine over a range of FAD concentration in the assay, by monitoring the production of N^6-hydroxylysine and H_2O_2 respectively. As shown in Figure 16, the rate of H_2O_2 production (occurring in the absence of lysine) parallels that of N-hydroxylysine formation when lysine is present in the assay. These findings indicate that the observed decline in the rate of lysine:N^6-hydroxylation at elevated levels of FAD is not a consequence of an uncoupling of the *r*IucD mediated reactions by a mechanism based on a

Figure 16. **Production of N^6-hydroxylysine and H_2O_2 by *r*IucD:**

Assays for monitoring H_2O_2 production consisted of potassium phosphate (100 mM, pH 7.0), NADPH (200 μM), FAD (33 μM) and *r*IucD (83.3 nM). For recording N^6-Hydroxylysine production, assays were the same as above except for the inclusion of the L-lysine (1 mM). ■-■, H_2O_2 and; •-•, N^6-hydroxylysine. Inset, production of H_2O_2 and N^6-hydroxylysine over a range of FAD concentration. Assay conditions same as above except for the change in FAD concentration as shown. H_2O_2 and N^6-hydroxylysine determined as described in the text. ■-■, H_2O_2 and; •-•, N^6-hydroxylysine.

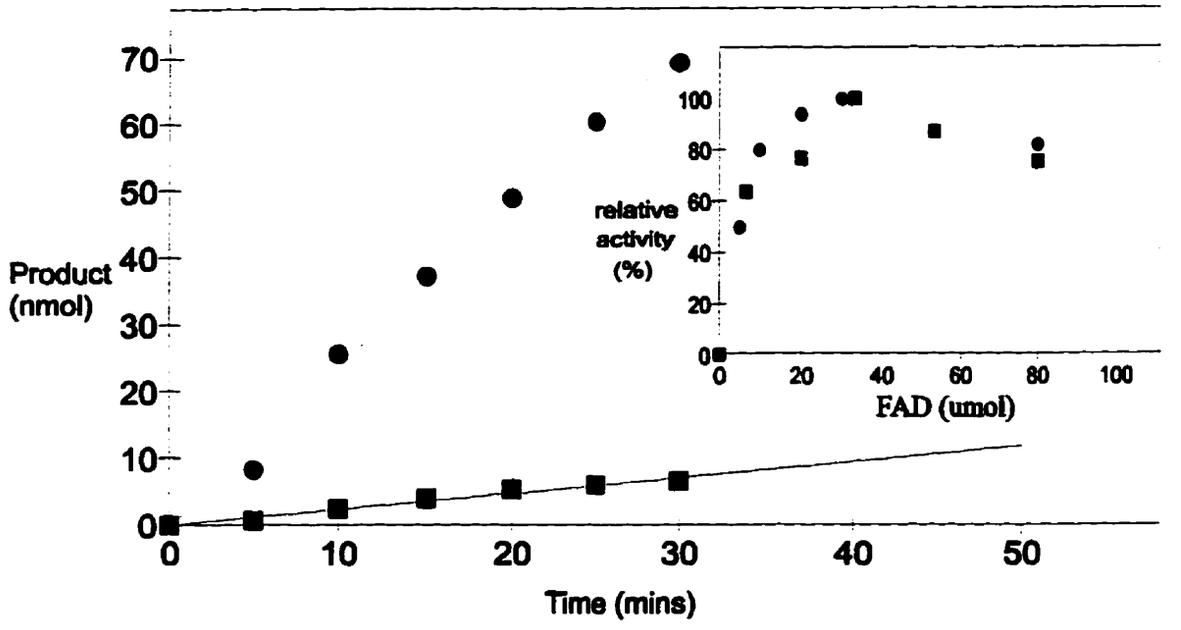
Product (nmol)
70
60
50
40
30
20
10
0
0
10
20
30
40
50
Time (mins)
relative activity (%)
100
80
60
40
20
0
0
20
40
60
80
100
FAD (umol)

reducing equivalent exchange between the enzyme bound flavin cofactor and that free in the medium (62). The occurrence of such a reducing equivalent exchange would have resulted in an enhancement in the rate of NADPH oxidation at elevated levels of FAD, a feature that would be reflected in an increase in H_2O_2 production.

4.1.4 Influence of cofactor analogs:

Both NADPH and FAD serve as obligatory cofactors in the catalytic mechanism of *r*IucD. Hence, the effect of analogs of these cofactors on the enzymatic activity of *r*IucD was investigated. These analogs included AMP, ADP, ADPR, NAD^+ and 2'-P-ADP. Among these, ADP, 2'-P-ADP and ADPR were found to serve as inhibitors of the enzyme, while AMP and NAD^+ were devoid of such activity. The adverse action of ADP and 2'-P-ADP could be reversed by increasing the concentration of FAD. In contrast, the inhibitory action of ADPR could not be overcome by an increase in the concentration of FAD in the assay. Indeed, ADPR appears to function synergistically by reinforcing the inhibitory effects observed at elevated concentrations of the flavin cofactor. These results are shown in Figure 17.

4.1.5 Proteolysis of *r*IucD:

The susceptibility of *r*IucD to proteolysis by endopeptidases and exopeptidases was investigated by monitoring both the extent of degradation by SDS-PAGE as well as of changes in the lysine:N^6-hydroxylase activity. TPCK-trypsin and TLCK-chymotrypsin served as endopeptidases while carboxypeptidases (CPD) A, B, and Y fulfilled the role of exopeptidases. Treatment of *r*IucD with either TPCK- trypsin or TLCK-chymotrypsin resulted in a rapid degradation of the protein with concomitant loss in lysine:N^6-hydroxylase

Figure 17. **Effects of analogs of FAD and NADPH on the lysine:N-hydroxylase activity of *r*IucD:**
The cofactor analogs were incubated with *r*IucD (~ 80 nM) at room temperature, for five minutes prior to assay of enzymatic activity.
A. ■-■, +ADP (4 mM); ◆-◆, without ADP
B. ■-■, +2′P-ADP (2 mM); ◆-◆, without 2′P-ADP
C. ■-■, +ADPR (2 mM); ◆-◆, without ADPR

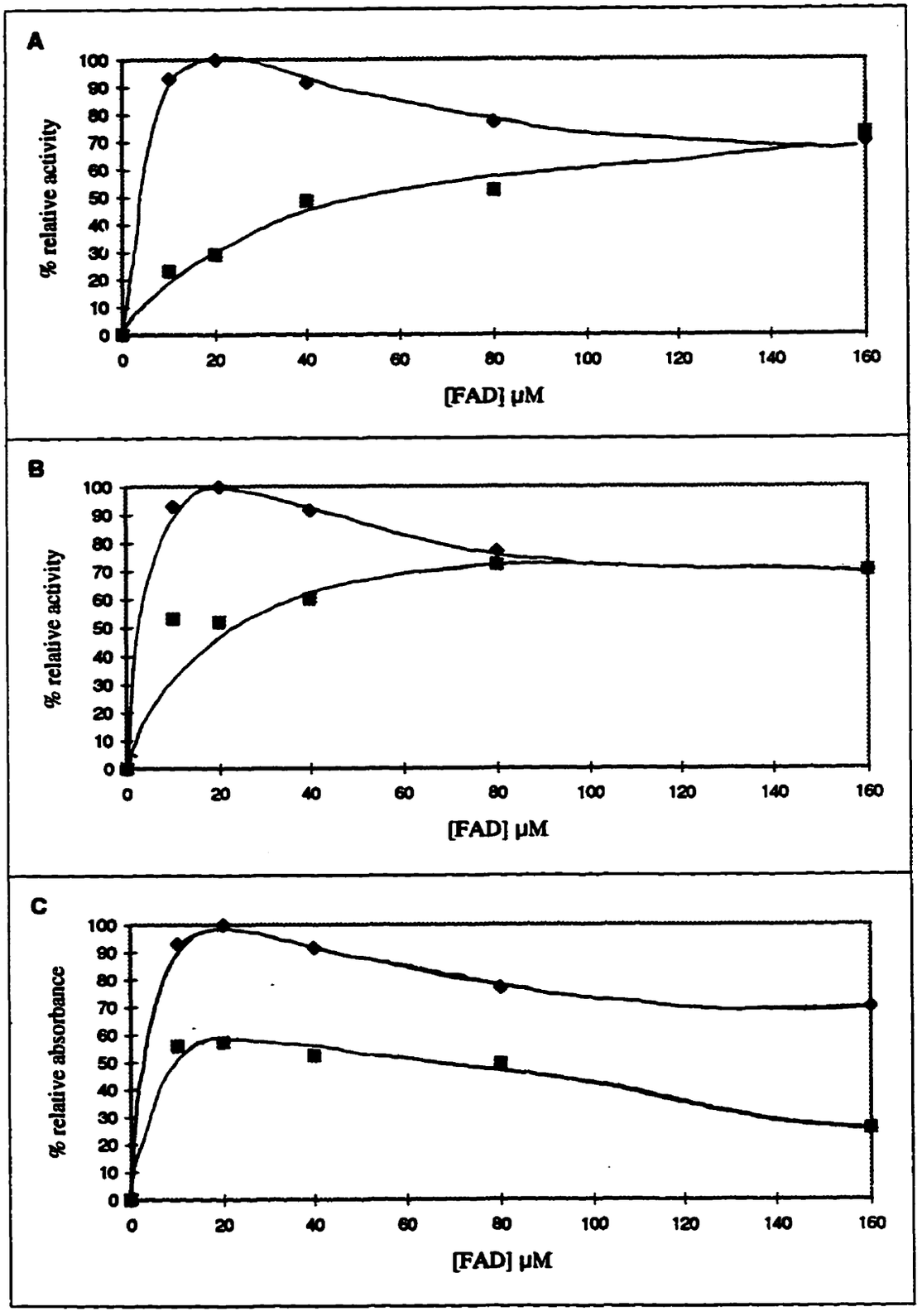
A
% relative activity
100
90
80
70
60
50
40
30
20
10
0
0
20
40
60
80
100
120
140
160
[FAD] µM
B
% relative activity
[FAD] µM
C
% relative absorbance
[FAD] µM

activity. FAD and ADP were found to protect *r*lucD from the deleterious action of these endopeptidases and in fact their presence would appear to not only stabilize but also enhance enzymatic activity of *r*lucD preparations. It is pertinent to mention that it is essential to inhibit TPCK-trypsin and TLCK-chymotrypsin by treatment with SBTI and PMSF respectively, prior to SDS-PAGE analysis to demonstrate the protective action of either FAD or ADP. Furthermore, the protective action of FAD is not due to its ability to inhibit trypsin, since the degradation of casein by this protease was not inhibited by the flavin cofactor. The results of these studies are shown in Figures 18 and 19.

Treatment of *r*lucD with CPD-A resulted in a marginal ($\leq$ 15 %) loss of enzymatic activity. This loss in enzymatic activity falls in the range of decline in the catalytic function that normally ensues upon incubation of the protein at 37°C over a period of 1-2 hours. Treatment with both CPD- A and CPD-B resulted in a relatively greater ($\approx$50 %) loss in lysine:N^6-hydroxylase activity. In contrast, treatment of *r*lucD with CPD-Y at pH 6.0 led to almost total loss of catalytic activity as shown in Figure 20. Both FAD and ADP were found to protect *r*lucD from the deleterious action of CDP-Y. Interestingly, L-norleucine was also found to prevent the deleterious effect of CPD-Y. L-norleucine was found to have no adverse effect on the CPD-Y catalyzed hydrolysis of its synthetic substrate, Furylacryloyl-L-Phe-L-Ala. Hence, it would appear that the observed protective action of L-norleucine is presumably due to its interaction with *r*lucD. The results are shown in Table 4.

Preliminary analyses of the amino acids released by the action of CPD-A or CPD-A and CPD-B or CPD-Y would appear to be consistent with the specificity features of these exopeptidases. These studies have revealed that treatment of *r*lucD with CPD-Y results in

Figure 18. **A. SDS PAGE profile of *r*IucD following treatment with TPCK-trypsin:**

rIucD (14 μM) was incubated (25°C, 12 minutes) with TPCK-trypsin (7 μM) in the presence of the substances indicated. The reactions were stopped with the addition of SBTI (15 μM) prior to analysis:

lane
1. FAD (0.5 mM)
2. ADP (1.0 mM)
3. $NADP^+$ (1.0 mM)
4. L-lysine (5 mM)
5. L-norleucine (5 mM)
6. none
7. control (trypsin added after SBTI)
8. molecular weight standards

B. Vertical bar graph representation of lysine:N^6-hydroxylase activity of *r*IucD following treatment with TPCK-trypsin:

The lysine:N^6-hydroxylase activity was assayed after the addition of SBTI as mentioned in Figure 18A. Bars 1 to 7 correspond to the respective lanes in Figure 18A.

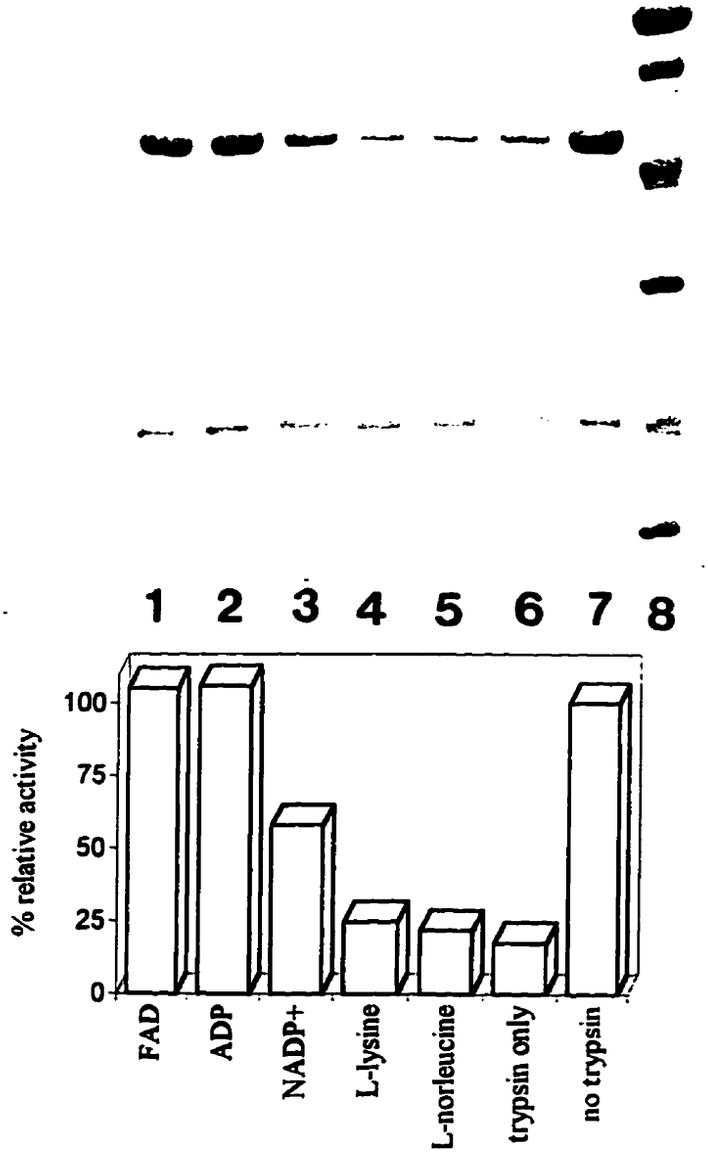
1 2 3 4 5 6 7 8
% relative activity
100
75
50
25
0
FAD
ADP
NADP+
L-lysine
L-norleucine
trypsin only
no trypsin

Figure 19. **SDS profile illustrating the effects of FAD on the proteolytic treatment of *r*lucD with TLCK-chymotrypsin:**

*r*lucD (13 μM) was treated with TLCK-chymotrypsin (11 μM) in the presence or absence of FAD (0.5 mM). At desired time intervals the reaction was stopped with the addition of PMSF.

lane 1. molecular weight standards
2. *r*lucD + chymotrypsin + FAD (0.5 mM) after 0 mins
3. *r*lucD + chymotrypsin + FAD (0.5 mM) after 20 mins
4. *r*lucD + chymotrypsin + FAD (0.5 mM) after 40 mins
5. *r*lucD + chymotrypsin after 0 mins
6. *r*lucD + chymotrypsin after 20 mins
7. *r*lucD + chymotrypsin after 40 mins
8. molecular weight standards

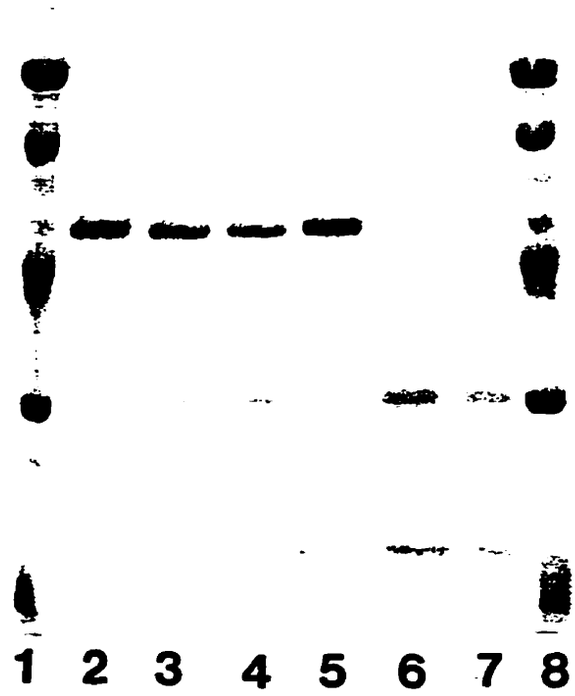
1 2 3 4 5 6 7 8

Table 4. **Carboxypeptidase Y-catalysed proteolysis of *r*IucD:**
Influence of substrate cofactors and their analogs.
*r*IucD (10 μM) was treated with CPD-Y (0.3 μM) at 37°C in 200 mM potassium phosphate, pH 6.0. After 2 hours, the emzyme mixture was assayed for lysine:N^6-hydroxylase activity.

Treatment	Relative activity (%)
none	100
CPD-Y	8
CPD-Y + FAD (1 mM)	139
CPD-Y + ADP (1 mM)	114
CPD-Y + AMP (1 mM)	46
CPD-Y + NADPH (1 mM)	7
CPD-Y + L-lysine (5 mM)	11.2
CPD-Y + L-norleucine (2 mM)	50.2
CPD-Y + L-norleucine (5 mM)	85.8

Figure 20. **The effect of carboxypeptidase Y on the Lysine:N^6-hydroxylase activity of *r*IucD:** *r*IucD (10 μM) was treated with CPD-Y (0.3 μM) at 37°C in 200 mM potassium phosphate, pH 6.0. After specific time intervals, the reaction was stopped by diluting the reaction mixture by (1:1000) into 200 mM potassium phosphate, pH 7.0.

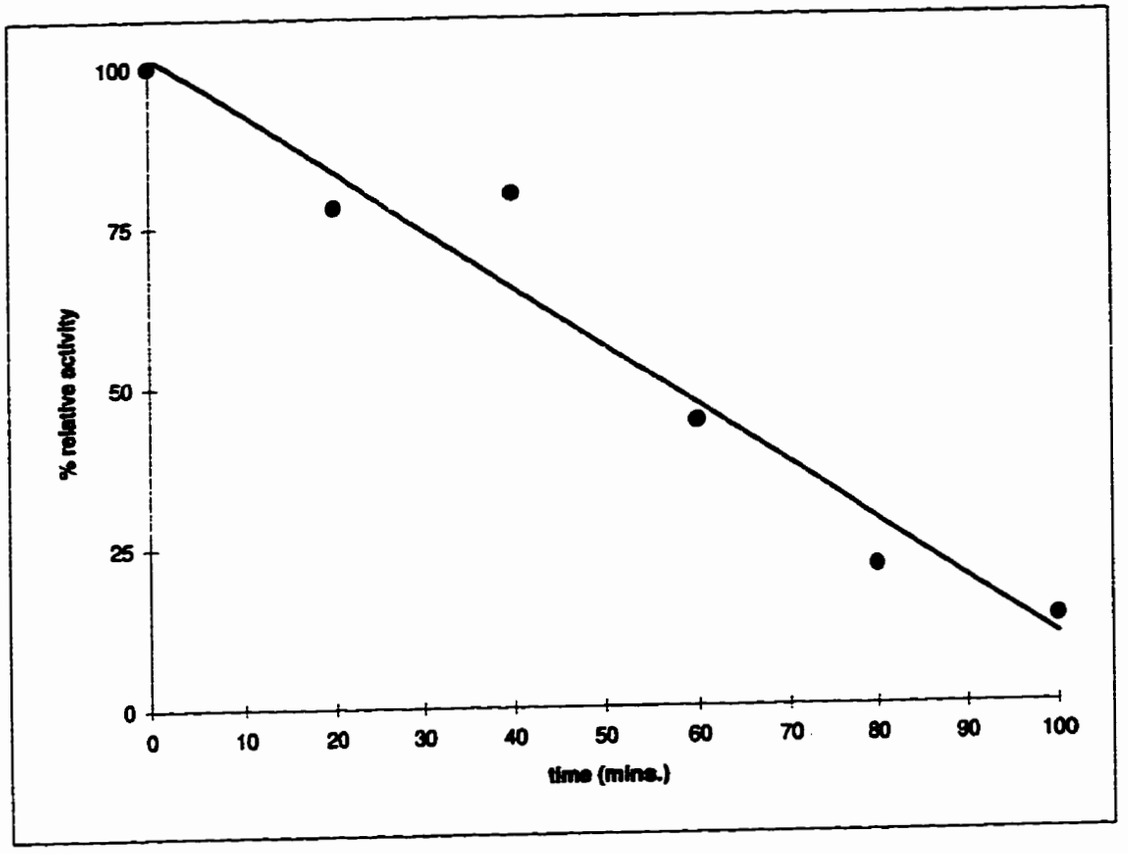
100
75
50
25
0
% relative activity
0
10
20
30
40
50
60
70
80
90
100
time (mins.)

the deletion of 12-13 C-terminal amino acid residues from the protein.

4.1.6 Attempts to produce truncated *r*IucD preparations:

The rapid loss of catalytic activity of *r*IucD upon treatment with CPD-Y suggests that the C-terminal segment of the protein may play a significant role in the promotion and maintenance of the conformation essential for the catalytic function(s) of the protein. In order to gain further insight into this aspect of the protein, attempts were made to produce truncated *r*IucD preparations by expression of iucD with a deletion mutation that would lead to removal of 27 amino acid residues from the C-terminus of its product. The incorporation of a deletion mutation in iucD was achieved by changing the triplet CGT encoding for Arg400 to TGA, a termination triplet, by site directed mutagenesis using the complementary primers shown in Table 3. The introduction of an *Eco*R I site accompanying this deletion mutation in iucD provided a means for assessing the success in the incorporation of the desired mutation. Indeed, the results obtained upon treatment of the plasmid carrying this iucD variant with *Eco*R I are those that can be expected of a termination codon, TGA, in a location that normally encodes for Arg400 in the parent iucD (Figure 21). This was further confirmed by nucleotide sequencing. However, *E. coli* cells transformed with the plasmid bearing this iucD variant were found to be incapable of producing N^6-hydroxylysine, a feature that is characteristic of cells transformed with plasmid carrying the parent iucD gene. Hence, it would appear that the C-terminal segment of IucD is important for the maintenance of the protein in a biologically, active conformation.

Figure 21. **Restriction enzyme analysis of Arg400stop *r*iucD mutation:**

E.coli cells were transformed with the Arg400stop *r*iucD constructs and streaked on LB agar plates containing ampicillin (100 mg/L). Two colonies were selected and analysed for the plasmid containing the Arg400stop mutation.

Plasmids (1.25 μg) were treated with *Eco*R I (14 units) for 12 hours at 37°C. Controls were incubated in similar buffer solutions without *Eco*R I.

lanes:
1. Arg400stop *r*iucD #1, control
2. Arg400stop *r*iucD #1, *Eco*R I digest
3. Arg400stop *r*iucD #2, control
4. Arg400stop *r*iucD #2, *Eco*R I digest
5. molecular weight standards, λ /*Hin*d III
6. *r*IucD (pAT5), control
7. *r*IucD (pAT5), *Eco*R I digest
8. molecular weight standards

λ DNA /*Hin*d III digest: standard weights (kilobase pairs)
23.130, 9.416, 6.557, 4.361, 2.322, 2.027, 0.564 and 0.125

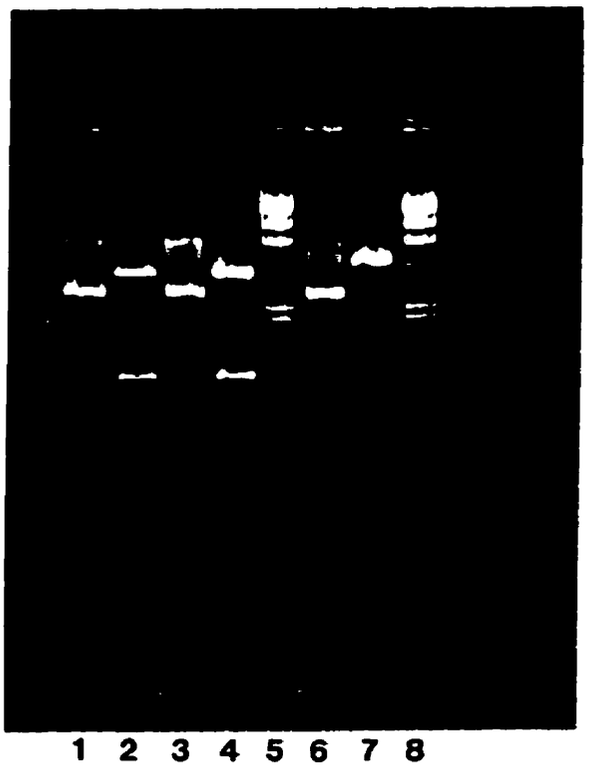
1 2 3 4 5 6 7 8

4.1.7 Influence of anions:

The final step in the purification of *r*IucD involves chromatography on Dyemātrex Orange A, and the lysine:N^6-hydroxylase activity is usually recovered in the fractions eluted with buffer containing high concentrations of NaCl (750 mM). Although *r*IucD has been found to be capable of its normal catalytic function of lysine:N^6-hydroxylation at concentrations of Cl^- ions ≤ 50 mM (a situation that prevails under assay conditions) a comprehensive study of the effect of these anions was initiated in view of their adverse action on a number of flavin dependent monooxygenases (78-81). Such information may prove useful in identifying the conditions that would promote the maintenance of *r*IucD in its native conformation, a prerequisite for the production of protein crystals in order to elucidate its three dimensional structure. Hence, the enzymatic activity was assessed as a function of increasing concentration of chloride ions in the assay. These results were compared with those obtained in the experiments performed in the presence of either phosphate or sulfate ions under conditions of identical ionic strength. As shown in Figure 22, the enzymatic activity of *r*IucD is not influenced by increases in either phosphate or sulfate ions. In contrast, the catalytic activity of *r*IucD declines steadily with increasing concentration of Cl^- ions in the assay, with almost complete loss of activity noted at 600 mM concentration of the anion. Since enzymatic activity is regained upon dilution (to 50 mM or less), *r*IucD would appear to be in a reversible, inactive conformation in a medium high in NaCl concentration (600 mM).

The destabilizing influence of Cl^- ions is further indicated by the observation that *r*IucD in a medium containing NaCl (≈600 mM) loses >75% of its enzymatic activity upon

Figure 22. **Effects of ionic strength on the activity of lysine N^6-hydroxylase:**
Assays for *r*IucD mediated lysine:N^6-hydroxylation are performed routinely in a medium of ionic strength ≈0.2 so as to maintain the enzyme in a catalytically functional oligomeric state. In this series of experiments, an ionic strength of approximately 0.2 was obtained by adding either Na_2SO_4 to HEPES buffer or by adding 100 mM potassium phosphate buffer. Additional increases in ionic strength were obtained by addition of KH_2PO_4 (■), Na_2SO_4 (●), and NaCl (▲).

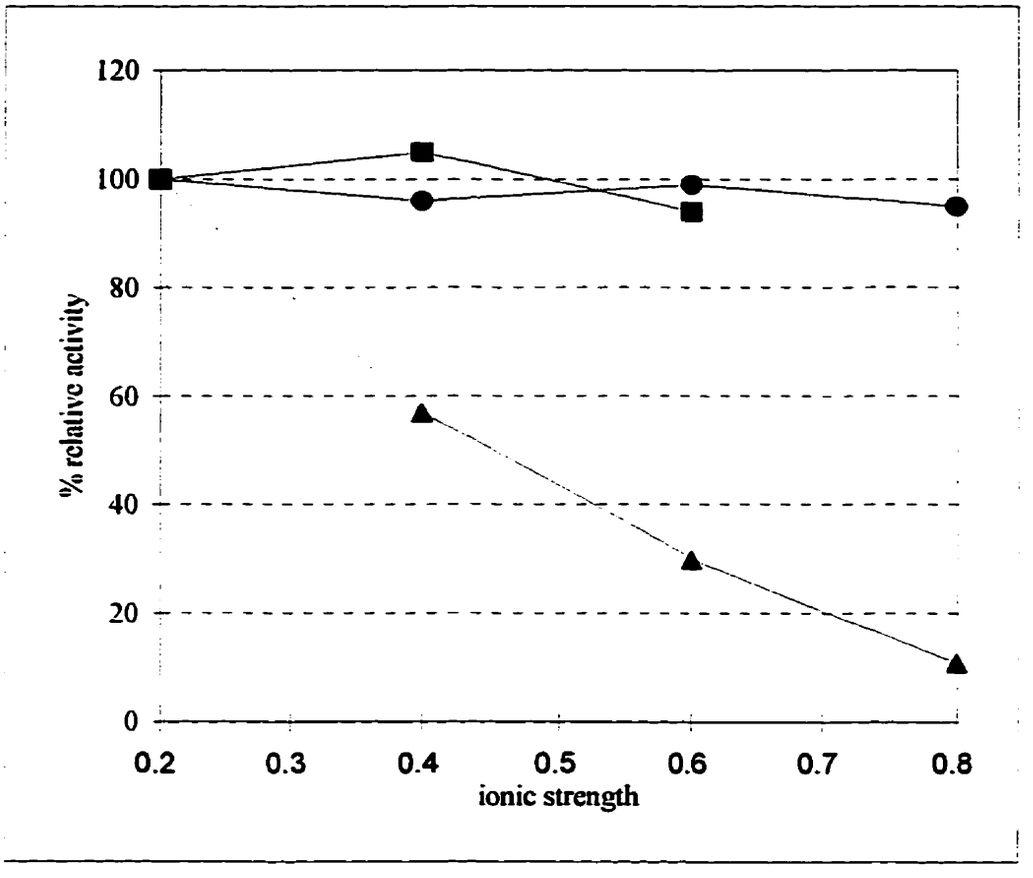
120
100
80
60
40
20
0
% relative activity
0.2
0.3
0.4
0.5
0.6
0.7
0.8
ionic strength

freezing in liquid nitrogen while similar treatment performed in the presence of phosphate ions (200 mM) results in the retention of >70% catalytic function (Figure 23). The deleterious effect associated with the freezing of the protein in the presence of Cl^- ions could, to a large extent, be overcome by the inclusion of glycerol (10-30 %) in the medium. Similar studies with *wt* (membrane bound) IucD indicate that the cryoprotective ability of glycerol is maximal at a concentration of approximately 10 % in the medium. Further increases in the concentration of glycerol results in a progressive decline in its ability to serve as a cryoprotectant (Figure 24).

During storage at pH 7.0, in a medium of high ionic strength, the enzymatic activity of *r*IucD declines steadily and this can be restored by treatment with thiols like DTT (1 mM) indicating that thiol functions may be involved in the catalytic mechanism of the protein.

4.2 Specificity of *r*IucD

Previous studies have shown that L-lysine and (S)-2-aminoethyl-L-cysteine are the only compounds that serve as substrates for *r*IucD (19,20). Hence, a systematic study with analogs of L-lysine was undertaken to gain an insight into the structural features governing the specificity of the enzyme with respect to its hydroxylatable substrate. The compounds chosen for these studies share certain structural features inherent in L-lysine, which consists of a positively charged amino group (A) at the α-carbon as well as a negatively charged carboxyl group (B) at the same position. Furthermore, L-lysine is characterized by a hydrophobic carbon side chain comprised of four methylene groups ($C_{n,}$ where n = 4), and a positively charged amino group at the end of this chain (D) (Figure 25). In addition, some compounds were also chosen in view of their documented ability to interact with lysine

Figure 23. **Effects of freezing on the lysine:N^6-hydroxylase activity of *r*IucD:**

The *r*IucD preparation in either 10 mM potassium phosphate buffer, pH 7.0, containing NaCl (≈600mM), or 200 mM potassium phosphate buffer, pH 7.0, was frozen in liquid nitrogen, in the presence of glycerol at concentrations indicated. After 20 minutes, the samples were thawed on ice and aliquots were used to determine lysine N^6-hydroxylase activity.

■-■, *r*IucD in 200 mM potassium phosphate buffer, pH 7.0;
▲-▲, *r*IucD in 10 mM potassium phosphate buffer, pH 7.0, containing NaCl (≈600mM)

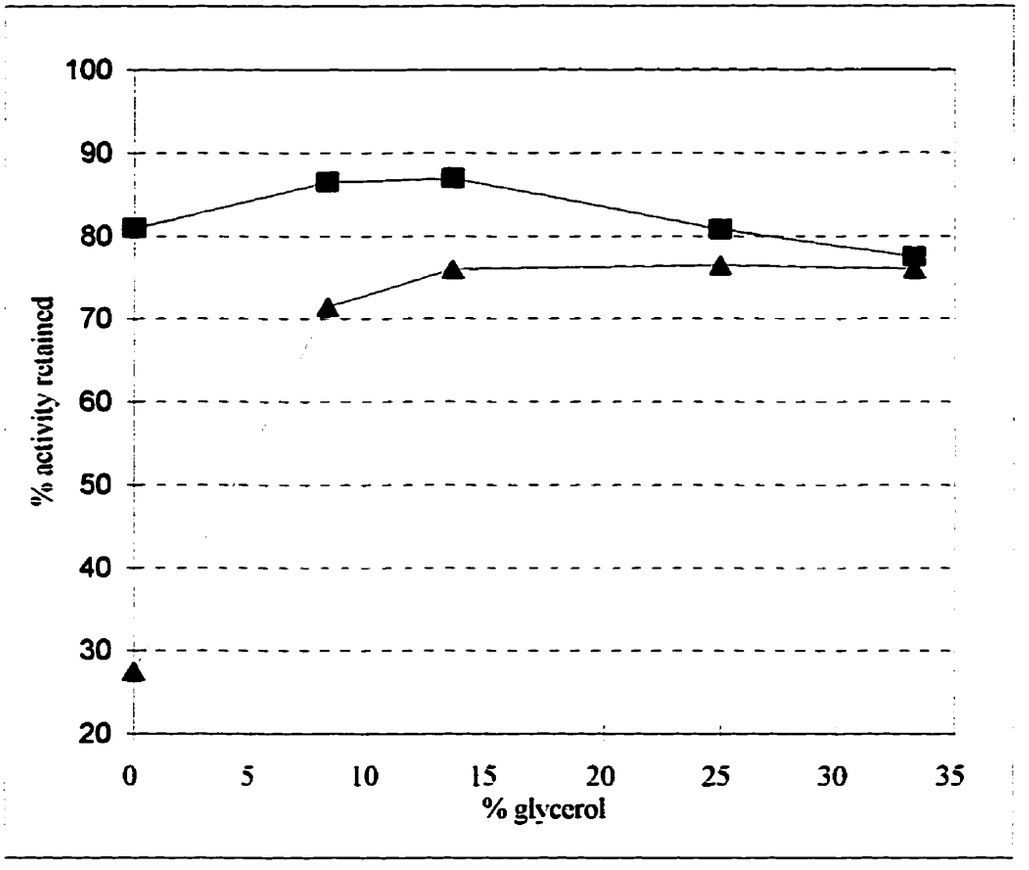
100
90
80
70
60
50
40
30
20
% activity retained
0
5
10
15
20
25
30
35
% glycerol

Figure 24. **Effects of freezing on the lysine:N6-hydroxylase activity of *wt*IucD:**
The *wt* enzyme preparation (15,16) in 10 mM potassium phosphate, pH 7.0, containing glycerol (as indicated) was frozen in liquid nitrogen. After 20 minutes, the samples were thawed on ice and an aliquot was used for the determination of lysine:N^6-hydroxylase activity.

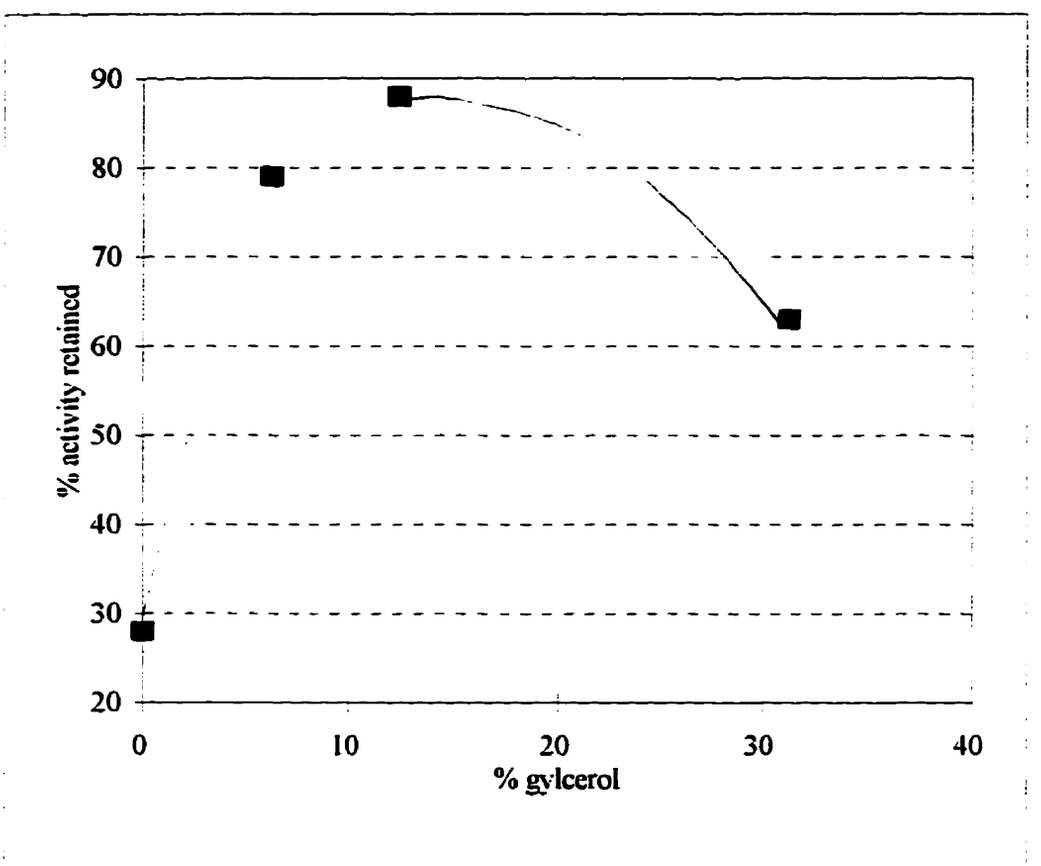
90
80
70
60
50
40
30
20
% activity retained
0
10
20
30
40
% glycerol

Figure 25. **Structural features inherent in L-lysine:**
A and **D** represent the positively charged amino acid group at the α and ϵ carbon, respectively. **B** symbolizes the negatively charged α-carboxyl function. $\mathbf{C_n}$ represents the hydrophobic side chain comprised of four methylene groups (**n** = 4).

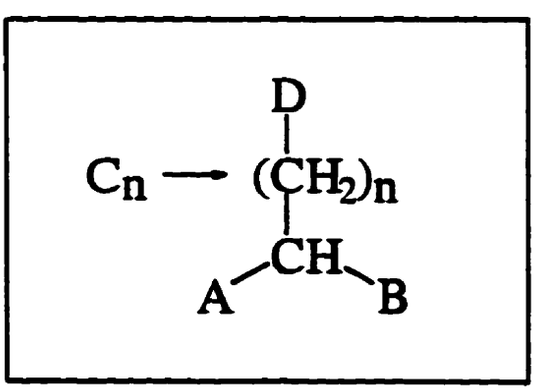
D
Cn
(CH2)n
CH
A
B

binding domains in other proteins. This latter class includes; (I) tranexamic acid (*trans*-4-(aminomethyl)-cyclohexanecarboxylic acid) and ϵ-aminocaproic acid, compounds known to bind lysine specific kringles in plasminogen (82); and (ii) benzamidine as well as p-aminobenzamidine which serve as inhibitors of trypsin (83), a protease with remarkable specificity for lysine (and arginine) substrates (84). The structures of some of these compounds are given in Figure 26.

As indicated in Table 5, lysine:N^6-hydroxylase would appear to be stringently specific with regard to its substrate. The substitution of the methylene group at the γ-position by a sulfur would appear to have no deleterious effect since (S)-2-aminoethyl-L-cysteine can still function as a substrate for the enzyme. Neither (S)-2-aminoethyl-DL-homocysteine (one additional methylene group) nor L-ethionine and S-propargyl-L-cysteine, which are devoid of the ϵ-amino function present in lysine, has been found to serve as potent substrates/inhibitors of *r*IucD. The importance of the presence of an unmodified ϵ-amino group gains further support from the observation that neither ϵ-N-methyl-L-lysine nor ϵ-N-acetyl-L-lysine is capable of serving as a substrate for the enzyme. However, methylation of L-lysine at the α-amino function (A) allows the analog to promote NADPH-oxidation as well as to serve as a substrate of lysine:N^6-hydroxylase, although only 20% as effective as the preferred substrate. These observations show that a free, unmodified α-amino group in the substrate is not absolutely necessary for hydroxylation by *r*IucD, whereas the modification of its ϵ-amino function leads to a total loss of such activity, suggesting the detrimental nature of any type of modification at this location. Even the presence of a carboxyl group in the vicinity of the ϵ-amino group, as in the case of α,ϵ-diaminopimelic acid, renders the compound incapable of

Figure 26. **Chemical structures of L-lysine and various substrate analogs of *r*lucD:**

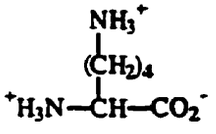

Lysine

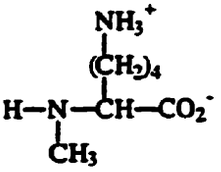

α-N-Methyllysine

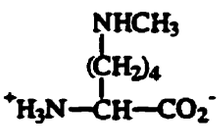

ε-N-Methyllysine

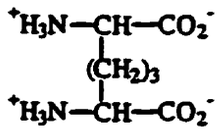

α,ε-Diaminopimelic acid

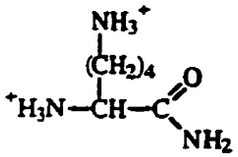

Lysineamide

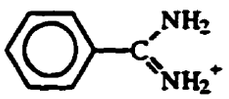

Benzamidine

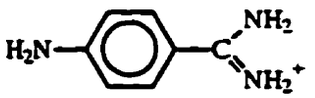

p-Aminobenzamidine

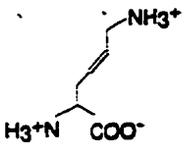

trans-4,5-dehydro-L-lysine

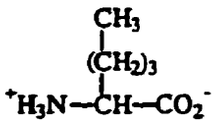

Norleucine
(HNleOH)

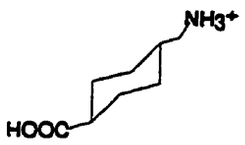

tranexamic acid

Table 5: Influence of various effectors on the enzymatic activity of *r*IucD

[a] All compounds listed below were purchased from Sigma Chem. Co., except α-N-methyl-L-lysine, trans-4,5-dehydro-L-lysine, (S)-aminoethyl-DL-homocysteine, and S-propargyl-L-cysteine (see Materials and Methods).

[b] The structural features of the effectors (A, B, C_n, D) are illustrated in Figure 26. The subscript n indicates the number of methylene groups present in the hydrophobic side chain of these compounds.

[c] The enzymatic activity of *r*IucD was determined as described earlier (Methods). The concentration of the effectors was 1 mM unless further specified.

[d] $C_\gamma H_2$ replaced by sulfur.

[e] $C_\delta H_2$ replaced by sulfur.

[f] $C_\gamma H_2$-$C_\delta H_2$ replaced by $C_\gamma H$=$C_\delta H$ (*trans*-conformation).

Effector[a]	Structural features[b]				Lysine:N^6-hydroxylase activity (%)[c]	
	A	B	C_n	D	+ L-Lysine	- L-Lysine
None					100	0
(S)-2-aminoethyl-L-cysteine	NH_3^-	CO_2^-	4[d]	NH_3^-	105	100
α-N-methyl-L-lysine	$NHCH_3$	CO_2^-	4	NH_3^-	103	21
D-lysine	NH_3^-	CO_2^-	4	NH_3^-	100	0
ε-N-methyl-L-lysine	NH_3^-	CO_2^-	4	$NHCH_3$	93	0
ε-N-acetyl-L-lysine	NH_3^-	CO_2^-	4	$NHCOCH_3$	100	0
DL-α-aminocaprylic acid	NH_3^-	CO_2^-	5	CH_3	100 (2 mM)	0
L-ethionine	NH_3^-	CO_2^-	4[e]	CH_3	85	n.d.
trans-4.5-dehydro-L-lysine	NH_3^-	CO_2^-	4[f]	NH_3^-	100	0
6-aminocaproic acid	H	CO_2^-	4	NH_3^-	100	0
L-lysineamide	NH_3^-	$CONH_2$	4	NH_3^-	100 (2 mM)	0
L-lysinemethylester	NH_3^-	CO_2CH_3	4	NH_3^-	100	0
1.6-diaminohexane	NH_3^-	H	5	NH_3^-	100	0
(S)-aminoethyl-DL-homocysteine	NH_3^-	CO_2^-	5[b]	NH_3^-	80	0
α.ε-diaminopimelic acid	NH_3^-	CO_2^-	3	$CH(NH_3^-)(CO_2^-)$	95	0
L-ornithine	NH_3^-	CO_2^-	3	NH_3^+	100	0
L-arginine	NH_3^+	CO_2^-	3	$NHC(NH_2)_2^+$	100	0
S-propargyl-L-cysteine	NH_3^-	CO_2^-	3[a]	C≡CH	100	n.d.
2.4-diaminobutyric acid	NH_3^-	CO_2^-	2	NH_3^-	100 (2 mM)	0

interacting with the enzyme.

Alteration in the site B of the substrate, either by a deletion of the carboxyl group (as in 1,6-diaminohexane) or by its modification (as in lysine amide or lysine methylester) results in a total loss of the ability to undergo the *r*IucD mediated hydroxylation.

The importance of the flexible hydrophobic backbone consisting of four methylene groups is emphasized by the observation that analogs with identical structural features (A, B, and D) but a change in the number of methylene groups in the side chain (as in L-2,4-diaminobutyric acid, L-ornithine, and (S)-2-aminoethyl-DL-homocysteine) do not serve as either substrates or inhibitors of *r*IucD to any significant extent. Hence, a C_4 chain length appears to be absolutely essential for a compound to function as a substrate, with a replacement of the methylene group at the γ-position by sulfur as in (S)-2-aminoethyl-L-cysteine being tolerated. Furthermore, a decrease in the flexibility of the hydrophobic side chain of the substrate, as in the case of *trans*-4,5-dehydro-L-lysine, results in a total loss of both the ability to promote NADPH-oxidation as well as to undergo hydroxylation. Moreover, none of the other compounds, benzamidine, p-aminobenzamidine as well as tranexamic acid, is utilized as a substrate by lysine:N^6-hydroxylase, providing further support for the essential role of a flexible hydrophobic backbone. It is pertinent to note that the small extent of inhibition observed in a few instances would appear to fall in the range of the experimental error of the assays based on either lysine:N^6-hydroxylation or NADPH-oxidation.

L-norleucine, a compound characterized by its C_4 hydrophobic side chain has been found to be the best effector of *r*IucD, inhibiting both NADPH-oxidation as well as

lysine:N^6-hydroxylation. L-norleucine analogs, such as L-α-aminobutyric acid, L-norvaline, and DL-α-aminocaprylic acid, which differ in the number of methylene groups present in the hydrophobic side chain, fail to exert any adverse effect on the reaction mediated by *r*IucD (Tables 5 and 6), providing further evidence for the stringent specificity of the enzyme for a C_4 backbone.

4.3 Cysteine residues in *r*IucD

Two approaches were employed for the estimation of the number of free thiol functions in *r*IucD. The first one involved the reaction of the protein with either DTNB or NTCB. Treatment of *r*IucD with DTNB or NTCB at pH 8.0 under conditions that ensure the maintenance of the protein in its native conformation results in the modification of approximately three cysteine residues per mole of protein. Of these, two are modified rapidly (reaction being complete in ≈ 10 seconds) while the third is slow to undergo modification requiring 2-3 minutes for completion of the reaction (The data are illustrated in Figure 27). Similar experiments performed in the presence of guanidine hydrochloride (4.0 M) indicate that approximately 5 thiol groups present in *r*IucD react rapidly with DTNB (reaction time ≤ 15 seconds).

The second approach to determine the number of free sulfhydryl groups pertains to an assessment of the cysteine residues accessible to alkylation upon treatment with [^{14}C]iodoacetate. Under nondenaturing conditions, treatment of *r*IucD with the alkylating agent at pH 7.0 for 20 minutes results in the incorporation of radioactive label which corresponds to a modification of approximately two cysteine residues (actual value 1.8 ±0.2) per mole of protein. Extending the time of the reaction to 40 minutes does not lead to any

Table 6: Influence of norleucine and its analogs on the catalytic function of *r*lucD[1]

[1] The relative activity of lysine:N^6-hydroxylation and NADPH-oxidation was determined as documented earlier (Methods). The concentration of the desired compound was 1 mM in the case of lysine:N^6-hydroxylation, and 5 mM in NADPH-oxidation experiments. NADPH oxidation was measured by observing the decrease in absorbance at 340 nm.

effector	**relative activity of lysine:N^6-hydroxylation (%)**	**relative activity of NADPH oxidation (%)**
None	100	100
L(+)-norleucine	50	18
L-norvaline	100	100
L-α-aminobutyric acid	100	100
DL-norleucine	75	n.d.

Figure 27. **Reaction of *r*IucD with DTNB:**
The *r*IucD preparation in one ml of 200 mM potassium phosphate, pH 8.0 was treated with an aliquot (100 μl) of DTNB (5 mM) and the progress of the reaction was monitored at 412 nm. After correction for the spontaneous hydrolysis of the reagent, ΔA values at 412 nm, at various intervals of the reaction, were used to determine the number of thiol group(s) modified per monomer of the protein.

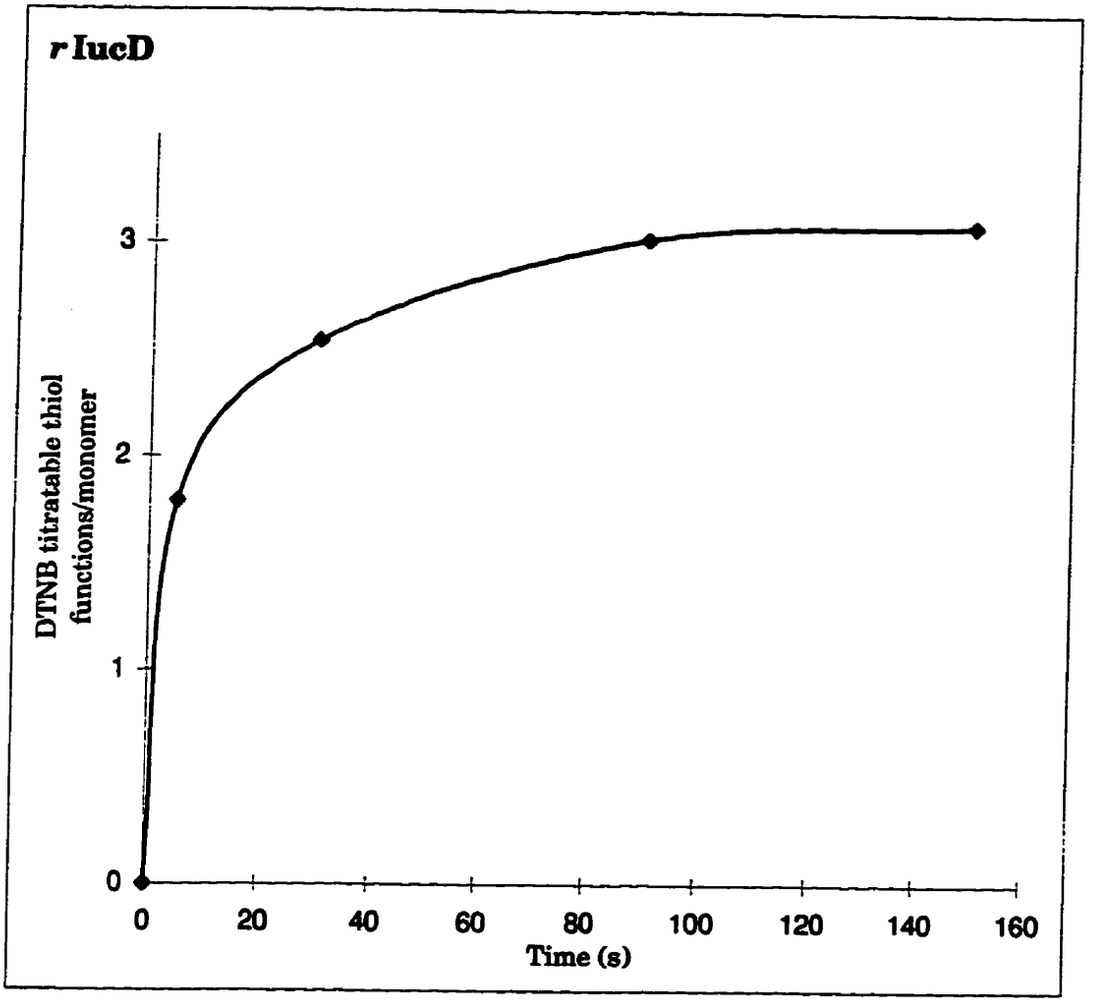
rIucD
DTNB titratable thiol functions/monomer
0
1
2
3
0
20
40
60
80
100
120
140
160
Time (s)

increase in the alkylation of the protein. Interestingly, similar experiments performed in the presence of FAD (1 mM) results in the modification of approximately one cysteine residue per mole of protein. Such modification of the thiol function in the presence of FAD also results in the loss of N-hydroxylase activity. When alkylation experiments were performed under denaturing conditions, approximately 4.8 ± 0.2 cysteine residues per mole of protein were found to be modified. These results are presented in Table 7.

4.3.1 Location of exposed thiol functions of *r*IucD:

The results presented in the previous section indicate that three of the cysteine residues present in *r*IucD are accessible to modification by DTNB in the native conformation of the protein and hence can be regarded to contribute to the "exposed" thiol functions in the protein. In contrast, alkylation of the protein with iodoacetate under identical conditions has revealed that only two of the cysteine residues are accessible to modification. In order to determine the location of these "exposed" thiol functions, *r*IucD preparations alkylated with [^{14}C] iodoacetate were treated with either CNBr or TPCK-trypsin to generate peptide fragments of the protein.

In the former instance, following removal of the excess CNBr and formic acid after cleavage, attempts were made to re-dissolve the residue in water (pH 7.0 - 9.0). Most of the material remained insoluble, presumably due to aggregation of the peptide fragments. However, the radioactive label was found to be distributed equally in the soluble and insoluble fractions. The soluble fraction was subjected to ultrafiltration with a 3 kDa cut off membrane. Under these conditions all of the radioactive label was found to be in the filtrate. The only cysteine containing peptides that are less than 3 kDa are the fragments

Table 7. **Reactivity of Thiol Functions of IucD:**
The thiol groups of *r*IucD were estimated by titration with DTNB or alkylation with [^{14}C]ICH_2COOH. The protein preparation was routinely maintained in the presence of DTT (1 mM). In the case of reaction with DTNB, the DTT was removed by chromatography on a 1x10 cm column of Biogel P4 with 200 M potassium phosphate, pH 8.0 serving as equilibration and elution medium.

For the native conformation of *r*IucD, the reaction mixture consisted of 200 mM potassium phosphate, pH 8.0 for DTNB or 200 mM potassium phosphate, pH 7.0 for ICH_2COOH. The "fast" thiol groups were modified within 10 seconds after the addition of DTNB where as the "slow" thiol functions were modified after 2-3 minutes. For the denatured form of *r*IucD, conditions were similar to that stated above except for the inclusion of guanidine hydrochloride (4.0 M).

DPIP-*r*IucD is the *r*IucD preparation covalently modified with DPIP as discussed in a later section 4.4.1.

The values represent an average of at least three determinations.
n.d. = not determined

Sample	Condition	Mole of thiol groups modified per mole of *r*IucD		Probable thiol functions modified per mole *r*IucD	
		DTNB	ICH_2COOH	DTNB	ICH_2COOH
*r*IucD	Native	1.9 ± 0.1 (fast) 1.2 ± 0.1 (slow)	1.8 ● 0.2	3	2
	Denatured	5.05 ± 0.27	4.8 ± 0.2	5	5
DPIP-*r*IucD	Denatured	2.89 ± 0.28	n.d.	3	n.d.

corresponding to amino acid sequences 47-53 and 163-172 with molecular weights 824 and 1198 Da, respectively (see Appendix D).

In order to gain unequivocal information regarding the cysteine residues susceptible to alkylation, the S-carboxymethyl *r*lucD preparation was subjected to degradation with TPCK-trypsin (for details see Methods, section 3.5). The insoluble component in the digest was recovered by centrifugation (13000 x g). Analysis revealed the presence of the radioactive label in both the insoluble and the soluble fractions of the digest. The insoluble component was subjected to CNBr cleavage. After removal of excess CNBr and formic acid, the material was subjected to HPLC. Fractions containing radioactive label were pooled and concentrated. ESMS analysis of the radioactive fraction indicated the presence of a major component (824 Da) and a minor component (842 Da) as shown in Figure 28. The molecular weight of the former would be compatible with the peptide segment 47-53 corresponding to the amino acid sequence, LVPDCHM, with homoserine lactone at the C-terminus (a feature expected of peptides generated by CNBr cleavage). The latter, minor component corresponds in molecular weight to that of the same peptide as above with homoserine at the C-terminus.

The soluble component of the tryptic digest was likewise subjected to HPLC. The profile of the peptides present are shown in Figure 29. Fractions containing radioactive label were pooled and resubjected to HPLC to obtain a relatively homogeneous preparation of the labelled peptide. ESMS analysis revealed the labelled peptide to be characterized by a mass of 1102 ± 2 Da, a value compatible with the peptide segment 152-160, corresponding to the amino acid sequence, QPYLPPCVK (Appendix E). These observations show that cysteine

Figure 28. **Chromatographic profile of the peptides produced upon CNBr treatment of the insoluble fraction of tryptic digest of S-carboxymethyl *r*IucD:**

The *r*IucD preparation alkylated with [^{14}C]-ICH_2COOH was digested with TPCK trypsin. Both the soluble and insoluble components of the digest were found to contain the readioactive label. *Inset*: The latter component was treated with CNBr and the resulting material was subjected to HPLC using a Vydac 214TP54 (C4, 5μ, 4.6 x 250 mm) 300 Å reverse phase column. Solvent: H_2O (0.1 % TFA) and CH_3CN (0.1 % TFA), a linear gradient over a period of 45 minutes. Flow rate, 0.8 ml/min; temperature, ambient; and detection 224nm. Fractions containing the radioactive label were collected. *Main figure*: ESMS spectra of the labelled peptide fragment indicated by the arrow in Figure 28, inset. The mass of the peptide corresponds to the segment 47-52 with the amino acid sequence. Further confirmation of the identity of the peptide was achieved by the analysis of the fragmentation pattern using $(MS)^2$ protocol (Appendix E).

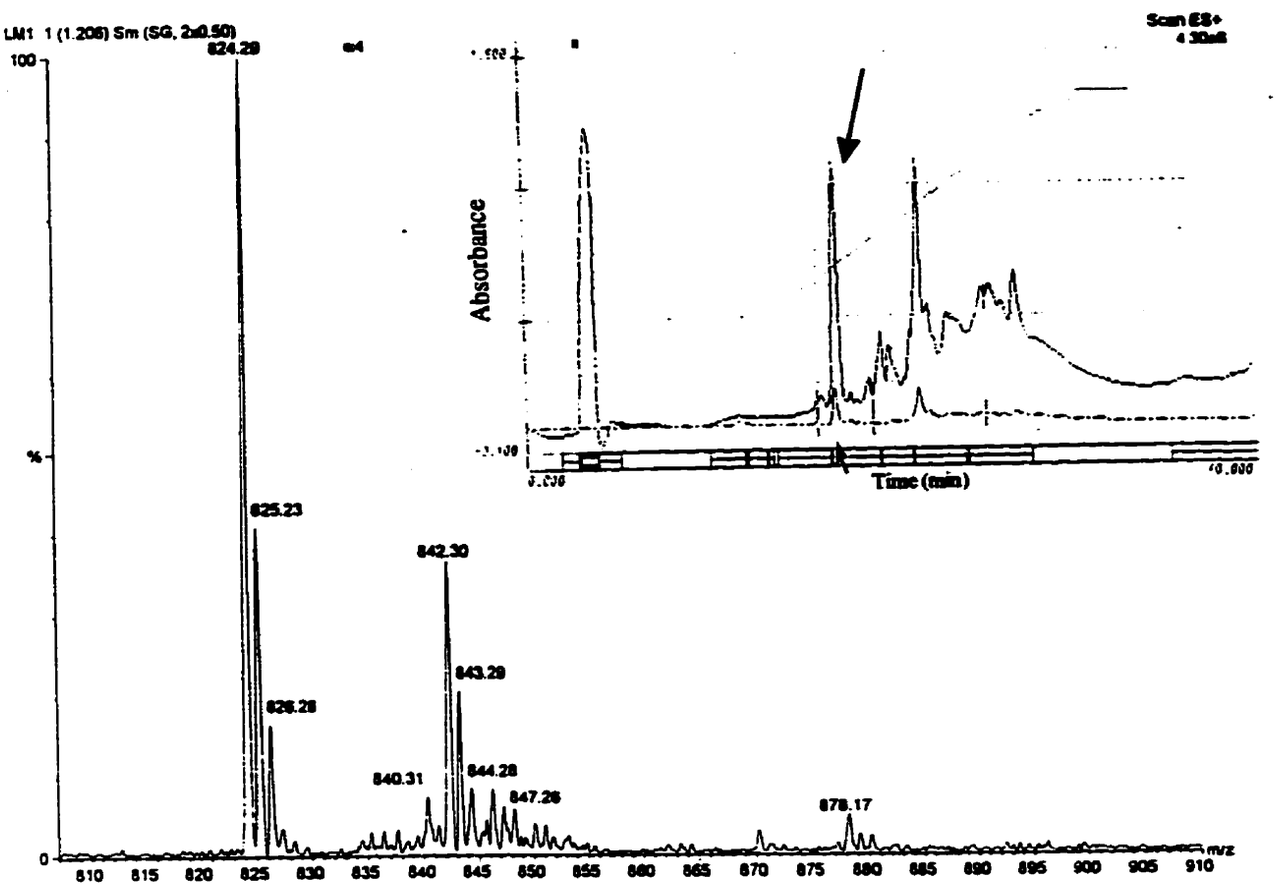
LM1 1 (1.206) Sm (SG, 2x0.50)
824.29
100
%
0
825.23
842.30
843.29
826.28
840.31
844.28
847.26
878.17
m/z
810 815 820 825 830 835 840 845 850 855 860 865 870 875 880 885 890 895 900 905 910
Absorbance
Time (min)
Scan ES+

Figure 29. **Chromatographic profile of the soluble component of the tryptic digest of [^{14}C]-S-carboxymethyl *r*lucD:**
A: An overall profile of the peptides present in the fraction. Conditions employed were same as in Figure 28 except the linear gradient was over a span of 100 minutes.
B: Chromatographic profile of the labelled material indicated by an arrow in Figure 29A. Conditions employed were same as above except the linear gradient was over a span of 90 minutes.

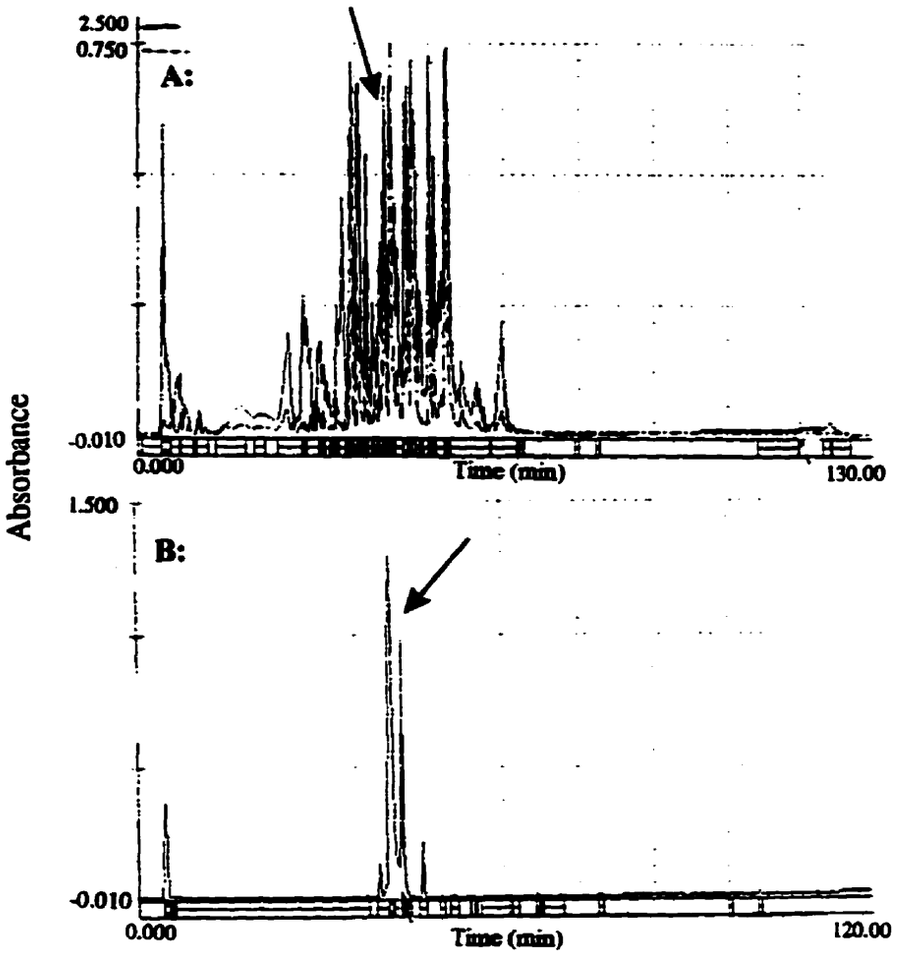
2.500
0.750
A:
-0.010
0.000
Time (min)
130.00
Absorbance
1.500
B:
-0.010
0.000
Time (min)
120.00

residues at location 51 and 158 are susceptible to alkylation in the native conformation of the protein.

As indicated earlier, treatment of *r*lucD with [^{14}C]iodoacetate in the presence of FAD resulted in the modification of approximately one cysteine residue per mole of protein. Thus, FAD would appear to shield one of the two cysteine residues and prevent its alkylation. Analyses of the protein modified with [^{14}C]ICH_2COOH in the presence of FAD by the above mentioned methods indicated the presence of radioactive label in the peptide fragment 47-53. These observations demonstrate that the Cys51 is one of the two cysteine residues susceptible to alkylation in the native conformation of the protein, regardless of the presence or the absence of FAD.

4.4 Reaction of *r*lucD with artificial electron acceptor

4.4.1 Reaction with DPIP:

DPIP in 100 mM potassium phosphate, pH 7.0 absorbs maximally at 600 nm and there is no detectable change in absorbance over an extended period. However, upon addition of *r*lucD, the absorbance at 600 nm declines steadily reaching a constant value after approximately 5-10 minutes and the magnitude of this decrease in absorbance value is proportional to the concentration of *r*lucD in the solution. Upon chromatography of the reaction mixture on Biogel P4 matrix, the protein is recovered as a blue coloured complex with the dye which can not be removed by extraction with ethanol. These observations are consistent with a covalent modification of *r*lucD by DPIP. The DPIP-*r*lucD complex is characterized, in addition to its typical UV absorption band at 280 nm, by a visible absorption band with a λ_{max} value at 654 nm. This observed red shift in λ_{max} of the dye

appears to be specific to its interaction with *r*IucD since DPIP bound to BSA retains its typical spectral features (Figure 30). Calculations based on the ϵ_m values of 6.75×10^4 M^{-1} cm^{-1} and 2×10^4 M^{-1} cm^{-1} for the protein and the dye respectively, suggest the incorporation of one mole of DPIP per *r*IucD monomer, the former being present equally between its reduced and oxidized states due to its innate ability to undergo auto-oxidation.

Since DPIP has been shown to conjugate with mercaptans (85-87), the thiol content of *r*IucD was assessed by titration with DTNB or NTCB both prior to and after its interaction with DPIP. As noted before, *r*IucD preparations used in this investigation are characterized by the presence of five DTNB (or NTCB) titratable functions per protein monomer, three of which are accessible in the native conformation, while the remaining two become susceptible to modification only upon denaturation of the protein. Analyses of the DPIP-*r*IucD complex have revealed the presence of approximately three DTNB titratable groups per *r*IucD monomer under denaturing conditions (Table 7). These observations indicate that two of the thiol functions present in the native conformation of *r*IucD are participating in an oxidative substitution reaction with DPIP, analogous to that recorded with mercaptans (85-87). Modification of the thiol groups of *r*IucD by DTNB results in a loss of ability to form a covalent conjugate with DPIP, a finding compatible with the above observations.

4.4.2 Catalytic properties of DPIP-*r*IucD conjugate:

The conjugation of *r*IucD with DPIP is accompanied by a loss in its ability to catalyse N-hydroxylation of lysine when assayed in the presence of FAD and NADPH, cofactors normally required for this function of the protein. However, the DPIP-*r*IucD

Figure 30. **Spectral and catalytic properties of DPIP-*r*IucD complex**:
DPIP-*r*IucD complex was prepared by treatment of *r*IucD (15 nmoles) with DPIP (100 μM) in potassium phosphate (200 mM, pH 7.0) and was isolated by chromatography on Biogel P4. For comparison DPIP-BSA complex was also produced by a similar procedure. Spectra of DPIP-*r*IucD (----) and DPIP-BSA complex (—).

Note: The covalent nature of the adduct was further demonstrated by the observation that the dye remains associated with the protein even after precipitation with trichloroacetic acid. The dye is decolorized under acidic conditions but turns blue at pH 7.0. In contrast, the complex with BSA is noncovalent since the dye is removed upon denaturation either with alcohol or trichloroacetic acid. Furthermore, such stable complexes are not formed with *r*IucD preparations containing modified thiol groups.

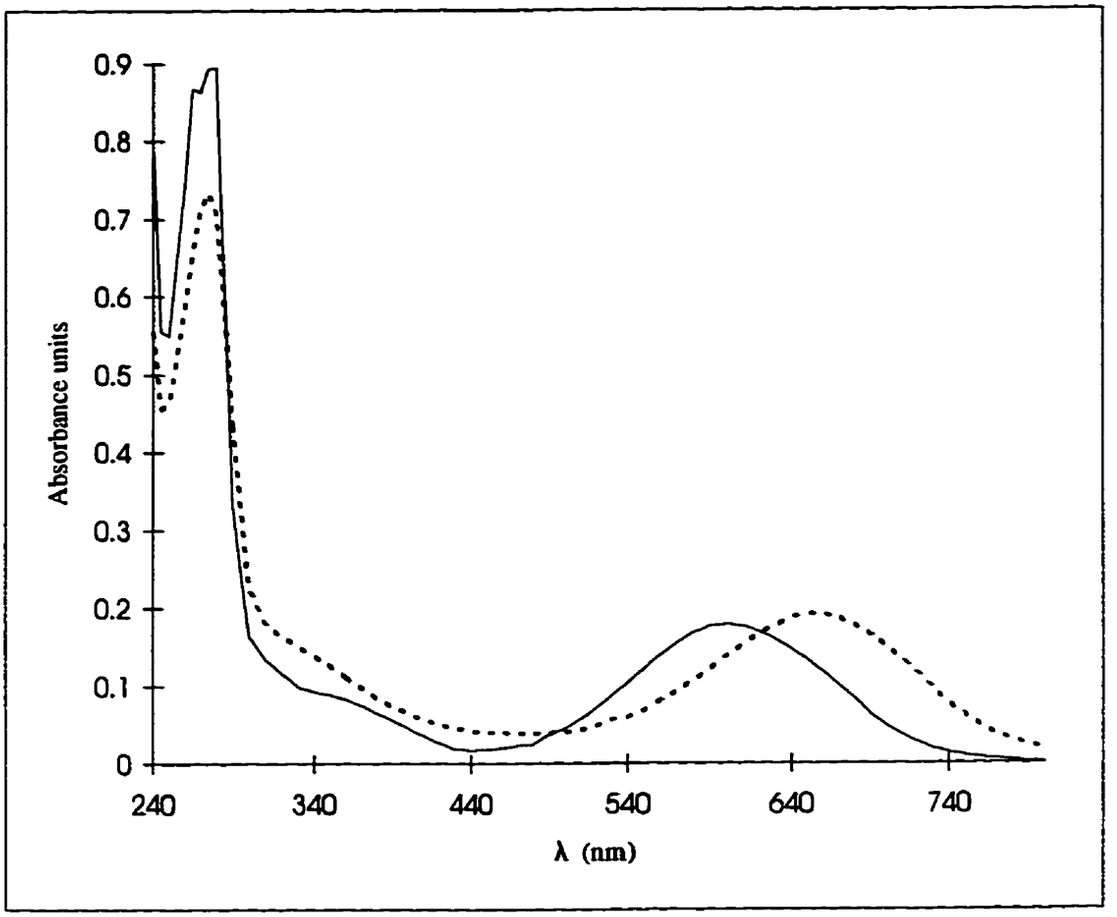
0.9
0.8
0.7
0.6
0.5
0.4
0.3
0.2
0.1
0
Absorbance units
240
340
440
540
640
740
λ (nm)

complex, either isolated or generated "in situ", is capable of promoting NADPH oxidation in the presence of exogenous DPIP (Figure 31). The DPIP-*r*IucD complex (4 μM) effects approximately a three fold increase in the rate of NADPH oxidation relative to that noted with DPIP alone. The process appears to involve an exchange of reducing equivalents between the protein bound DPIP and that free in the medium. Further studies of the above noted phenomenon of reducing equivalent exchange have revealed the process to require unmodified DPIP, since its conjugate with 2-mercaptoethanol fails to elicit NADPH oxidation by *r*IucD. Furthermore, *r*IucD preparations which do not show the presence of DTNB titratable thiol groups and are devoid of lysine:N^6-hydroxylase activity (a situation that develops on prolonged storage of the protein) have been found to catalyse NADPH oxidation in the presence of DPIP. Similarly, *r*IucD preparations with thiol functions modified either by DTNB or NTCB still retain their ability to promote DPIP dependent NADPH oxidation. Hence, it would appear that a noncovalent interaction between *r*IucD and DPIP could result in the formation of a species which is also capable of promoting NADPH oxidation. However, it has not been possible to demonstrate such a noncovalent complex of the protein and the dye presumably due to its facile dissociation even under mild conditions employed for its isolation. Finally, as reported before (86), NADH can also undergo a slow rate of oxidation in the presence of DPIP. However, this process is not enhanced by *r*IucD. Thus, the promotion of DPIP dependent NADPH oxidation by *r*IucD is in accordance with the preference for this particular cofactor in its catalytic function.

Figure 31. **Reaction of DPIP-*r*IucD complex catalysing NADPH dependent reduction of exogenous DPIP:**

1, DPIP in potassium phosphate (100 mM, pH 7.0); **2**, reaction with *r*IucD leading to the formation of DPIP-*r*IucD complex; **3**, NADPH dependent reduction of exogenous DPIP mediated by the DPIP-*r*IucD complex. The introduction of *r*IucD and NADPH is indicated by the first and second arrows, respectively. **4**, Reaction of DPIP with NADPH in the absence of DPIP-*r*IucD complex shown for comparison. The DPIP-*r*IucD complex recovered from the reaction mixture was also found to exhibit the ability to promote NADPH dependent reduction of exogenous DPIP.

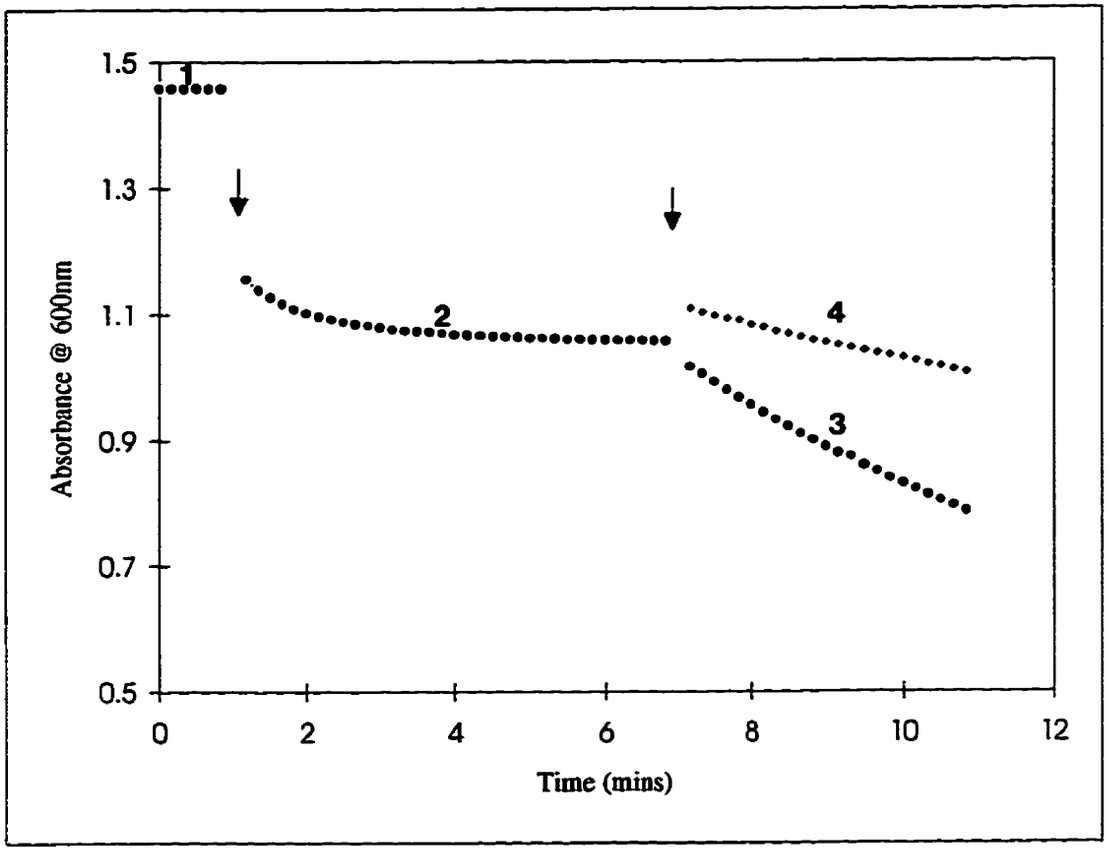
1.5
1.3
1.1
0.9
0.7
0.5
Absorbance @ 600nm
1
2
3
4
0
2
4
6
8
10
12
Time (mins)

4.4.3 Influence of FAD on the interaction between DPIP and *r*IucD:

The observations recorded above pertained to the reactions between DPIP and *r*IucD performed in the absence of FAD. Hence, experiments were designed to assess the influence of the flavin cofactor on the interaction between DPIP and *r*IucD.

FAD, if present, would appear to cause a diminution in the amount of DPIP bound to *r*IucD. Thus, under experimental conditions involving an incubation period of 5 minutes, the amount of DPIP bound in the presence of FAD (200 μM) corresponds approximately to 0.6 moles per mole of *r*IucD compared to the value of one mole per mole of protein noted in the experiments performed in the absence of the flavin cofactor. However, in view of the covalent nature of its interaction, DPIP would appear eventually to overcome the interference by FAD which can only bind the protein reversibly. In light of these findings, the effect of FAD at various stages after the initiation of the interaction between DPIP and *r*IucD was investigated. These studies have revealed that the introduction of FAD immediately after the start of the reaction would result in a stimulation of NADPH oxidation, with the rate of the process being considerably higher relative to that noted in experiments with DPIP serving as the sole electron acceptor. The ability of FAD to stimulate NADPH oxidation has been found to diminish progressively with the increase in the duration of the interaction between the dye and the protein. Thus, the enhancement of NADPH oxidation by FAD is considerably less with preparations of *r*IucD and DPIP preincubated for five minutes relative to that observed with those after just one minute of interaction. FAD has a marginal influence on NADPH oxidation mediated by the preparations of DPIP and *r*IucD which have been allowed to interact for fifteen minutes. These results are shown in Figure 32. As noted

Figure 32. **Influence of FAD on the NADPH oxidase activity of *r*lucD in the presence of DPIP**:
*r*lucD was incubated with DPIP and the effect of FAD, added at different time intervals of the initiation of the reaction on NADPH oxidation, was determined.
●-●, no FAD (-0.06 ΔA/min); ▲-▲, FAD after 1 minute (-0.105 ΔA/min): ◆-◆, FAD after 5 minutes (-0.085 ΔA/min); and ■-■, FAD after 15 minutes (-0.073 ΔA/min).

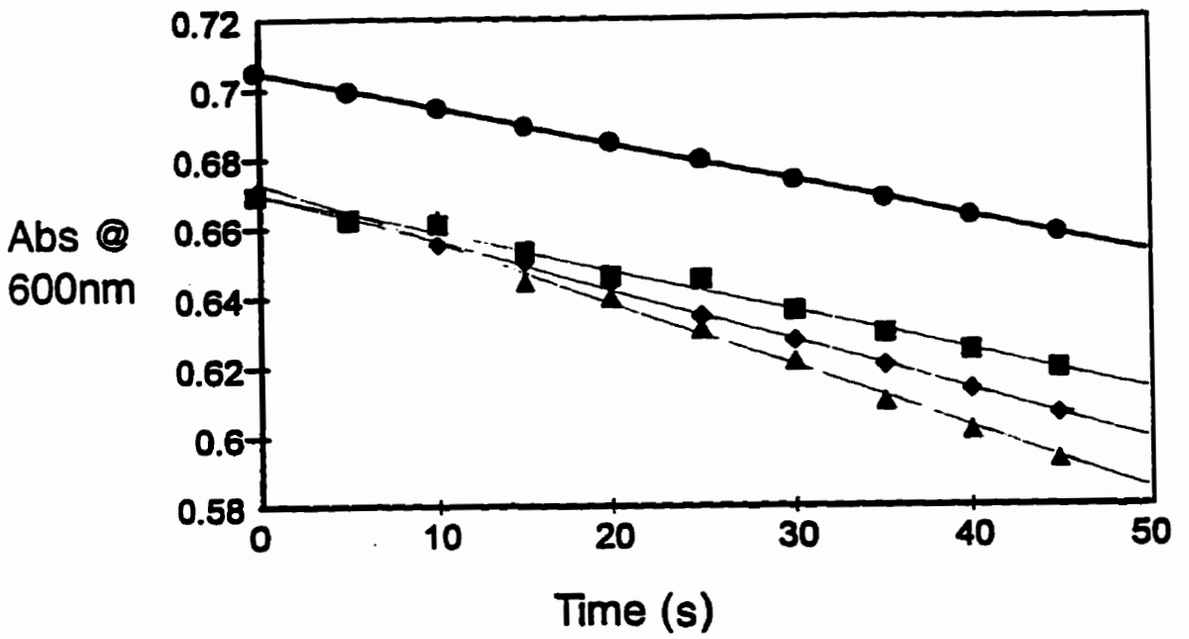
0.72
0.7
0.68
0.66
0.64
0.62
0.6
0.58
Abs @
600nm
0
10
20
30
40
50
Time (s)

earlier, *r*IucD preparations with thiol groups modified (due to oxidation or chemical modification) are also capable of mediating the DPIP dependent NADPH oxidation and this process has been found to be further enhanced in the presence of FAD. Since preincubation of *r*IucD with DPIP leads to the formation of a covalent conjugate, the above findings suggest that the stimulation of NADPH oxidation by FAD can occur only in the absence of a covalent interaction between the dye and the protein. Thus, the covalent modification of *r*IucD by DPIP is accompanied by a decline in the FAD dependent activity of NADPH oxidation presumably due to a loss in its ability to interact with the flavin cofactor.

4.5 Site directed mutagenesis of *r*IucD

4.5.1 Characterization of iucD and its variants:

In order to elucidate the role of thiol groups in the catalytic functions of *r*IucD, Cys51 and Cys158 were replaced with alanine residue(s) either individually or in combination. (see Methods, section 3.4). The occurrence of the desired mutation(s) in the iucD gene was confirmed both on the basis of the profile of the product(s) generated upon treatment of the plasmid preparation with appropriate restriction enzyme(s) as well as by the determination of the nucleotide sequence of iucD and its variants. The consequences of either single or double mutation in iucD has been mentioned earlier (see Table 3). Thus, in the design of C51A mutation, the primers employed would lead not only to the replacement of the desired triplet (TGT) for cysteine with that for alanine (GCT) but also to the elimination of one of the two *Kpn* I restriction endonuclease sites. Hence, the plasmid carrying this iucD variant would contain a unique *Kpn* I restriction endonuclease site and become linearized upon treatment by that restriction endonuclease. In the case of C158A

mutation, the primers employed result not only in the replacement of the triplet TGT with GCT but also in the elimination of the unique *Dra* III restriction endonuclease site. Consequently, the plasmid carrying this iucD variant will not be susceptible to cleavage by *Dra* III. The results, shown in Figures 33 and 34, conform to the above predictions and thus provide evidence for the incorporation of the desired mutations in iucD. The C51A/C158A double mutation was performed starting with both iucD encoding for either C51A IucD or C158A IucD using appropriate complementary primers to effect the second mutation. The plasmid preparation carrying iucD variant encoding for C51A/C158A IucD was treated with the restriction endonucleases *Kpn* I and *Dra* III, individually. The results obtained (Figure 35) confirm the incorporation of the desired mutations. In all these analyses, the parent pAT5 preparations treated with the above restriction endonucleases served as controls.

4.5.2 Characterisation of *r*IucD muteins:

Each of the iucD variants has been found to encode for a functional lysine:N^6-hydroxylase which was isolated in a homogeneous state by procedures analogous to those employed in the case of the parent iucD gene product (Figure 36) (19,20). An examination of the lysine:N-hydroxylase activity of these *r*IucD muteins has revealed that C51A *r*IucD and C51A/C158A *r*IucD are approximately 1.5 times more active, while C158A *r*IucD is similar to the parent *r*IucD in their specific activity.

All three *r*IucD muteins, like the parent protein, are stringently specific with L-lysine serving as the preferred hydroxylatable substrate. The cysteine replacement in *r*IucD does not lead to any significant change in the affinity for its cofactors. Thus, in the case of all three muteins, the K_M values for FAD (≈ 4 μM) and for NADPH (≈ 70 μM) are similar to

Figure 33. **Restriction enzyme analysis of Cys51Ala *r*iucD mutation:**

E.coli cells were transformed with the Cys51Ala *r*iucD constructs and streaked on LB agar plates containing ampicillin (100 mg/L). Two colonies were selected and analysed for the plasmid containing the Cys51Ala mutation.

Plasmids (1.25 μg) were treated with *Kpn* I (18 units) for 6 hours at 37°C. Controls were incubated in similar buffer solutions without *Kpn* I.

lanes:
1. molecular weight standards, λ /*Hin*d III
2. Cys51Ala *r*iucD #1, control
3. Cys51Ala *r*iucD #1, *Kpn* I digest
4. Cys51Ala *r*iucD #2, control
5. Cys51Ala *r*iucD #2, *Kpn* I digest
6. *r*IucD (pAT5), control
7. *r*IucD (pAT5), *Kpn* I digest
8. molecular weight standards

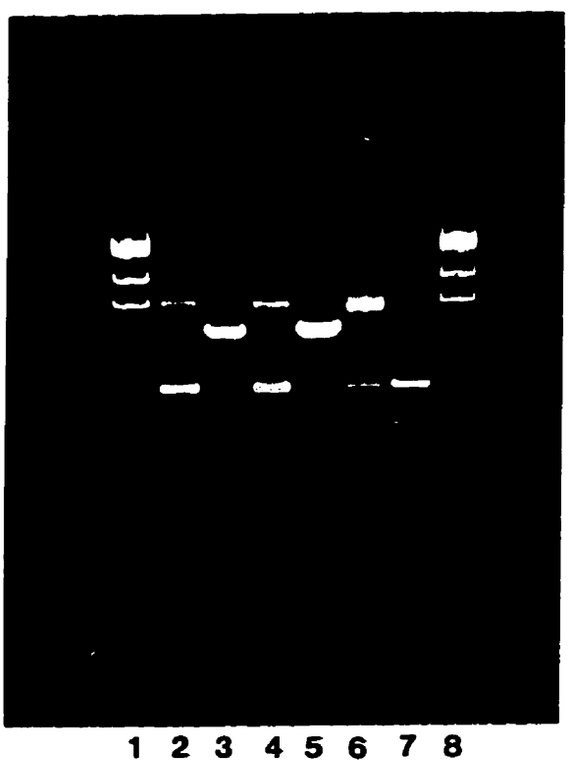
1 2 3 4 5 6 7 8

Figure 34. **Restriction enzyme analysis of Cys158Ala *r*iucD mutation:**

E.coli cells were transformed with the Cys158Ala *r*iucD constructs and streaked on LB agar plates containing ampicillin (100 mg/L). One colony was selected and analysed for the plasmid containing the Cys158Ala mutation.

Plasmids (1.25 μg) were treated with *Dra* III (3 units) for 6 hours at 37°C. Controls were incubated in similar buffer solutions without *Dra* III.

lanes:
1. molecular weight standards, λ /*Hin*d III
2. Cys158Ala *r*iucD #1, control
3. Cys158Ala *r*iucD #1, *Dra* III digest
4. molecular weight standards
5. *r*IucD (pAT5), control
6. *r*IucD (pAT5), *Dra* III digest

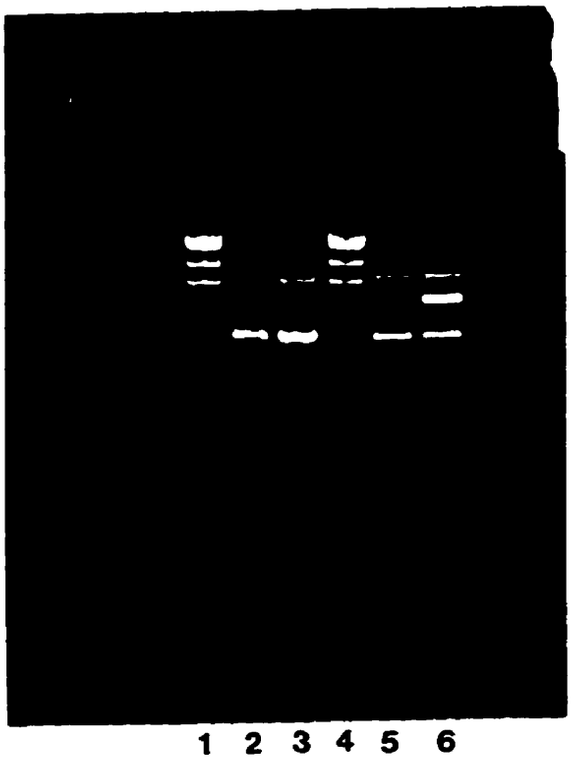
1 2 3 4 5 6

Figure 35. **Restriction enzyme analysis of Cys51Ala/Cys158Ala *r*iucD mutation:**
E.coli cells were transformed with the Cys51Ala/Cys158Ala *r*iucD constructs and streaked on LB agar plates containing ampicillin (100 mg/L). Four colonies were selected and analysed for the plasmid containing the Cys51Ala/Cys158Ala mutation.
Plasmids (1.25 μg) were treated with either *Dra* III (3 units) or *Kpn* I (18 units) for 6 hours at 37°C. Controls were incubated in similar buffer solutions without *Dra* III or *Kpn* I, respectively.
pAT5 with iucD encoding for Cys51Ala *r*IucD was used to effect the second mutation, Cys158Ala. Hence, the second mutation was analysed by digesting with *Dra* III (samples #1 and #2).
pAT5 with iucD encoding for Cys158Ala *r*IucD was employed to effect the second desired mutation, Cys51Ala. Hence, the second mutation was analysed by digesting with *Kpn* I (#3 and #4).

A. lanes:
1. molecular weight standards, λ /*Hin*d III
2. Cys51Ala/Cys1581Ala *r*iucD #1, *Dra* III control
3. Cys51Ala/Cys158Ala *r*iucD #2, *Dra* III control
4. *r*IucD (pAT5), *Dra* III control
5. Cys158Ala/Cys51Ala *r*iucD #3, *Kpn* I control
6. Cys158Ala/Cys51Ala *r*iucD #4, *Kpn* I control
7. *r*IucD (pAT5), *Kpn* I control
8. molecular weight standards

B. lanes:
1. molecular weight standards, λ /*Hind* III
2. Cys51Ala/Cys1581Ala *r*iucD #1, *Dra* III digest*
3. Cys51Ala/Cys158Ala *r*iucD #2, *Dra* III digest*
4. *r*IucD (pAT5), *Dra* III digest
5. Cys158Ala/Cys51Ala *r*iucD #3, *Kpn* I digest
6. Cys158Ala/Cys51Ala *r*iucD #4, *Kpn* I digest
7. *r*IucD (pAT5), *Kpn* I digest
8. molecular weight standards

* Colonies chosen for #1 and #2 did not contain plasmids with a successful second mutation.

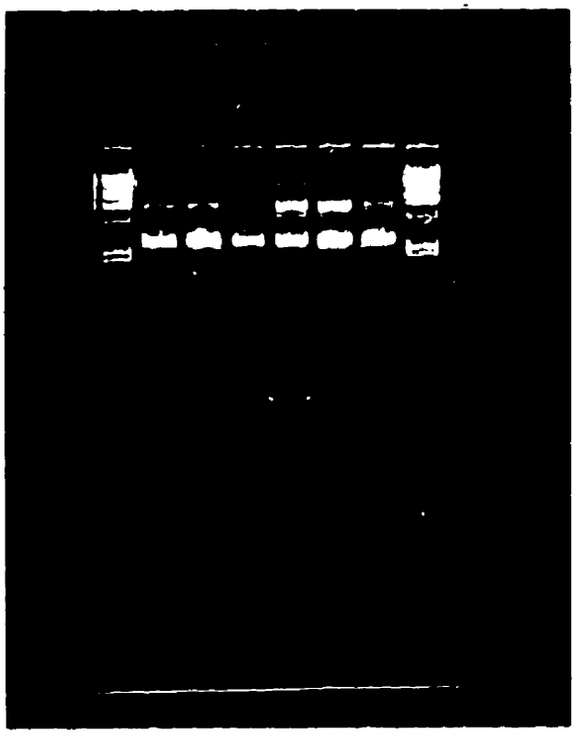
1 2 3 4 5 6 7 8

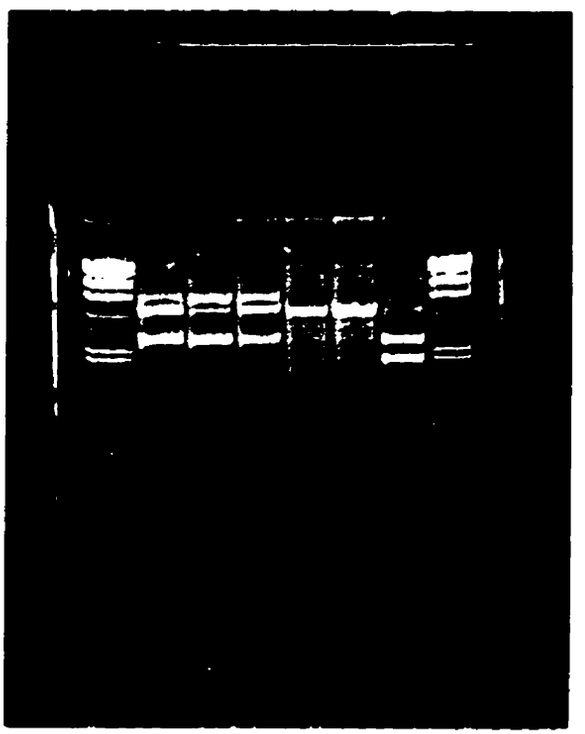
1 2 3 4 5 6 7 8

Figure 36. **SDS-PAGE profile of *r*IucD and *r*IucD mutein preparations recovered from the affinity matrix Orange A.**

Lanes **1**. *r*IucD; **2**. Cys51Ala *r*IucD; **3**. molecular weight standards (94 kDa, 67 kDa, 43 kDa, 30 kDa, 20.1 kDa); **4**. Cys158Ala *r*IucD; **5**. Cys51Ala/Cys158Ala *r*IucD; and **6**. *r*IucD

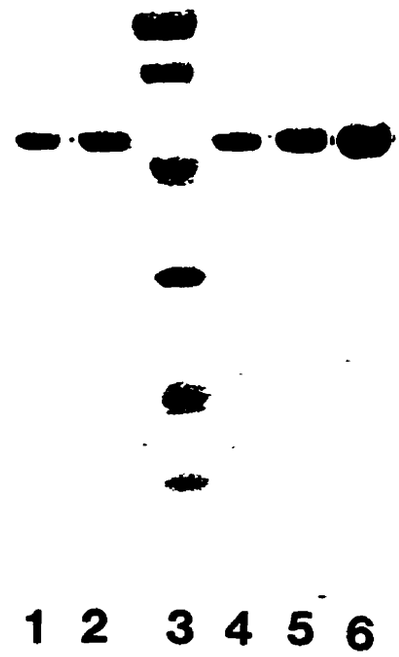
1 2 3 4 5 6

that recorded in the case of the parent *r*IucD. Furthermore, all the three *r*IucD muteins are capable of promoting NADPH oxidation in the absence of lysine (a process which results in the production of H_2O_2) at considerably enhanced rates relative to that noted in the case of parent *r*IucD (Figure 37).

4.5.3 Reactivity of cysteine residues in *r*IucD muteins:

The susceptibility of the thiol functions accessible in the native conformation of the *r*IucD muteins was examined by reaction with DTNB. The results can be summarized as follows: As noted before, experiments with parent *r*IucD preparations have revealed the presence of three accessible thiol functions, two of them reacting fast (reaction time ≈ 10 seconds) and the other requiring approximately 2-3 minutes for completion of the modification. In the case of C51A *r*IucD, such analyses have revealed the presence of two thiol groups, one reacting fast (time ≈ 10 seconds) and the other relatively slow requiring approximately 2-3 minutes for completion of the reaction. With C158A *r*IucD, two thiol groups (actual value = 1.5) have been found to react rapidly with DTNB. Finally, under similar experimental conditions, the C51A/C158A *r*IucD has been found to contain one rapidly modifiable thiol function. These results are shown in Figure 38.

Treatment of the parent *r*IucD and C158A *r*IucD with iodoacetate results in the loss of lysine:N^6-hydroxylase activity. In contrast, such treatment has no adverse effect on the catalytic function of C51A *r*IucD and C51A/C158A *r*IucD.

4.5.4 Reaction of *r*IucD muteins with DPIP:

As reported previously, DPIP can form either a covalent or a noncovalent adduct with *r*IucD (62). The salient features of the phenomenon leading to the covalent adduct are:

Figure 37. **NADPH oxidtion by *r*IucD and its muteins in the presence and in the absence of lysine:**
The rates of NADPH oxidation by *r*IucD and its muteins in the presence and absence of lysine were determined on the basis of the production of N^6-hydroxylysine and H_2O_2, respectively. Assays were performed under identical enzyme concentrations.

Legend: •-•, N^6-hydroxylysine; and ○-○ H_2O_2

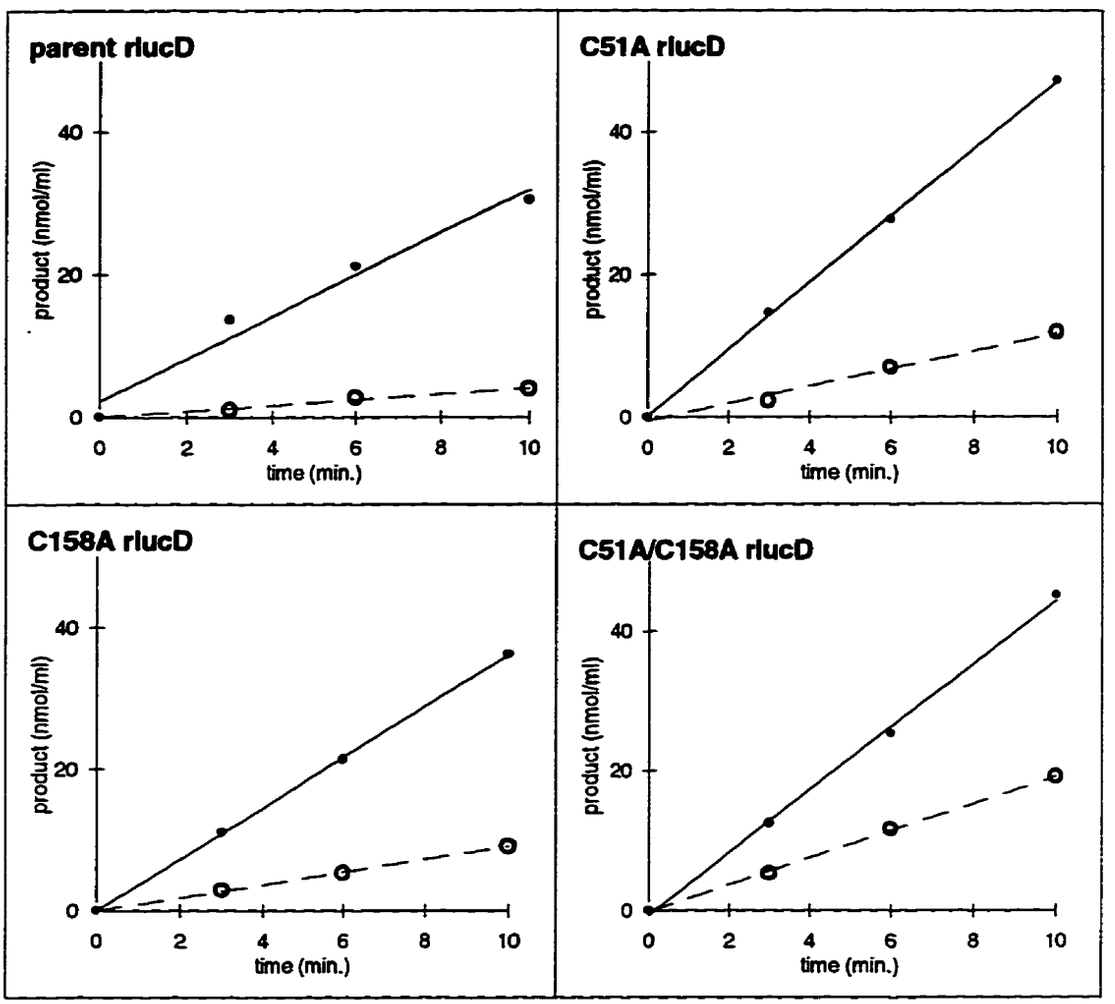
parent rlucD
C51A rlucD
C158A rlucD
C51A/C158A rlucD
product (nmol/ml)
time (min.)
0
20
40
0
2
4
6
8
10

Figure 38. **Reaction of *r*lucD or its muteins with DTNB:** The desired protein preparation in one ml of 200 mM potassium phosphate, pH 8.0 was treated with an aliquot (100 μl) of DTNB (5 mM) and the progress of the reaction was monitored at 412 nm. After correction for the spontaneous hydrolysis of the reagent, ΔA values at 412 nm, at various intervals of the reaction, were used to determine the number of thiol group(s) modified per monomer of the protein.

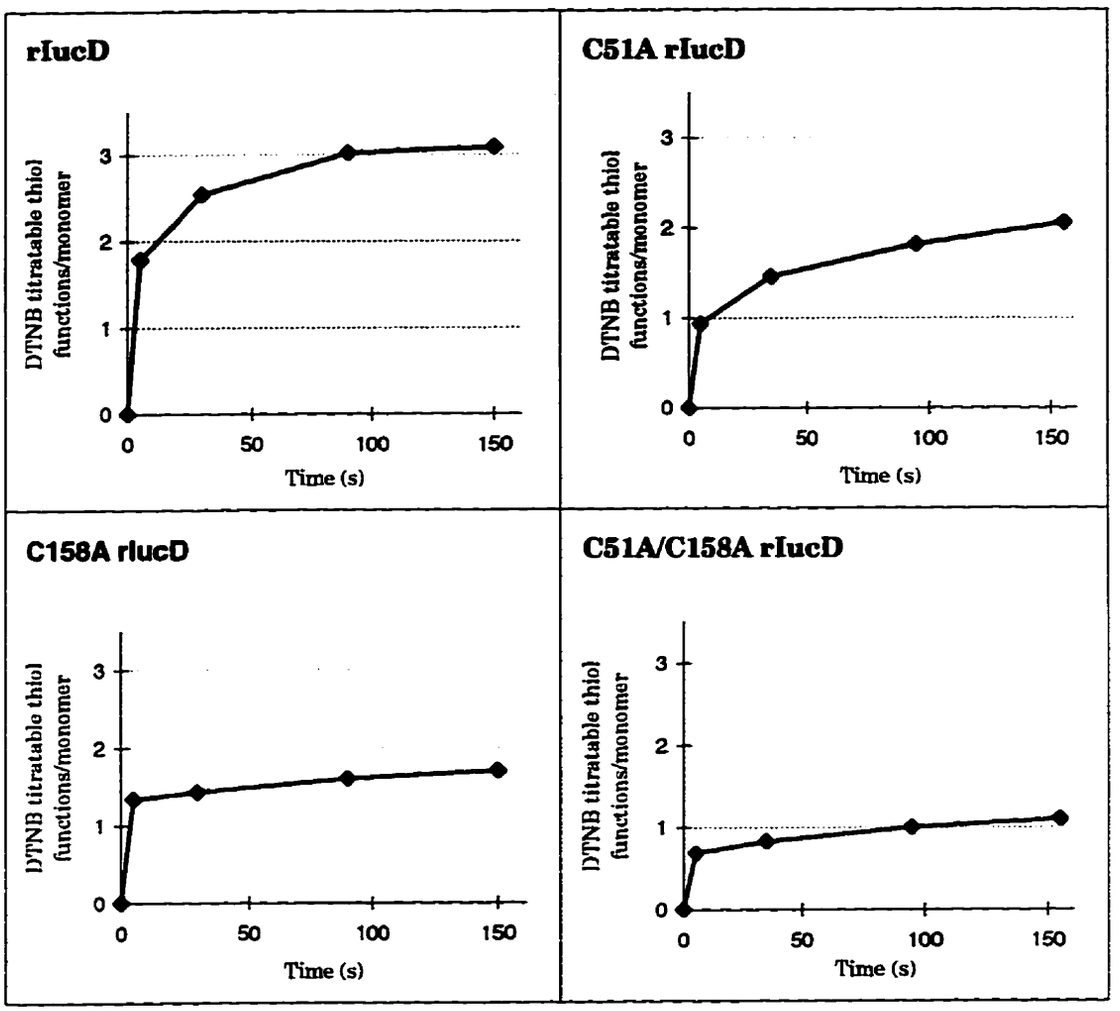
rIucD
DTNB titratable thiol functions/monomer
0
1
2
3
0
50
100
150
Time (s)
C51A rIucD
DTNB titratable thiol functions/monomer
0
1
2
3
0
50
100
150
Time (s)
C158A rIucD
DTNB titratable thiol functions/monomer
0
1
2
3
0
50
100
150
Time (s)
C51A/C158A rIucD
DTNB titratable thiol functions/monomer
0
1
2
3
0
50
100
150
Time (s)

(i) the process requires the presence of unmodified thiol functions in the protein; (ii) the reaction is accompanied by a steady diminution in the absorbance at 600 nm reaching a constant value after approximately 10 minutes; and (iii) a steady decline in the diaphorase activity with total loss after 10-15 minutes of the incubation with the dye, a period required for the completion of the covalent modification of the protein. The covalent DPIP-*r*IucD adduct is capable of promoting NADPH oxidation by a mechanism based on a reducing equivalent exchange between the protein bound DPIP and that free in the medium (62). On the other hand, the latter type of complex exhibits diaphorase activity regardless of the period of preincubation of the protein with the dye. Hence, in the studies on the interaction between DPIP and the *r*IucD muteins, attention was focussed on the above mentioned aspects. Concerning the diminution in absorbance at 600 nm, the following observations were noted: (I) in the case of C51A *r*IucD and C51A/C158A *r*IucD, the decrease in the absorbance at 600 nm corresponds to approximately half as that noted in the case of the parent *r*IucD; and (ii) in the case of C158A *r*IucD, such diminution in the absorbance at 600 nm is similar to that noted in the parent *r*IucD (data not shown). Regarding the other aspects, the replacement of Cys51 with alanine, as in C51A *r*IucD, has no marked effect (relative to the parent *r*IucD) on the ability to promote NADPH oxidation. However, the diaphorase activity is no longer sensitive to the presence of DPIP, the time of preincubation being irrelevant. In contrast, the presence of Cys51, as in the of C158A *r*IucD, the rate of NADPH oxidation, via the phenomenon of a reducing equivalent exchange between the protein bound DPIP and that free in the medium, is enhanced and the diaphorase activity declines steadily with the time of preincubation with the dye. The observations, in the case

of C51A/C158A *r*IucD, would appear to reflect essentially those recorded with C51A *r*IucD with respect to diaphorase activity. These findings, which are illustrated in Figure 39, indicate that Cys51 of *r*IucD plays a pivotal role in the oxidative addition reaction with DPIP, a prerequisite for the formation of the covalent adduct.

A summary of the consequences of the replacement of Cys51 and Cys158 of *r*IucD with an alanine residue on both the reactivity of the thiol functions towards DTNB and DPIP as well as on the dissociation constant of the protein • FAD complex and the kinetic parameters are presented in the Appendix F.

Figure 39. **Reaction of *r*IucD and its muteins with DPIP:** An aliquot of the indicated *r*IucD preparation was introduced into one ml of DPIP (100 μM) in potassium phosphate (200 mM, pH 7.0) to achieve a final concentration of 2.5 μM with respect to the protein. After either one or fifteen minutes of incubation, an aliquot of NADPH was introduced to achieve a final concentration of 200 μM and the rate of NADPH oxidation was recorded by monitoring the decrease in absorbance at 600 nm for 40 seconds. After the introduction of FAD (indicated by the arrow) to a final concentration of 100 μM, the NADPH oxidation (the diaphorase activity) was monitored by the decrease in absorbance at 600 nm.

1. NADPH oxidation in the absence of FAD after preincubation of the protein and the dye for 1 minute, ●-●, and 15 minutes, o-o, respectively; **2.** NADPH oxidation in the presence of FAD (the diaphorase activity) after preincubation of the protein and the dye for 1 minute, ●-●, and 15 minutes, o-o, respectively.

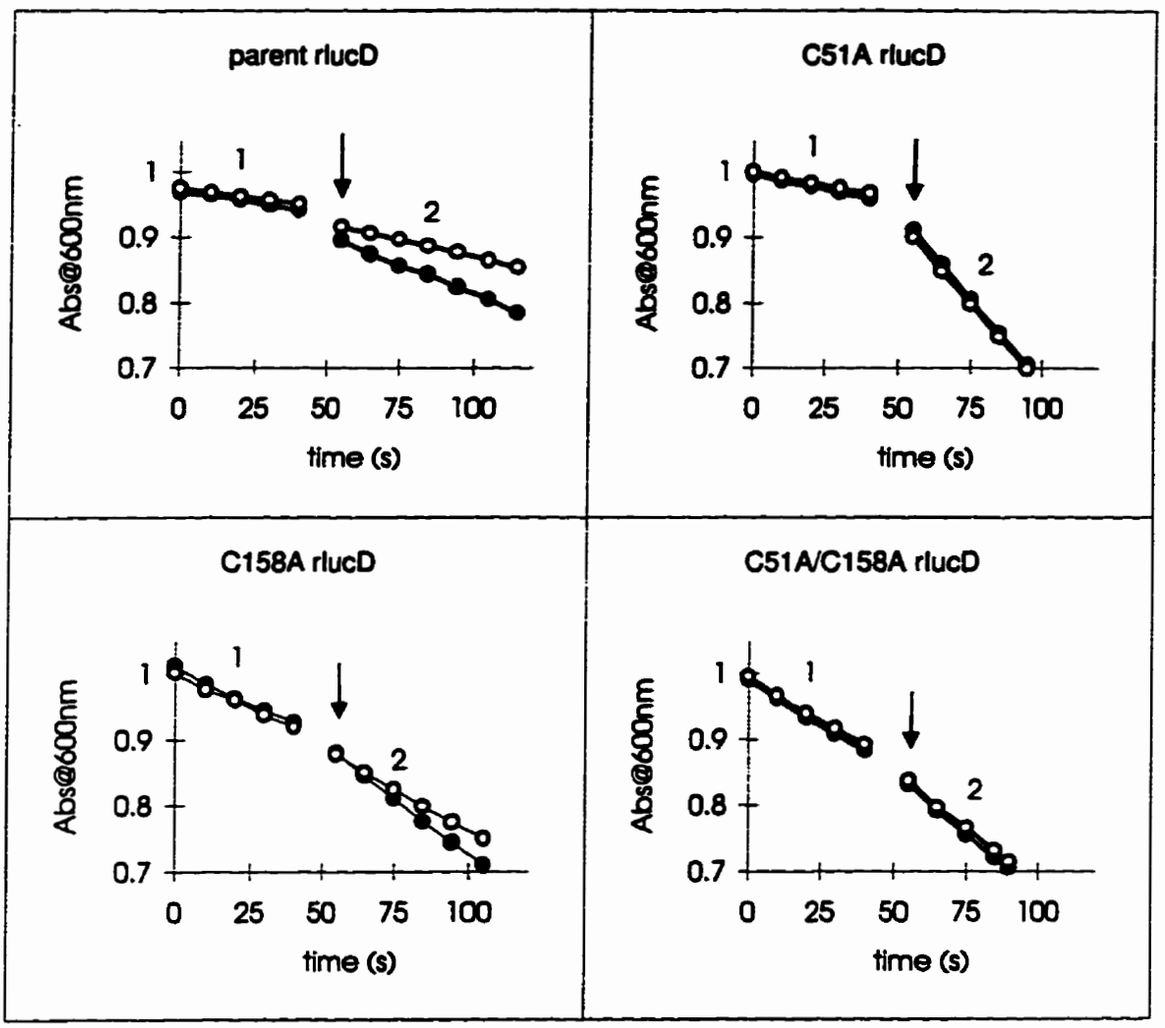
parent rlucD
C51A rlucD
C158A rlucD
C51A/C158A rlucD
Abs@600nm
time (s)
1
2
0.7
0.8
0.9
1
0
25
50
75
100

5.0

DISCUSSION

Lysine:N^6-hydroxylase, (IucD), as noted in the introduction section of this dissertation, catalyses the conversion of L-lysine to its N^6-hydroxy derivative, the initial event in the biosynthesis of the siderophore, aerobactin. This enzyme normally occurs in a membrane environment, a feature that has prevented characterization of both its physicochemical properties as well as its catalytic mechanism (13). Recently, this problem has been circumvented by the development of recombinant, cytoplasmic forms of the enzyme by employing a gene fusion methodology (19). These recombinant forms of IucD are capable of catalysing N^6-hydroxylation of L-lysine upon supplementation with cofactors NADPH and FAD (19,20). Since the cofactor requirement(s) of *wt*IucD could not be identified, the availability of the recombinant cytoplasmic forms of IucD has allowed for an unequivocal demonstration of the participation of the flavin cofactor in the catalytic mechanism of the protein. This feature is consistent with the extensively documented evidence for the pivotal role of flavins in the activation of molecular oxygen (88). As in the case of other flavin dependent monooxygenases, the catalytic cycle of lysine:N^6-hydroxylase is a multistep event involving several reactants. The initial step of FAD-dependent NADPH oxidation is linked to lysine:N-hydroxylation with 4a-peroxyflavin (produced by the interaction of the reduced flavin cofactor with molecular oxygen) serving as the oxygenating agent (Scheme 3). In the absence of a hydroxylatable substrate, the process of NADPH

Scheme 3: **A general mechanism for *r*lucD mediated N-hydroxylation of lysine:**

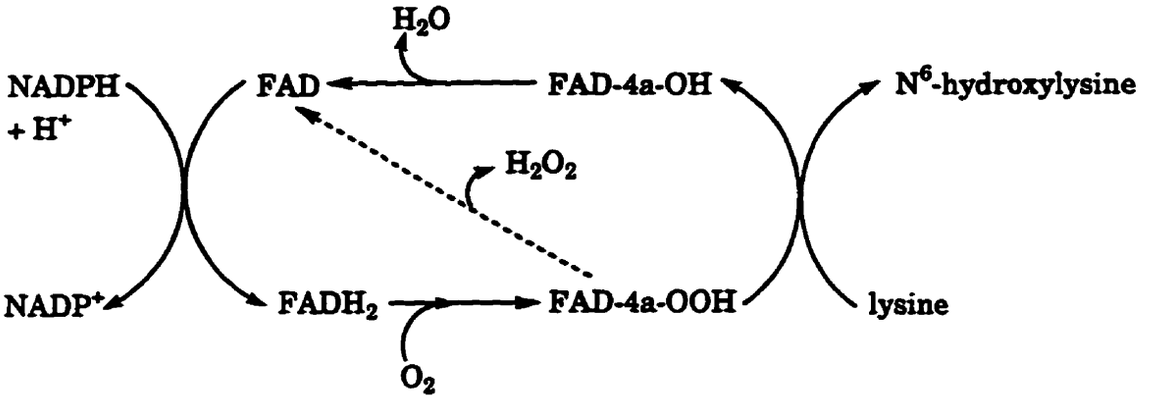
H2O
NADPH
+ H+
FAD
FAD-4a-OH
N6-hydroxylysine
H2O2
NADP+
FADH2
FAD-4a-OOH
lysine
O2

oxidation is channelled toward H_2O_2 production (20).

At the time of the development of the recombinant forms of IucD, sequence analysis was restricted to the region comprising the lacZ-iucD fusion segment (19). Attempts were not made to determine the entire nucleotide sequence of iucD present in the recombinant genetic construct(s). The nucleotide sequence of iucD in these constructs was presumed to be the same as that documented in the literature (76). One of the endeavours undertaken in the current investigations pertained to the manipulation of iucD by site directed mutagenesis and this aspect of the studies necessitated sequencing of *r*iucD and its variants to ensure that not only the desired mutation has been incorporated but also that there has been no other change in iucD accompanying the intended mutation. The nucleotide sequence of *r*iucD and its variants used in this study as well as that of iucD present in pABN5, the plasmid that served as the source for the sequence documented in literature (76), was determined. These analyses have revealed several discrepancies (see Results, section 4.1) in the previously reported sequence (76). This matter has been brought to the attention of Prof. J.B. Neilands and steps are being taken for making the appropriate corrections in the literature regarding the nucleotide sequence of iucD.

An important outcome of this correction in the nucleotide sequence of iucD concerns the reduction in the number of tryptophan and cysteine residues present in the gene product, IucD. The revised nucleotide sequence of iucD calls for the presence of eight tryptophan and five cysteine residues per mole of IucD instead of the value of nine and six residues respectively, of these amino acids predicted by the sequence documented in the literature. Although there are changes in other amino acid residues, these two have been singled out in

view of their contribution to molar absorptivity (tryptophan) and thiol content (cysteine) of the protein. Finally, the enzyme preparation, *r*IucD439, used in the current investigations is actually *r*IucD438 since the revised iucD nucleotide sequence encodes for 425 amino acids instead of the 426 amino acid residues reported previously (76). The appended β-galactosidase peptide segment of 13 amino acid residues is susceptible to removal by means of post-translational processing mechanisms (77). Hence, the molecular weight of *r*IucD would depend on the number of amino acid residues deleted by such an event.

The above mentioned findings necessitating a revision of the published nucleotide sequence of iucD are indeed fortuitous in as much as such an undertaking was not planned at the time of the initiation of these investigations. The major objective of the study pertains to the elucidation of the structure-function relationship of the enzyme by an examination of its stability in different environments, its specificity with respect to its hydroxylatable substrate, the role of its thiol functions in the delineation of its catalytic functions and its interaction with artificial electron acceptor(s). Each of these aspects, although not in the same order outlined above, will be addressed in the ensuing sections.

First, attention was focussed on the influence of various anions on the stability as well as the catalytic function of the enzyme since the procedure for the purification involved the use of high concentration of NaCl in the elution buffer medium to achieve the ionic strength conditions required for its recovery from the affinity matrix (19). The choice of NaCl was primarily based on the low cost of the material and its bacteriostatic effects at high concentrations. However, the catalytic function of many flavin dependent monooxygenases has been shown to be adversely affected by monovalent anions such as SCN^-, Cl^-, and N_3^-.

These enzymes include phenol hydroxylase (78-80), *p*-hydroxybenzoate hydroxylase (81) and salicylate hydroxylase (89) and there appears to be considerable debate concerning the basis for the adverse effects exerted by these monovalent anions. Thus, in the case of phenol hydroxylase, studies by Massey and coworkers suggest that the adverse influence of Cl^- ions may be due to their ability to retard the regeneration of the flavin cofactor from its 4a-hydroxy derivative, the terminal step in the catalytic mechanism of the protein (78). On the other hand, Neujahr and associates attribute the inhibition of this enzyme by Cl^- ion to its ability to function as a chaotrope and perturb the hydrophobic environment of its FAD binding domain (79,80). In contrast to the above mentioned proposals, investigations on *p*-hydroxybenzoate hydroxylase by Müller and coworkers indicate that the inhibitory action of Cl^- ion may be due to its ability to compete for the NADPH binding domain and to interfere in the turnover of the cofactor (81). Current studies have shown that *r*IucD is susceptible to the adverse actions of Cl^- ions although the concentration required for the inactivation is considerably higher than that observed with the enzymes mentioned above. Both phosphate and sulfate ions have no inhibitory effect on *r*IucD, an observation in accordance with their position in the Hoffmeister series which is a reflection of the chaotropic abilities of the various ions, the basis for which has been recently addressed (90).

The flexibility in the conformation of *r*IucD was also probed by an assessment of its susceptibility to proteolysis by endo- and exo-peptidases. The protein is rapidly degraded by endopeptidases, TPCK-trypsin and TLCK-chymotrypsin with concomitant loss of catalytic function(s). Deletion of its amino acid residues by treatment with CPD-Y also results in a loss of enzymatic activity. Both FAD and ADP have been found to provide total protection

to *r*IucD from the adverse effects of these proteases. NADPH is only marginally effective in preventing the action of proteases while lysine, the hydroxylatable substrate, is totally devoid of protective function. It would appear that FAD and ADP exert their effect by virtue of their interaction in the flavin cofactor binding domain present in *r*IucD (20). The failure of NADPH to exert a similar influence may be related to the absence, in *r*IucD, of a unique domain specific for interaction with this cofactor (20). The inactivation of *r*IucD upon treatment with CPD-Y suggests that the C-terminal tail constitutes an essential region for the maintenance of the protein in a biologically active conformation. This observation is analogous to that recorded with *Drosophila* alcohol dehydrogenase which requires the C-terminal region to provide the needed hydrophobicity of the catalytic pocket for the binding of the substrate (91). However, in the case of *r*IucD, L-lysine, the hydroxylatable substrate, fails to prevent the adverse effects of CPD-Y. Interestingly, L-norleucine protects rIucD from the deleterious action of CPD-Y. The protective action of FAD, ADP and norleucine is a consequence of their interaction with *r*IucD since these substances do not function as inhibitors of the proteases used in this study.

The second aspect of these investigations concerns the specificity requirements of the enzyme with respect to its hydroxylatable substrate and their implications on its catalytic mechanism. A comprehensive study of the ability of a number of compounds to serve as substrates for lysine:N^6-hydroxylase has revealed that the enzyme is stringently specific in its function. L-lysine and (S)-2-aminoethyl-L-cysteine are the only known compounds that are hydroxylated by the enzyme. Besides its unique substrate specificity, lysine:N^6-hydroxylase also exhibits exclusive preference for its cofactors, NADPH and FAD. The enzyme

mediated processes of NADPH- oxidation and lysine:N^6-hydroxylation are coupled (19,77). However, the coupling of the two above mentioned processes catalysed by *r*IucD does not appear to be as rigid as that noted in the case of other flavin dependent monooxygenases. For example, in the case of p-hydroxybenzoate hydroxylase, the rate of NADPH oxidation is stimulated by a factor of 10^4-10^5 in the presence of substrate, p-hydroxybenzoate (46). In contrast, the substrate, L-lysine, elicits only a moderate, approximately 10-15 fold increase in the rate of NADPH-oxidation mediated by lysine:N^6-hydroxylase (62). Furthermore, the low k_{cat} value (0.1-0.2 sec^{-1}) of lysine:N^6-hydroxylase relative to that of p-hydroxybenzoate hydroxylase, approximately 45 sec^{-1} (49), would seem to correlate with the differences in the substrate induced rate enhancement of NADPH oxidation in the two enzyme systems. Such vast differences in the rates of NADPH oxidation and the k_{cat} values in these two enzyme systems do not appear to be due to a change in the nature of the hydroxylating species, since 4a-peroxyflavin has been shown to be the oxygenating species in a number of flavin dependent monooxygenases (88). This view derives additional support from the previous report which provides evidence for the exclusion of a cytochrome P-450 and/or a metalloenzyme system in the lysine:N^6-hydroxylation mediated by the wild type IucD (17).

The rate enhancement of an enzyme catalysed reaction relative to that in solution can be achieved by lowering the activation barrier of the process either through stabilization of transition state and/or by increasing the energy content or the reactivity of the substrate(s). Serine proteases serve as typical examples of the former route (92,93) while the 4(a)-peroxyflavin dependent hydroxylation of aromatic substrates exemplifies the latter option (94,95). Furthermore, similar catalytic efficiency in the hydroxylation of substrates with

differing reactivities can be achieved by appropriate adjustment of the dielectric constant of the active site and of the proximity of the reactants (94,95). These considerations raise the possibility that the low rate of NADPH oxidation induced by the substrate and the consequent low k_{cat} value of the *r*IucD mediated N-hydroxylation process may be a reflection of the low reactivity of lysine in its extended conformation. This view derives support from the following observations: (i) *trans*-4,5-dehydro-L-lysine, which is characterized by a non-flexible, extended conformation is not a substrate of the enzyme. This situation is in distinct contrast to that noted in the case of trypsin, which utilizes the esters and amides of the *trans*-4,5-dehydro-L-lysine as substrates, but not those of the *cis*-isomer (96); and (ii) studies with model 4a-peroxyflavins have shown that the reaction with primary amines is slow relative to that of secondary and tertiary amines, and may result in the destruction of the flavin cofactor (25,26). In light of these considerations, it would appear appropriate to propose that lysine:N^6-hydroxylase participates in the enhancement of the reactivity of L-lysine by its cyclization to 2-aminocaprolactam, a transient intermediate which reacts rapidly with the 4a-peroxyflavin species, to yield N^6-hydroxylysine via the hydroxamate intermediate (Scheme 4). Unorthodox as it may appear at first glance, it is pertinent to note that although the N-hydroxylation process is an obligatory event in the biosynthesis of hydroxamate siderophores, there appears to be no precise order with regard to the sequence of events leading to the production of hydroxamate constituents of the siderophores. In the case of ferrichrome (97), rhodotorulic acid (98,99) and hadacidin (100), available evidence indicates that N-hydroxylation precedes the acylation reaction. In contrast, the sequence of events appears to be reversed, i.e. acylation reaction occurs prior to N-hydroxylation, in the biosynthesis of

Scheme 4. **Proposed mechanism for *r*IucD mediated lysine:N^6-hydroxylase:**
The interaction of 2-aminocaprolactam with 4a-peroxyflavin species is shown.

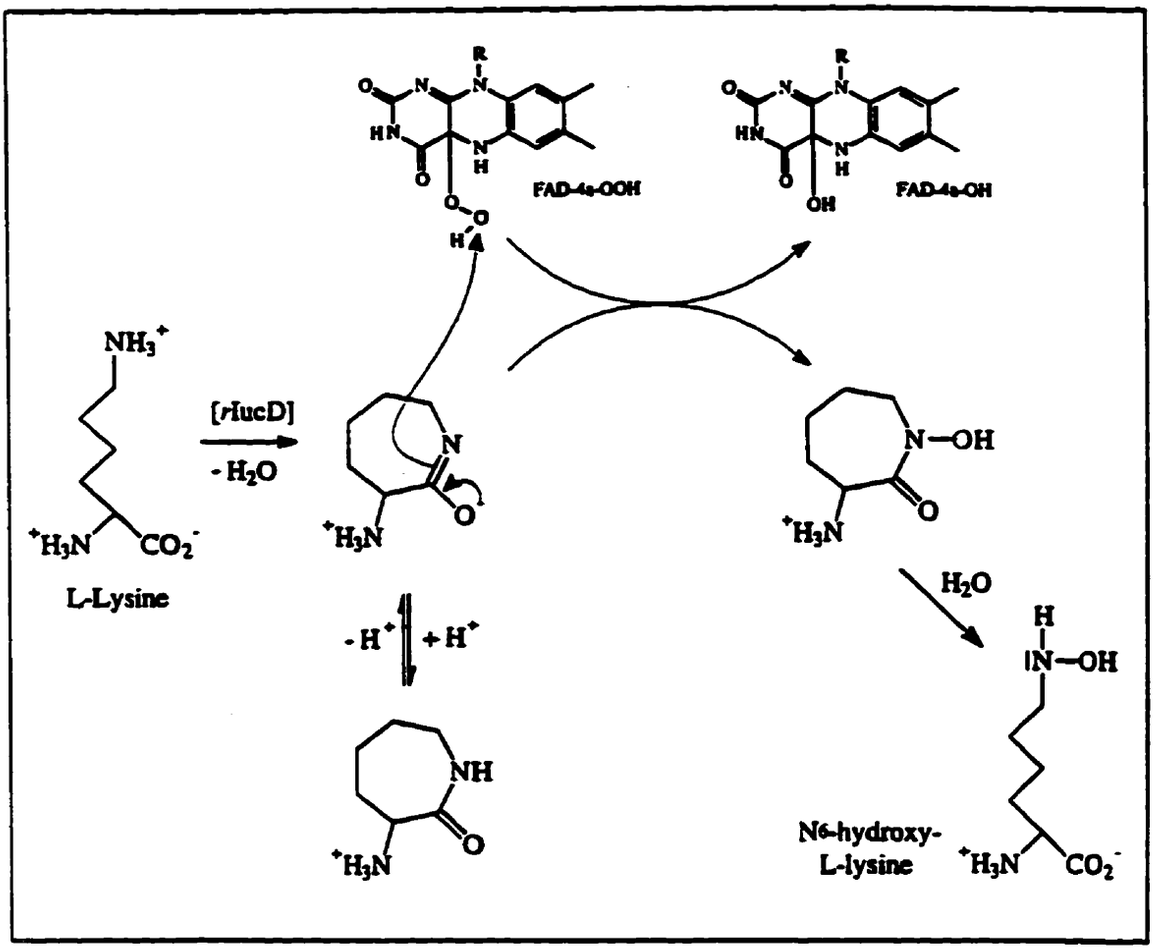
FAD-4a-OOH
FAD-4a-OH
[rIucD]
- H2O
L-Lysine
- H+
+ H+
H2O
N6-hydroxy-
L-lysine

mycobactins (101,102) and pulcherriminic acid (103,104). Indeed, the production of an acyl intermediate has been noted to occur during the production of mycobactin (101).

The conversion of L-lysine to its lactam derivative involves an intramolecular condensation reaction between its α-carboxyl and ∈-amino functions. Such an amide or peptide bond formation, a non-ribosomal event in this case, could be expected to involve ATP dependent activation of the carboxyl function (105,106). Since lysine:N^6-hydroxylase does not require ATP for its function, the bond formation reaction would have to be a consequence of the lysine binding in such a way as to sterically compress the α-carboxylic and ε-amino functions in close proximity of each other. The importance of binding energy in the compensation for the loss in entropy has been elegantly reviewed (107). Furthermore, the vast enhancement in the rates of bond formation that ensues due to the restricted rotation and stereo population control has been documented (108,109). Experiments to generate 2-amino caprolactam from L-lysine methyl ester for an assessment of its ability to function as a substrate have not been successful, primarily in view of its facile conversion to lysine under the conditions of the assay. However, the preformed lactam may not be recognized as a substrate since the conformational changes in the enzyme accompanying its binding of the substrate may be essential not only for the production of the lactam intermediate but also for the promotion of electron transfer between the cofactors. Finally, the formation of a lactam intermediate may be the rate determining step and is likely responsible for the low catalytic efficiency of the N-hydroxylation process. The reactivity of the free hydroxylamine function has been well documented (110,115), and it is toxic by virtue of its ability to interact with a variety of active acyl intermediates essential for cellular function. The participation of a

lactam in the N-hydroxylation reaction would result in the formation of a hydroxamate derivative, which would be less toxic than its parent hydroxylamine function. A mechanism for the N-hydroxylation process, relying on the initial conversion of the substrate to a lactam, may serve as an effective means for minimizing the accumulation of the undesirable hydroxylamine function in addition to that available by the post hydroxylation acylation step in the biosynthetic pathway of aerobactin (2-4). An added benefit of such a lactam intermediate would be that not only the reactivity of the compound is enhanced, but it also minimizes the possibility of the destruction of the cofactor that serves as the source of the oxygenating species (26). It should be emphasized that these proposals, attractive as they may seem, fall in the realm of conjecture at the present time in view of the lack of concrete evidence in their support.

The last aspect of these investigations concerns the role of thiol groups in the catalytic function(s) of the protein. Of the five cysteine residues present in *r*IucD, three are accessible to titration with DTNB in the native conformation of the protein. In contrast, only two such groups have been found to be alkylatable by iodoacetate under similar conditions and these are Cys51 and Cys158 residues of the protein. Modification of thiol groups of flavin dependent enzymes has been found to be accompanied by profound changes in the catalytic function of the proteins. In the case of lipoamide dehydrogenase, which serves as a classical example for the demonstration of the phenomenon, oxidation of its thiol groups is accompanied by a loss of its normal function as a dehydrogenase with a concomitant enhancement of the diaphorase activity (116,117). Other examples include xanthine dehydrogenase and phenol hydroxylase. In the former case, modification of thiol

groups of the enzyme results in its conversion to an oxidase with altered affinities for the cofactor and the substrate (118). With phenol hydroxylase, thiol modification leads to a loss of catalytic activity due to a displacement of its flavin cofactor (119). As recorded earlier, treatment of *r*IucD with thiol modifying agents results in a loss of the lysine:N^6-hydroxylase activity (77). In the assessment of the action of DPIP, its ability to serve in a dual capacity needs to be considered. First, it can function as a thiol modifying agent by virtue of its ability to conjugate with mercaptans (85-87). This feature of DPIP would appear to prevail during its interaction with *r*IucD preparations possessing unmodified thiol functions. The second role of DPIP concerns its ability to serve as a terminal electron acceptor in the studies designed to demonstrate the diaphorase activity of dehydrogenases. Such a function of DPIP has been widely documented with lipoamide dehydrogenase (117), glutathione reductase (120) and D-amino acid oxidase (121) serving as typical examples of the phenomenon. In all these instances, the electron transfer reactions involve the intermediacy of a flavin cofactor, however, the situation with *r*IucD would appear to be distinct from the examples cited above. Both the covalent and the noncovalent complexes of DPIP and *r*IucD appear to be capable of mediating NADPH oxidation in the presence of exogenous dye by a mechanism involving a reducing equivalent exchange between the protein bound DPIP and that free in the medium. FAD enhances the rate of NADPH oxidation mediated by the latter type of complex between *r*IucD and DPIP, rendering the system to function as a diaphorase analogous to that recorded in the case of lipoamide dehydrogenase (117). These reactions are illustrated in Scheme 5 and 6. In contrast, FAD has little influence on the NADPH oxidation mediated by the covalent DPIP-*r*IucD conjugate. These observations, taken

Scheme 5. **Mechanism for NADPH-dependent reduction of exogenous DPIP by covalent *r*lucD-DPIP complex**

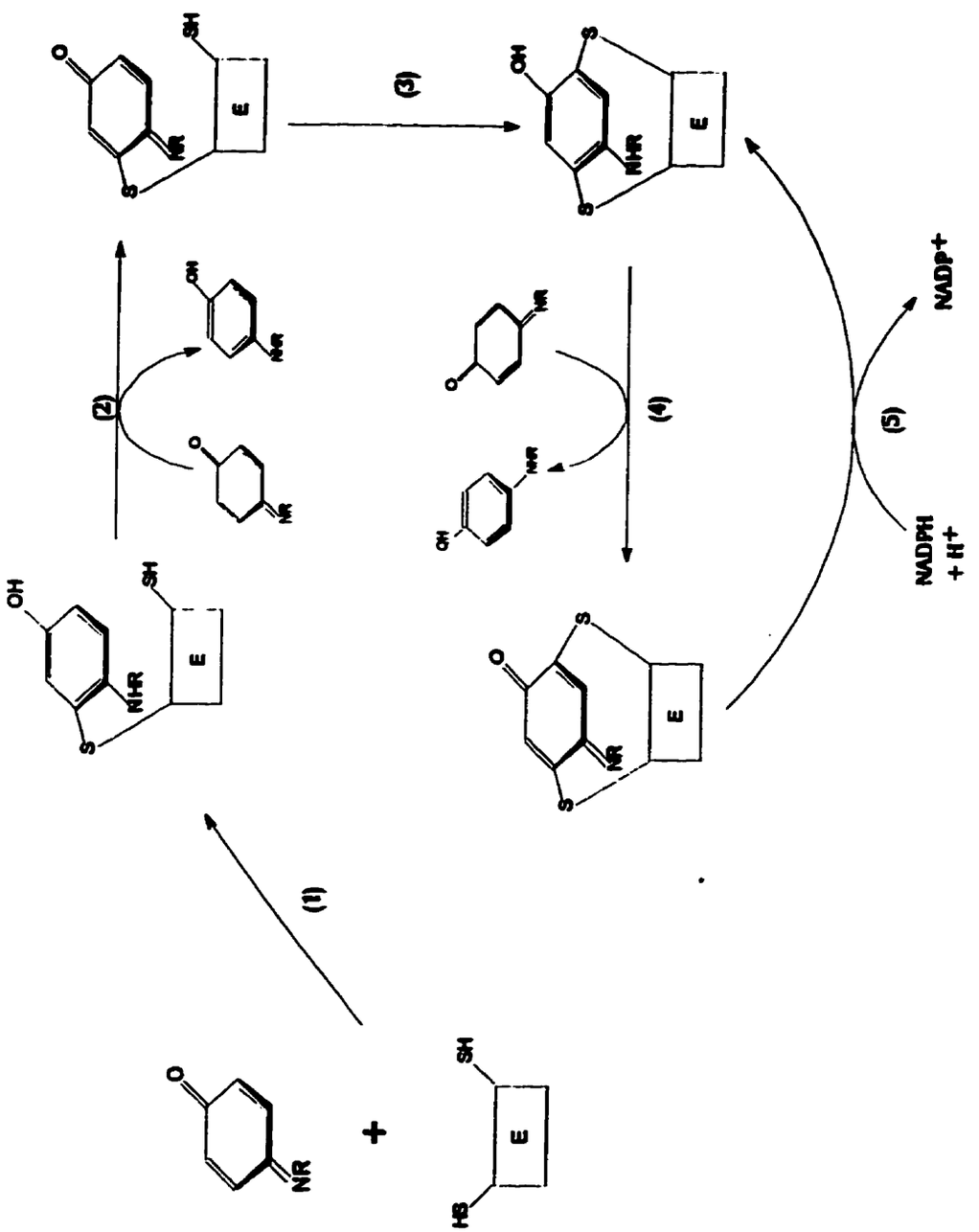
(1)
(2)
(3)
(4)
(5)
NADP+
NADPH
+ H+
E
SH
HS
OH
NHR
NR
O
S

Scheme 6. **Mechanism for NADPH-dependent reduction of exogenous DPIP by noncovalent complex of *r*lucD and DPIP:**
(A) Reducing equivalent exchange
(B) Diaphorase activity

A. FAD ABSENT

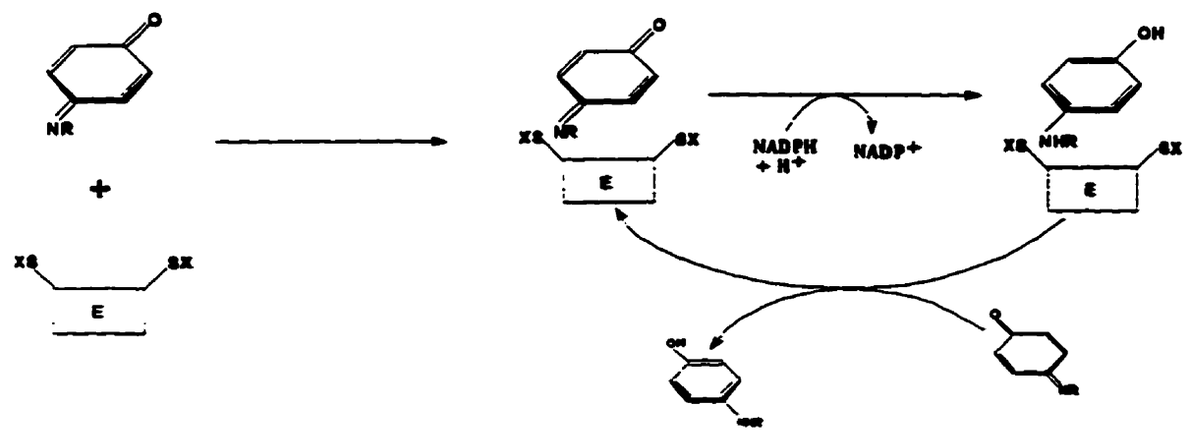

B. FAD PRESENT

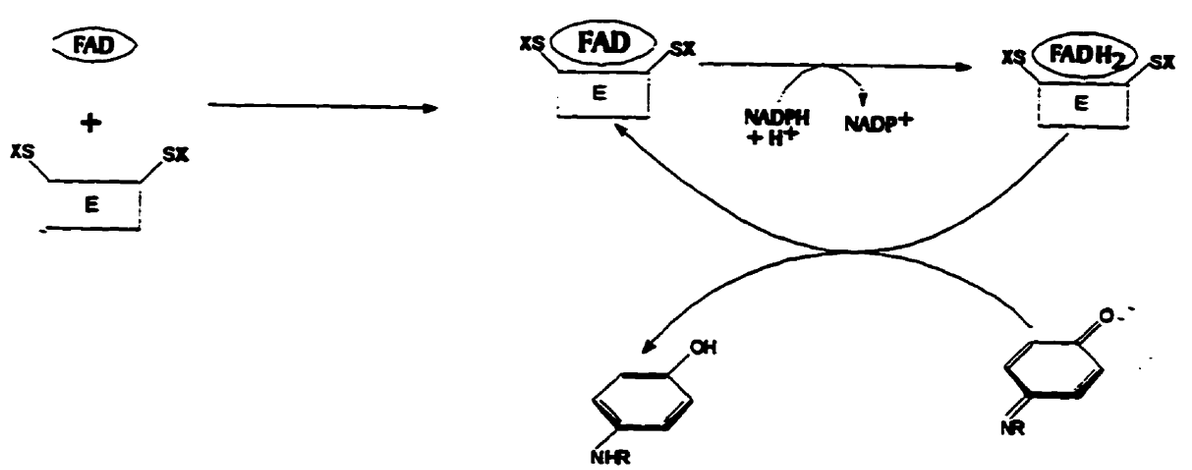

together with the ability of the flavin cofactor to interfere in the process of the formation of the covalent protein-dye conjugate, raise the possibility of DPIP and FAD competing for the same site in *r*IucD, a view which would appear to be consistent with the similarity in the structural features of the redox segments of the two electron acceptors (Figure 40).

Site directed mutagenesis of *r*IucD has proved extremely informative in several aspects. First, as noted above, it provided an elegant means to demonstrate that certain cysteine residues in *r*IucD can be replaced by alanine without any adverse effect on its catalytic functions. Second, it provided an insight into the reactivity of cysteine residues susceptible to chemical modification in the native conformation of the protein. Thus, an examination of the rates of reaction of the *r*IucD and its muteins with DTNB (Figure 38) reveals that of the three accessible residues, the rate of modification of Cys158 is slow relative to that of the other two. However, although Cys158 is sluggish in its reactivity towards DTNB, it is one of the two cysteine residues, the other one being Cys51, to undergo alkylation with iodoacetate. Hence, a cysteine residue in *r*IucD, other than Cys51, is capable of rapid reaction with DTNB and yet not amenable to alkylation by iodoacetate.

Finally, studies on *r*IucD muteins have aided in the identification of the cysteine residue(s) participating in the oxidative addition reaction with DPIP. As reported earlier, *r*IucD can form either a covalent or a non-covalent adduct with DPIP, the presence of unmodified thiol functions being an obligatory requirement for the production of the former type of complex (62). Furthermore, the diaphorase activity of *r*IucD monitored after its incubation with DPIP has been found to decline progressively with time, indicating that upon completion of the covalent interaction, the binding of the flavin cofactor and the dye to the

Figure 40. **Similarities in the structural features of DPIP and the isoalloxazine segment of FAD:**

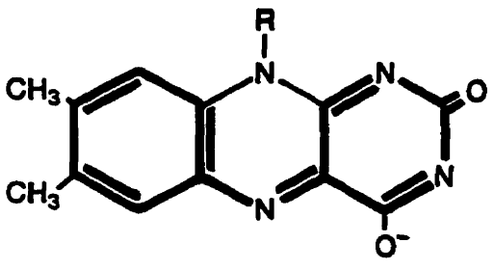

FAD (enol form)

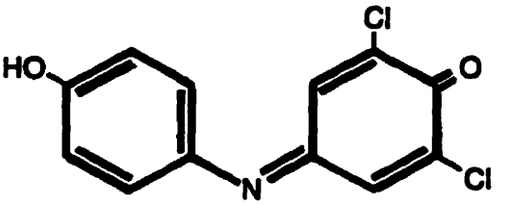

DPIP

R = ADPR

protein is mutually exclusive (62). Examination of *r*IucD muteins (Figure 39) has revealed that the replacement of Cys51 with alanine, as in C51A *r*IucD and C51A/C158A *r*IucD, results in the protein's diaphorase function becoming insensitive to the time of incubation with DPIP. Indeed, these muteins exhibit greater diaphorase activity relative to that noted in the case of parent protein. In contrast, its presence as in C158A *r*IucD, renders the diaphorase activity of the protein to decline progressively with the time of incubation with DPIP.

The differences between *r*IucD and its muteins with respect to their susceptibility to inactivation by iodoacetate further emphasize the pivotal role played by Cys51 in the catalytic mechanism of the protein. Thus, *r*IucD preparations containing the Cys51 residue, the parent *r*IucD and C158A *r*IucD, are inactivated upon treatment with iodoacetate while those lacking this residue, C51A *r*IucD and C51A/C158A *r*IucD are not inhibited by the reagent. With respect to the promotion of NADPH oxidation that occurs in the absence of lysine, the hydroxylatable substrate, the replacement of either Cys51 or Cys158 with alanine results in an enhancement of the process, the rate being approximately twice that noted in the case of parent *r*IucD. The effect of replacement of both the cysteine residues with alanine appears to be additive in that the rate of such NADPH oxidation in the case of C51A/C158A *r*IucD is approximately twice that noted with either C51A *r*IucD or C158A *r*IucD. These findings suggest that Cys51 and Cys158 may play a prominent role in the coupling of the *r*IucD catalysed processes of NADPH oxidation and lysine:N-hydroxylation.

In the assessment of structure-function relationship of biologically active proteins, both chemical modification of the constituent amino acid residues (122) as well as their

replacement by site directed mutagenesis have been widely employed (123). The former, the older of the two strategies, has the advantage in that the modification involves the protein which has undergone appropriate post-translational events of folding and processing essential for the attainment of its catalytically active conformation. Its limitations are: (i) the modifying agent(s) may not be stringently specific in its action; and (ii) the modification may lead to an imposition of steric constraints that could perturb the catalytically active conformation of the protein. In contrast, the amino acid replacement by the relatively recent approach of site directed mutagenesis occurs during the translation process and hence may influence the subsequent events of folding and post-translational processing of the polypeptide. The limitations and the potential application of this approach to the study of structure-function relationship of proteins has been recently reviewed (124). In view of the above considerations, a correspondence between the results obtained by chemical modification with those noted by the use of site directed mutagenesis would provide unambiguous information regarding the role of amino acid residue(s) in the protein's biological function.

In the current investigations, chemical modification of certain cysteine residues in *r*lucD is accompanied by a loss of its lysine-monooxygenase activity. In contrast, replacement of the same amino acid residues with alanine has no such adverse effect on this catalytic function of the protein. This paradoxical finding is not unique, since a similar phenomenon has been noted in a number of instances. Some of these examples include: His21 of *Rhodosprillum rubrum* ribulose carboxylase (125), Tyr166 of the catalytic subunit if *E. Coli* aspartate transcarbamoylase (126), Cys148 of *E. Coli* lac permease (127), Cys395

of *E. Coli* glycine t-RNA synthetase (128) and Cys5 and Cys214 of Fre, the *E. Coli* NADPH flavin oxidoreductase (129). In all these cases, chemical modification of the indicated amino acid residues in the protein results in the loss of catalytic activity while their replacement has no adverse effect.

As noted before, the catalytic cycle of *r*IucD is a multi-step event (Scheme 3). As in the case of other flavin dependent monooxygenases, the first (flavin reduction) and the last (hydroxylation) enzyme catalysed steps are coupled, emphasizing the importance of substrate induced conformational changes in the *r*IucD's catalytic mechanism. Hence, the chemical modification of thiol functions (by introduction of either carboxymethyl group or 2-nitro 5-thiobenzoate moiety by the use of iodoacetate and DTNB respectively) may impose constraints on the conformational flexibility of *r*IucD leading to a loss in its monooxygenase activity. On the other hand, replacement of these cysteine residues with alanine would appear not to interfere in the protein's conformational response to its hydroxylatable substrate resulting in the maintenance of its monooxygenase function. In contrast to the above observations, *r*IucD preparations, regardless of whether their cysteine residues have been modified chemically or have been replaced with alanine, exhibit diaphorase activity. The enhancement in the diaphorase function of the parent *r*IucD at the expense of its monooxygenase activity is analogous to that recorded in the case of lipoamide dehydrogenase (117).

The intriguing aspect of *r*IucD's catalytic mechanism concerns the differences in the conformational states required for the expression of its monooxygenase and diaphorase activities. In the former instance, the catalytically active conformation of *r*IucD is induced

by its hydroxylatable substrate. In contrast, the latter type of activity has no such prerequisite and manifests itself in the protein's conformation that is not conducive for the expression of the monooxygenase activity. These observations can be accommodated by envisaging the possibility of the flavin cofactor being able to reside in either of the two distinct conformational states of *r*IucD, one to promote monooxygenase function and the other to express the diaphorase activity of the protein. These proposals have a precedent in the case of *p*-hydroxybenzoate hydroxylase which, based on the X-ray crystallographic data, has been shown to be capable of accommodating the flavin cofactor in two distinct, the "in" and the "out"orientations (54,55). The hydroxylation of the substrate is suggested to occur exclusively in the former conformation of the protein, with switching of the cofactor between the two conformations being governed by the substrate (54). By analogy, one could visualize a similar situation in *r*IucD with lysine promoting a conformation that would favour exclusively the hydroxylation event and under these conditions the flavin cofactor may be expected to be shielded form the aqueous environment. In contrast, the diaphorase function would require the presence of the flavin cofactor accessible to the aqueous environment. However, since the rate of NADPH oxidation in the absence of lysine is approximately 10 % of that noted in the presence of lysine, it would appear that the alternate conformation permits only a partial exposure of the flavin to the environment. The enhanced rate of diaphorase activity in the absence of Cys51 and/or Cys158 in *r*IucD would indicate that these residues may serve as a constraint on the mobility of the flavin and thus prevent the wasteful process of NADPH oxidation that would occur in the absence of a hydroxylatable substrate. It is needless to emphasize that the above mentioned proposals fall

in the realm of conjecture at the present time and an assessment of their validity has to await the elucidation of the three dimensional structure of the protein.

In conclusion, the salient achievements of the current investigations are: (i) a rectification of errors in the published nucleotide sequence of iucD; (ii) formulation of a novel proposal for the activation of the hydroxylatable substrate, L-lysine; and (iii) elucidation of the role of the thiol functions in the demarkation of the catalytic functions of *r*IucD and its interaction with an artificial electron acceptor. Finally, as is true of all scientific investigations, the current endeavour has opened up new venues for further research in order to gain an insight into the anatomy of *r*IucD catalysed processes. Some of these are: (i) the elucidation of the three dimensional structure of the protein so as to identify its mechanism at the molecular level as has been achieved in the classic example, *p*-hydroxy-benzoate hydroxylase; (ii) the identification of the size of the catalytically functional unit of the protein by an approach based on radiation inactivation techniques (130,131), an endeavour which had to be discontinued during the course of the current study: and (iii) manipulation of iucD to achieve the production of two distinct domains of rIucD, one solely capable of NADPH oxidation and the other possessing the ability to restore N-hydroxylation of lysine, a feature analogous to that recorded in the case of *p*-hydroxy phenylacetate hydroxylase (36,37). These approaches should lead to a clear understanding of the protein's catalytic mechanism.

6.0

Appendix A

Composition of growth media and transformation buffer:

(a) ***Nutrient agar***

One litre of LB nutrient agar contained the following:

bacto agar	15 g
bacto tryptone	10 g
yeast extract	5 g
sodium chloride	10 g

The solution was adjusted to pH 7.2 with NaOH and then the preparation was autoclaved for 20 minutes at 121°C. Once the solution was cooled to 50°C the liquid agar was aseptically distributed to sterile petri plates (approximately 15 ml) and cooled to room temperature.

(b) ***LB media***

The composition of the LB medium was similar to that described above, except for the omission of the bacteriological agar.

(c) ***2X YT medium***

One litre of 2X YT medium contained the following:

bacto tryptone	16 g
yeast extract	10 g
sodium chloride	5 g

The solution was adjusted to pH 7.0 with NaOH and then the preparation was autoclaved for 20 minutes at 121°C.

(d) ***Modified version of Monod minimal medium***

One litre of the modified minimal medium contained the following:

ampicillin	100 mg
ammonium sulphate	2 g
calcium chloride, dihydrate	10 mg
casamino acids	1 g
glucose	5 g
magnesium sulfate-7 H_2O	200 mg
potassium phosphate, dibasic	13.8 g
potassium phosphate, monobasic	2.73 g
yeast extract	1 g

The glucose, yeast extract, and casamino acids were autoclaved separately from the salt solution and mixed prior to inoculation. The ampicillin was either filter sterilized or added directly to the medium prior to inoculation.

(e) ***Transformation buffer***

$CaCl_2$	100 mM
MOPS	10 mM
glucose	0.5 % (w/v)
glycerol	sterilized separately and added to the transformation when applicable

Appendix B:

Composition of buffers used in the Qiagen plasmid purification procedure. Data from QIAGEN® plasmid handook, Feb. 1995, Qiagen Inc. Chatsworth CA.

Composition of Buffers		Storage
Buffer P1: (Resuspension Buffer)	50 mM Tris-HCl, pH 8.0; 10 mM EDTA; 100 µg/ml RNase A	4°C
Buffer P2: (Lysis Buffer)	200 mM NaOH, 1% SDS	room temp.
Buffer P3: (Neutralization Buffer)	3.0 M potassium acetate, pH 5.5	room temp. or 4°C
Buffer QBT: (Equilibration Buffer)	750 mM NaCl; 50 mM MOPS, pH 7.0; 15% ethanol; 0.15% Triton X-100	room temp.
Buffer QC: (Wash Buffer)	1.0 M NaCl; 50 mM MOPS, pH 7.0; 15% ethanol	room temp.
Buffer QF: (Elution Buffer):	1.25 M NaCl; 50 mM Tris-HCl, pH 8.5; 15% ethanol	room temp.
TE:	10 mM Tris-HCl, pH 8.0; 1 mM EDTA	room temp.
STE:	100 mM NaCl; 10 mM Tris-HCl, pH 8.0; 1mM EDTA	room temp.

Preparation of Buffers

Buffer compositions are given per liter of solution. Do not autoclave MOPS- or ethanol-containing buffers; sterilize by filtration instead.

P1: Dissolve 6.06 g Tris base, 3.72 g EDTA·2H_2O in 800 ml H_2O. Adjust the pH to 8.0 with HCl. Adjust the volume to 1 liter with H_2O.

P2: Dissolve 8.0 g NaOH pellets in 950 ml H_2O, 50 ml 20% SDS solution. The final volume should be 1 liter.

P3: Dissolve 294.5 g potassium acetate in 500 ml H_2O. Adjust the pH to 5.5 with glacial acetic acid (~110 ml). Adjust the volume to 1 liter with H_2O.

QBT: Dissolve 43.83 g NaCl, 10.46 g MOPS (free acid) in 800 ml H_2O. Adjust the pH to 7.0. Add 150 ml pure ethanol and 15 ml 10% Triton X-100 solution. Adjust the volume to 1 liter with H_2O.

QC: Dissolve 58.44 g NaCl and 10.46 g MOPS (free acid) in 800 ml H_2O. Adjust the pH to 7.0. Add 150 ml pure ethanol. Adjust the volume to 1 liter with H_2O.

QF: Dissolve 73.05 g NaCl and 6.06 g Tris base in 800 ml H_2O and adjust the pH to 8.5 with HCl. Add 150 ml pure ethanol. Adjust the volume to 1 liter with H_2O.

STE: Dissolve 5.84 g NaCl, 1.21 g Tris base and 0.37 g EDTA·2H_2O in 800 ml H_2O. Adjust the pH to 8.0 with HCl. Adjust the volume to 1 liter with H_2O.

Appendix C

Nucleotide sequence of iucD: the sequence documented documented in literature,"I" (77), and that revised in the current investigation, "II", are provided. The regions of discrepancy are underlined in "II".

Figure C.1 **Nucleotide sequence of iucD (I)**

Met Lys Lys Ser Val Asp Phe Ile Gly Val[10] Gly Thr Gly Pro Phe Asn[16]
ATG AAA AAA AGT GTC GAT TTT ATT GGT GTA GGG ACA GGG CCA TTT AAT

Leu Ser Ile Ala[20] Ala Leu Ser His Gln Ile Glu Glu Leu Asp[30] Cys Leu[32]
CTC AGC ATT GCT GCG TTG TCA CAT CAG ATC GAA GAA CTG GAC TGT CTC

Phe Phe Asp Glu His Pro His Phe[40] Ser Trp His Pro Gly Met Leu Val[48]
TTC TTT GAT GAA CAT CCT CAT TTT TCC TGG CAT CCG GGT ATG CTG GTA

Pro Asp[50] Cys His Met Gln Thr Val Phe Leu Lys Asp[60] Leu Val Ser Ala[64]
CCG GAT TGT CAT ATG CAG ACC GTC TTT CTG AAA GAT CTG GTC AGT GCT

Val Ala Pro Thr Asn Pro[70] Tyr Ser Phe Val Asn Tyr Leu Val Lys His[80]
GTT GCA CCT ACA AAT CCC TAC AGT TTT GTT AAC TAT CTG GTG AAG CAC

Lys Lys Phe Tyr Arg Phe Leu Thr Ser Arg[90] Leu Arg Thr Val Ser Arg[96]
AAA AAG TTC TAT CGC TTC CTT ACA AGC AGA CTA CGT ACA GTA TCC CGT

Glu Glu Phe Ser[100] Asp Tyr Leu Arg Trp Ala Ala Glu Asp Met[110] Asn Asn[112]
GAA GAG TTT TCT GAC TAC CTC CGC TGG GCT GCT GAA GAT ATG AAT AAC

Leu Tyr Phe Ser His Thr Val Glu[120] Asn Ile Asp Phe Asp Lys Lys Arg[128]
CTG TAT TTC AGT CAT ACC GTT GAA AAC ATT GAT TTC GAT AAA AAA CGT

Arg Leu[130] Phe Leu Val Gln Thr Ser Gln Gly Gln Tyr[140] Phe Ala Arg Asn[144]
CGA TTG TTT CTG GTG CAA ACC AGC CAG GGA CAA TAT TTT GCC CGC AAT

Ile Cys Leu Gly Thr Gly[150] Lys Gln Pro Tyr Leu Pro Pro Cys Val Lys[160]
ATC TGC CTT GGT ACA GGA AAA CAA CCT TAT TTA CCA CCC TGT GTG AAG

His Met Thr Gln Ser Cys Phe His Ala Ser[170] Glu Ser Asn Leu Arg Arg[176]
CAT ATG ACA CAA TCC TGT TTC CAT GCC AGT GAA AGT AAT CTT CGT CGG

Pro Asp Leu Ser[180] Gly Lys Arg Ile Thr Val Val Gly Gly Gly[190] Gln Ser[192]
CCG GAT CTT AGT GGA AAA CGG ATA ACC GTG GTT GGT GGA GGA CAG AGT

Gly Ala Asp Leu Phe Leu Asn Ala[200] Leu Arg Gly Glu Trp Gly Glu Ala[208]
GGT GCA GAC CTG TTC CTT AAT GCA TTA CGC GGG GAA TGG GGA GAA GCG

Ala Glu[210] Ile Asn Trp Val Ser Arg Arg Asn Asn Phe[220] Asn Ala Leu Asp[224]
GCG GAA ATA AAC TGG GTG TCC CGG CGT AAT AAT TTT AAC GCA CTG GAT

Glu Ala Ala Phe Ala Asp[230] Asp Tyr Phe Thr Pro Glu Tyr Ile Ser Gly[240]
GAG GCT GCT TTT GCT GAT GAT TAT TTT ACA CCT GAA TAT ATT TCA GGC

Phe Ser Gly Leu Glu Glu Asp Ile Arg His[250] Gln Leu Leu Asp Glu Gln[256]
TTC TCC GGA CTG GAG GAA GAT ATT CGC CAT CAG TTA CTG GAT GAG CAG

Lys Thr Asp Ile[260] Gly Trp His His Cys Pro Ile Leu Leu Leu[270] Thr Ile[272]
AAA ACT GAC ATC GGA TGG CAT CAC TGC CCG ATT CTT TTA CTG ACC ATT

Tyr Arg Glu Leu Tyr His Arg Phe[280] Glu Val Leu Arg Lys Pro Arg Asn[288]
TAT CGT GAG TTG TAC CAC CGT TTT GAA GTT CTG AGA AAA CCA AGA AAT

Ile Arg[290] Leu Leu Pro Ser Arg Ser Val Thr Thr Leu[300] Glu Ser Ser Gly[304]
ATC CGT CTG CTA CCC AGC CGC TCG GTA ACA ACT CTG GAA AGT AGT GGT

Pro Gly Trp Lys Leu Leu[310] Met Glu His His Leu Asp Gln Gly Arg Glu[320]
CCT GGC TGG AAG TTG CTG ATG GAG CAT CAT CTG GAT CAG GGC AGG GAG

Ser Leu Glu Ser Asp Val Val Ile Phe Ala[330] Thr Gly Tyr Arg Ser Ala[336]
AGC CTG GAA AGT GAT GTG GTG ATT TTC GCC ACA GGT TAC CGT TCT GCG

Leu Pro Gln Ile[340] Leu Pro Ser Leu Met Pro Leu Ile Thr Met[350] His Asp[352]
TTG CCA CAA ATA CTT CCC TCA CTG ATG CCC CTG ATC ACC ATG CAC GAT

Lys Asn Thr Phe Lys Val Arg Asp[360] Asp Phe Thr Leu Glu Trp Ser Gly[368]
AAG AAC ACC TTT AAA GTG CGT GAT GAC TTC ACT CTG GAA TGG AGT GGC

Pro Lys[370] Glu Asn Asn Ile Phe Val Val Asn Ala Ser[380] Met Gln Thr His[384]
CCG AAA GAG AAC AAC ATC TTC GTG GTC AAC GCC AGT ATG CAA ACC CAT

Gly Ile Ala Glu Pro Gln[390] Leu Ser Leu Met Ala Trp Arg Ser Ala Arg[400]
GGC ATC GCC GAA CCC CAG CTC AGC CTG ATG GCA TGG AGA TCT GCA CGT

Ile Leu Asn Arg Val Met Gly Arg Asp Leu[410] Phe Asp Leu Ser Met Pro[416]
ATT CTT AAT CGC GTA ATG GGA CGT GAT TTA TTC GAT CTC AGT ATG CCG

Pro Ala Leu Ile[420] Gln Trp Arg Ser Gly Thr[426] ter
CCC GCC CTG ATT CAG TGG CGC AGC GGC ACC TAG

Figure C.2 **Nucleotide sequence of iucD (II)**

Met Lys Lys Ser Val Asp Phe Ile Gly Val[10] Gly Thr Gly Pro Phe Asn[16]
ATG AAA AAA AGT GTC GAT TTT ATT GGT GTA GGG ACA GGG CCA TTT AAT

Leu Ser Ile Ala[20] Ala Leu Ser His Gln Ile Glu Glu Leu Asp[30] Cys Leu[32]
CTC AGC ATT GCT GCG TTG TCA CAT CAG ATC GAA GAA CTG GAC TGT CTC

Phe Phe Asp Glu His Pro His Phe[40] Ser Trp His Pro Gly Met Leu Val[48]
TTC TTT GAT GAA CAT CCT CAT TTT TCC TGG CAT CCG GGT ATG CTG GTA

Pro Asp[50] Cys His Met Gln Thr Val Phe Leu Lys Asp[60] Leu Val Ser Ala[64]
CCG GAT TGT CAT ATG CAG ACC GTC TTT CTG AAA GAT CTG GTC AGT GCT

Val Ala Pro Thr Asn Pro[70] Tyr Ser Phe Val Asn Tyr Leu Val Lys His[80]
GTT GCA CCT ACA AAT CCC TAC AGT TTT GTT AAC TAT CTG GTG AAG CAC

Lys Lys Phe Tyr Arg Phe Leu Thr Ser Arg[90] Leu Arg Thr Val Ser Arg[96]
AAA AAG TTC TAT CGC TTC CTT ACA AGC AGA CTA CGT ACA GTA TCC CGT

Glu Glu Phe Ser[100] Asp Tyr Leu Arg Trp Ala Ala Glu Asp Met[110] Asn Asn[112]
GAA GAG TTT TCT GAC TAC CTC CGC TGG GCT GCT GAA GAT ATG AAT AAC

Leu Tyr Phe Ser His Thr Val Glu[120] Asn Ile Asp Phe Asp Lys Lys Arg[128]
CTG TAT TTC AGT CAT ACC GTT GAA AAC ATT GAT TTC GAT AAA AAA CGT

Arg Leu[130] Phe Leu Val Gln Thr Ser Gln Gly Glu Tyr[140] Phe Ala Arg Asn[144]
CGA TTG TTT CTG GTG CAA ACC AGC CAG GGA GAA TAT TTT GCC CGC AAT

Ile Cys Leu Gly Thr Gly[150] Lys Gln Pro Tyr Leu Pro Pro Cys Val Lys[160]
ATC TGC CTT GGT ACA GGA AAA CAA CCT TAT TTA CCA CCC TGT GTG AAG

His Met Thr Gln Ser Cys Phe His Ala Ser[170] Glu Met Asn Leu Arg Arg[176]
CAT ATG ACA CAA TCC TGT TTC CAT GCC AGT GAA ATG AAT CTT CGT CGG

Pro Asp Leu Ser[180] Gly Lys Arg Ile Thr Val Val Gly Gly Gly[190] Gln Ser[192]
CCG GAC CTT AGT GGA AAA CGG ATA ACC GTG GTT GGT GGA GGA CAG AGT

Gly Ala Asp Leu Phe Leu Asn Ala[200] Leu Arg Gly Glu Trp Gly Glu Ala[208]
GGT GCA GAC CTG TTC CTT AAT GCA TTA CGC GGG GAA TGG GGA GAA GCG

Ala Glu[210] Ile Asn Trp Val Ser Arg Arg Asn Asn Phe[220] Asn Ala Leu Asp[224]
GCG GAA ATA AAC TGG GTC TCC CGG CGT AAT AAT TTT AAC GCA CTG GAT

Glu Ala Ala Phe Ala Asp[230] Glu Tyr Phe Thr Pro Glu Tyr Ile Ser Gly[240]
GAG GCT GCT TTT GCT GAT GAG TAT TTT ACA CCT GAA TAT ATT TCA GGC

Phe Ser Gly Leu Glu Glu Asp Ile Arg His[250] Gln Leu Leu Asp Glu Gln[256]
TTC TCC GGA CTG GAG GAA GAT ATT CGC CAT CAG TTA CTG GAT GAG CAG

Lys Met Thr Ser[260] Asp Gly Ile Thr Ala Asp Ser Leu Leu Thr[270] Ile Tyr[272]
AAA ATG ACA TCG GAT GGC ATC ACT GCC GAT TCT TTA CTG ACC ATT TAT

Arg Glu Leu Tyr His Arg Phe Glu[280] Val Leu Arg Lys Pro Arg Asn Ile[288]
CGT GAG TTG TAC CAC CGT TTT GAA GTT CTG AGA AAA CCA AGA AAT ATC

Arg Leu[290] Leu Pro Ser Arg Ser Val Thr Thr Leu Glu[300] Ser Ser Gly Pro[304]
CGT CTG CTA CCC AGC CGC TCG GTA ACA ACT CTG GAA AGT AGT GGT CCT

Gly Trp Lys Leu Leu Met[310] Glu His His Leu Asp Gln Gly Arg Glu Ser[320]
GGC TGG AAG TTG CTG ATG GAG CAT CAT CTG GAT CAG GGC AGG GAG AGC

Leu Glu Ser Asp Val Val Ile Phe Ala Thr[330] Gly Tyr Arg Ser Ala Leu[336]
CTG GAA AGT GAT GTG GTG ATT TTC GCC ACA GGT TAC CGT TCT GCG TTG

Pro Gln Ile Leu[340] Pro Ser Leu Met Pro Leu Ile Thr Met His[350] Asp Lys[352]
CCA CAA ATA CTT CCC TCA CTG ATG CCC CTG ATC ACC ATG CAC GAT AAG

Asn Thr Phe Lys Val Arg Asp Asp[360] Phe Thr Leu Glu Trp Ser Gly Pro[368]
AAC ACC TTT AAA GTG CGT GAT GAC TTC ACT CTG GAA TGG AGT GGC CCG

Lys Glu[370] Asn Asn Ile Phe Val Val Asn Ala Ser Met[380] Gln Thr His Gly[384]
AAA GAG AAC AAC ATC TTC GTG GTC AAC GCC AGT ATG CAA ACC CAT GGC

Ile Ala Glu Pro Gln Leu[390] Ser Leu Met Ala Trp Arg Ser Ala Arg Ile[400]
ATC GCC GAA CCC CAG CTC AGC CTG ATG GCA TGG AGA TCT GCA CGT ATT

Leu Asn Arg Val Met Gly Arg Asp Leu Phe[410] Asp Leu Ser Met Pro Pro[416]
CTT AAT CGC GTA ATG GGA CGT GAT TTA TTC GAT CTC AGT ATG CCG CCC

Ala Leu Ile Gln[420] Trp Arg Ser Gly Thr[425] ter
GCC CTG ATT CAG TGG CGC AGC GGC ACC TAG

Appendix D

The family of peptides generated by treatment of IucD with CNBr and trypsin:
The protein cleavage analysis was achieved with the aid of PC/GENE® program, Release 6.6, August, 1991. IntelliGenetics, Inc. Mountain View, CA.

Analyses includes the IucD with amino acid sequence deduced from the previously documented nucleotide sequence of iucD (labelled "I") And that with the amino acid sequence deduced from .the revised nucleotide sequence in the current study labelled "II")

Figure D.1 **Peptide fragments of *r*lucD (I) upon CNBr treatment**

Nb)	Position in sequence				Weight	[Fragment.....]
1)	Lys-	2	to Met-	46	5056	KKSVDFIGVGT/.../EHPHFSWHPGM
2)	Leu-	47	to Met-	53	814	LVPDCHM
3)	Gln-	54	to Met-	110	6836	QTVFLKDLVSA/.../SDYLRWAAEDM
4)	Asn-	111	to Met-	162	6119	NNLYFSHTVEN/.../EPYLPPCVKHM
5)	Thr-	163	to Met-	311	17004	TQSCFHASESN/.../ESSGPGWKLLM
6)	Glu-	312	to Met-	345	3810	EHHLDQGRESL/.../SALPQILPSLM
7)	Pro-	346	to Met-	350	574	PLITM
8)	His-	351	to Met-	381	3640	HDKNTFKVRDD/.../ENNIFVVNASM
9)	Gln-	382	to Met-	394	1425	QTHGIAEPQLSLM
10)	Ala-	395	to Met-	406	1473	AWRSARILNRVM
11)	Gly-	407	to Met-	415	1053	GRDLFDLSM
12)	Pro-	416	to Thr-	426	1225	PPALIQWRSGT

Figure D.2 **Peptide fragments of *r*IucD (II) upon CNBr treatment**

Nb)	Position in sequence			Weight	[Fragment.....]
1)	Lys-	2	to Met- 46	5056	KKSVDFIGVGT/.../EHPHFSWHPGM
2)	Leu-	47	to Met- 53	814	LVPDCHM
3)	Gln-	54	to Met- 110	6836	QTVFLKDLVSA/.../SDYLRWAAEDM
4)	Asn-	111	to Met- 162	6118	NNLYFSHTVEN/.../QPYLPPCVKHM
5)	Thr-	163	to Met- 172	1140	TQSCFHASEM
6)	Asn-	173	to Met- 258	9673	NLRRPDLSGKR/.../IRHQLLDEQKM
7)	Thr-	259	to Met- 310	5989	TSDGITADSLL/.../ESSGPGWKLLM
8)	Glu-	311	to Met- 344	3810	EHHLDQGRESL/.../SALPQILPSLM
9)	Pro-	345	to Met- 349	574	PLITM
10)	His-	350	to Met- 380	3640	HDKNTFKVRDD/.../ENNIFVVNASM
11)	Gln-	381	to Met- 393	1425	QTHGIAEPQLSLM
12)	Ala-	394	to Met- 405	1473	AWRSARILNRVM
13)	Gly-	406	to Met- 414	1053	GRDLFDLSM
14)	Pro-	415	to Thr- 425	1225	PPALIQWRSGT

Figure D.3 **Peptide fragments of *r*lucD (I) upon trypsin treatment**

Nb)	Position in sequence				Weight	[Fragment.....]
1)	Met-	1	to Lys-	2	277	MK
2)	Ser-	4	to Lys-	59	6312	SVDFIGVGTGP/.../PDCHMQTVFLK
3)	Asp-	60	to Lys-	79	2197	DLVSAVAPTNPYSFVNYLVK
4)	His-	80	to Lys-	81	283	HK
5)	Phe-	83	to Arg-	85	485	FYR
6)	Phe-	86	to Arg-	90	623	FLTSR
7)	Leu-	91	to Arg-	92	287	LR
8)	Thr-	93	to Arg-	96	462	TVSR
9)	Glu-	97	to Arg-	104	1058	EEFSDYLR
10)	Trp-	105	to Lys-	126	2660	WAAEDMNNLYFSHTVENIDFDK
11)	Leu-	130	to Arg-	143	1658	LFLVQTSQGQYFAR
12)	Asn-	144	to Lys-	151	805	NICLGTGK-
13)	Glu-	152	to Lys-	160	1045	EPYLPPCVK
14)	His-	161	to Arg-	175	1748	HMTQSCFHASESNLR
15)	Arg-	176	to Lys-	182	772	RPDLSGK
16)	Ile-	184	to Arg-	202	1888	ITVVGGGQSGADLFLNALR
17)	Gly-	203	to Arg-	216	1604	GEWGEAAEINWVSR
18)	Asn-	218	to Arg-	249	3632	NNFNALDEAAF/.../SGFSGLEEDIR
19)	His-	250	to Lys-	257	1010	HQLLDEQK
20)	Thr-	258	to Arg-	274	2051	TDIGWHHCPILLLTIYR
21)	Glu-	275	to Arg-	279	717	ELYHR
22)	Phe-	280	to Arg-	284	663	FEVLR
23)	Lys-	285	to Arg-	287	399	KPR
24)	Asn-	288	to Arg-	290	401	NIR
25)	Leu-	291	to Arg-	295	585	LLPSR
26)	Ser-	296	to Lys-	308	1348	SVTTLESSGPGWK
27)	Leu-	309	to Arg-	319	1349	LLMEHHLDQGR
28)	Glu-	320	to Arg-	334	1686	ESLESDVVIFATGYR
29)	Ser-	335	to Lys-	353	2106	SALPQILPSLMPLITMHDK
30)	Asn-	354	to Lys-	357	509	NTFK
31)	Val-	358	to Arg-	359	273	VR
32)	Asp-	360	to Lys-	370	1294	DDFTLEWSGPK
33)	Glu-	371	to Arg-	397	3057	ENNIFVVNASMQTHGIAEPQLSLMAWR
34)	Ser-	398	to Arg-	400	332	SAR
35)	Ile-	401	to Arg-	404	515	ILNR
36)	Val-	405	to Arg-	408	462	VMGR
37)	Asp-	409	to Arg-	423	1802	DLFDLSMPPALIQWR
38)	Ser-	424	to Thr-	426	263	SGT

Figure D.4 **Peptide fragments of *r*lucD (II) upon trypsin treatment**

Nb)	Position in sequence				Weight	Fragment.....]
1)	Met-	1	to Lys-	2	277	MK
2)	Ser-	4	to Lys-	59	6312	SVDFIGVGTGP/.../PDCHMQTVFLK
3)	Asp-	60	to Lys-	79	2197	DLVSAVAPTNPYSFVNYLVK
4)	His-	80	to Lys-	81	283	HK
5)	Phe-	83	to Arg-	85	485	FYR
6)	Phe-	86	to Arg-	90	623	FLTSR
7)	Leu-	91	to Arg-	92	287	LR
8)	Thr-	93	to Arg-	96	462	TVSR
9)	Glu-	97	to Arg-	104	1058	EEFSDYLR
10)	Trp-	105	to Lys-	126	2660	WAAEDMNNLYFSHTVENIDFDK
11)	Leu-	130	to Arg-	143	1658	LFLVQTSQGQYFAR
12)	Asn-	144	to Lys-	151	805	NICLGTGK
13)	Gln-	152	to Lys-	160	1044	QPYLPPCVK
14)	His-	161	to Arg-	175	1792	HMTQSCFHASEMNLR
15)	Arg-	176	to Lys-	182	772	RPDLSGK
16)	Ile-	184	to Arg-	202	1888	ITVVGGGQSGADLFLNALR
17)	Gly-	203	to Arg-	216	1604	GEWGEAAEINWVSR
18)	Asn-	218	to Arg-	249	3646	NNFNALDEAAF/.../SGFSGLEEDIR
19)	His-	250	to Lys-	257	1010	HQLLDEQK
20)	Met-	258	to Arg-	273	1757	MTSDGITADSLLTIYR
21)	Glu-	274	to Arg-	278	717	ELYHR
22)	Phe-	279	to Arg-	283	663	FEVLR
23)	Lys-	284	to Arg-	286	399	KPR
24)	Asn-	287	to Arg-	289	401	NIR
25)	Leu-	290	to Arg-	294	585	LLPSR
26)	Ser-	295	to Lys-	307	1348	SVTTLESSGPGWK
27)	Leu-	308	to Arg-	318	1349	LLMEHHLDQGR
28)	Glu-	319	to Arg-	333	1686	ESLESDVVIFATGYR
29)	Ser-	334	to Lys-	352	2106	SALPQILPSLMPLITMHDK
30)	Asn-	353	to Lys-	356	509	NTFK
31)	Val-	357	to Arg-	358	273	VR
32)	Asp-	359	to Lys-	369	1294	DDFTLEWSGPK
33)	Glu-	370	to Arg-	396	3057	ENNIFVVNASMQTHGIAEPQLSLMAWR
34)	Ser-	397	to Arg-	399	332	SAR
35)	Ile-	400	to Arg-	403	515	ILNR
36)	Val-	404	to Arg-	407	462	VMGR
37)	Asp-	408	to Arg-	422	1802	DLFDLSMPPALIQWR
38)	Ser-	423	to Thr-	425	263	SGT

Appendix E

Confirmation of amino acid sequence of the alkylated cysteine containing peptides of *r*IucD. Analysis was achieved by $(MS)^2$ experiment on the peptides (61).

Figure E.1 **$(MS)^2$ analysis of the peptide of mass 842 Da.**
(refer to Figure 15)

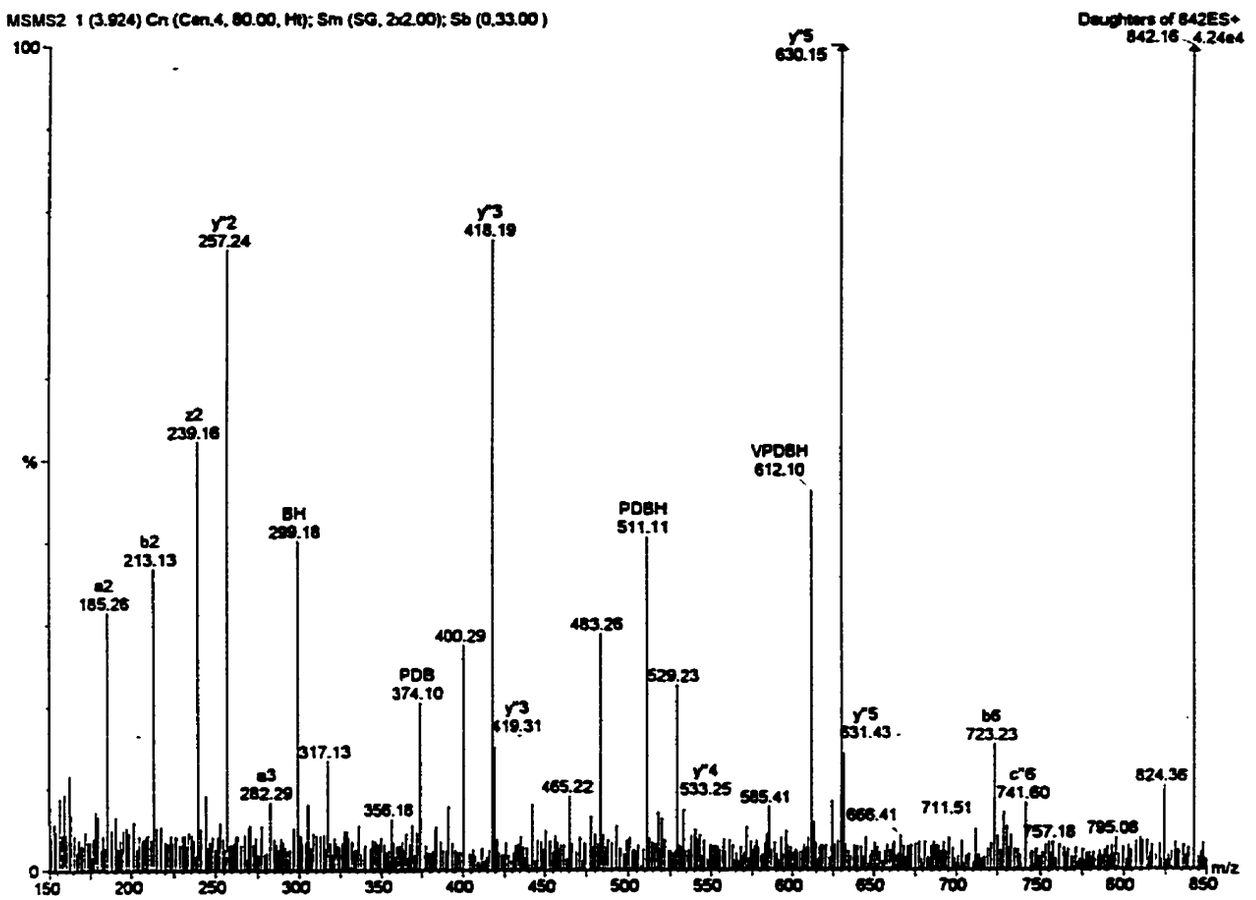
MSMS2 1 (3.924) Cn (Cen,4, 80.00, Ht); Sm (SG, 2x2.00); Sb (0,33.00)
Daughters of 842ES+
842.16 4.24e4
100
%
0
y"5
630.15
y"2
257.24
y"3
418.19
z2
239.16
VPDBH
612.10
BH
299.18
PDBH
511.11
b2
213.13
a2
185.26
483.26
400.29
PDB
374.10
529.23
y"3
419.31
y"5
631.43
b6
723.23
317.13
a3
282.29
y"4
533.25
c"6
741.60
824.36
465.22
585.41
666.41
711.51
757.18
795.08
356.18
m/z
150
200
250
300
350
400
450
500
550
600
650
700
750
800
850

Figure E.2 **ESMS data of the peptide with mass 1102 Da (A) and $(MS)^2$ analysis of its doubly charged species (B):**

A

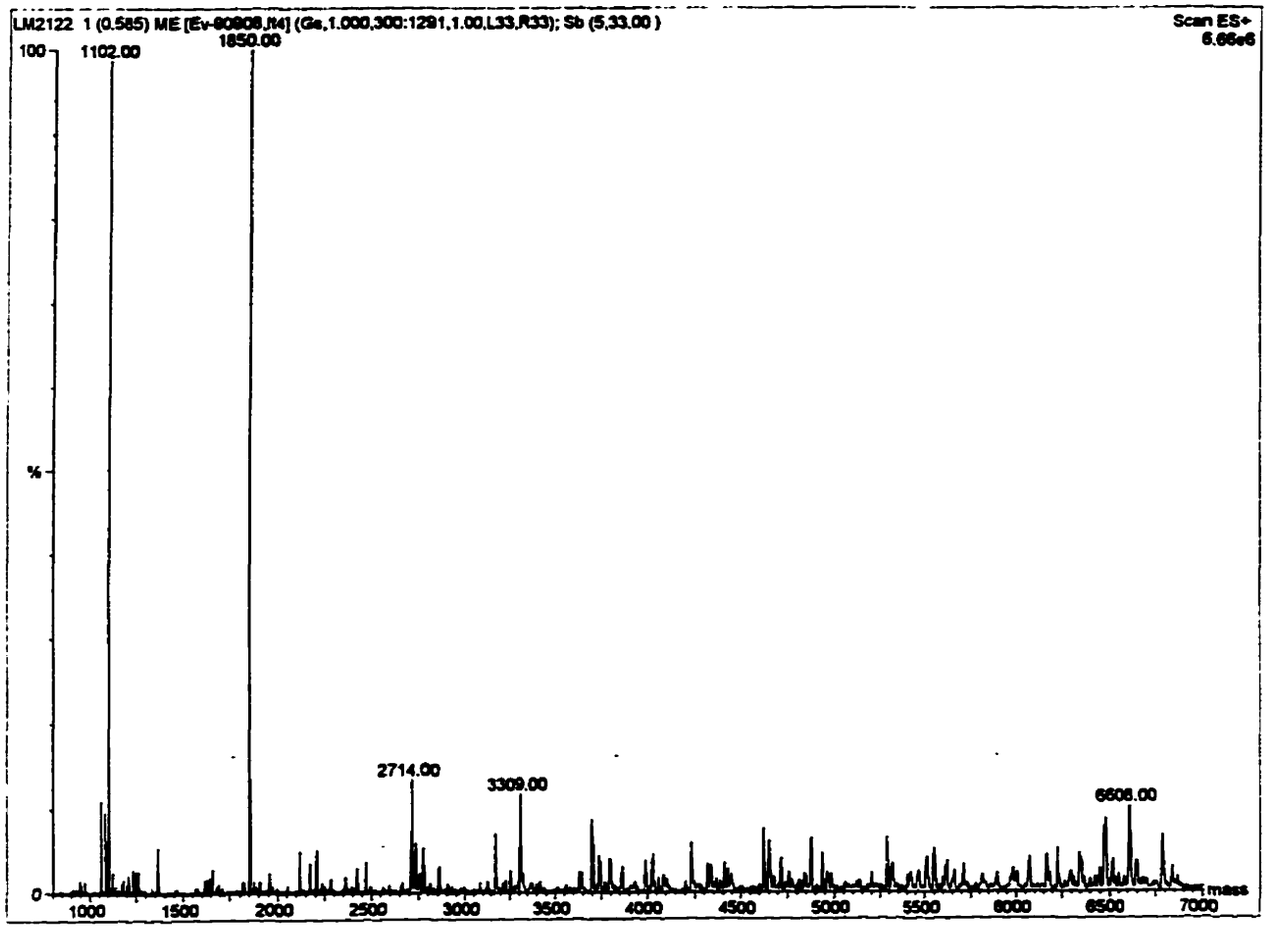
LM2122 1 (0.585) ME [Ev-80808,R4] (Ge,1.000,300:1291,1.00,L33,R33); Sb (5,33.00)
Scan ES+
6.66e6
100
%
0
1102.00
1850.00
2714.00
3309.00
6606.00
mass
1000
1500
2000
2500
3000
3500
4000
4500
5000
5500
6000
6500
7000

B

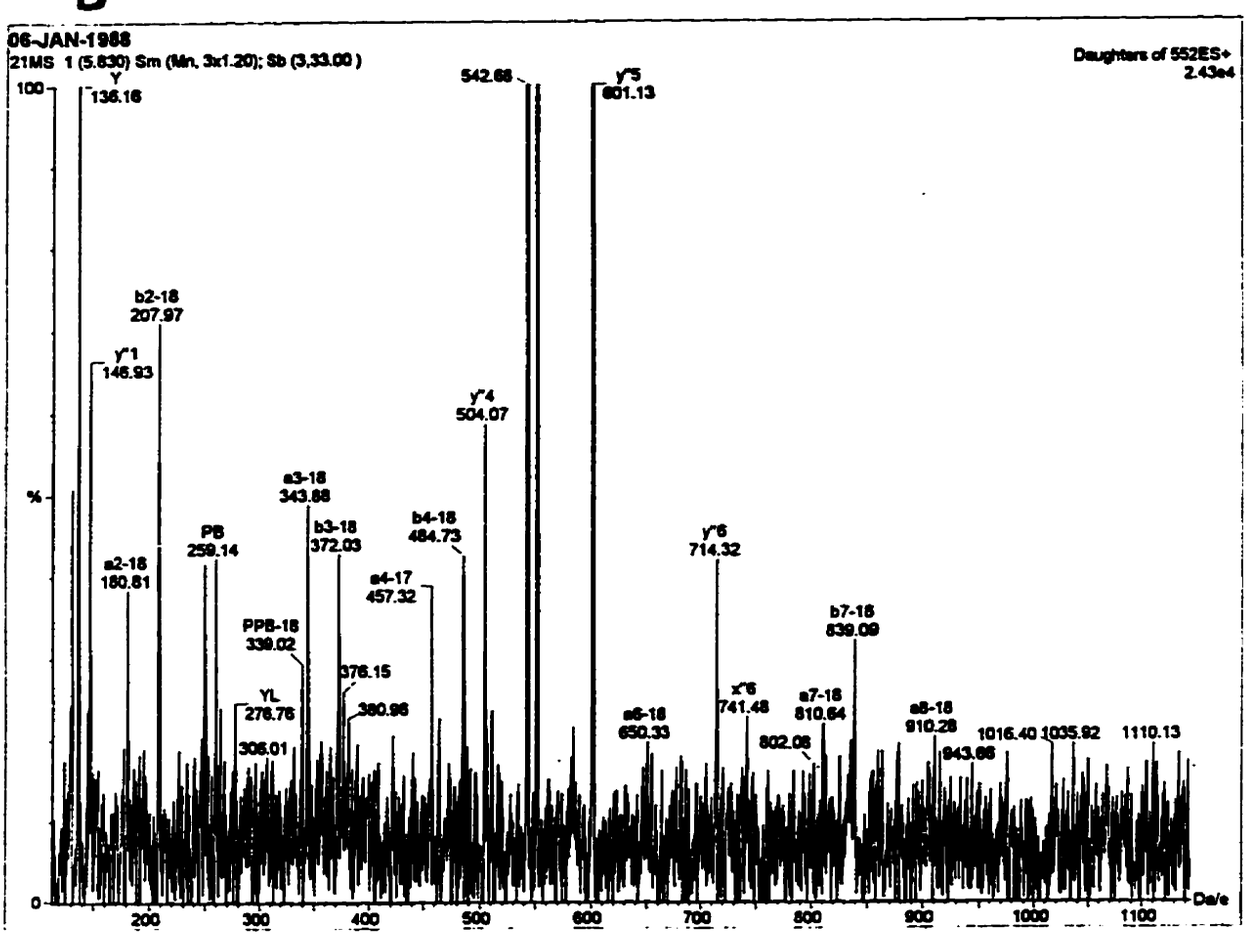
06-JAN-1988
21MS 1 (5.630) Sm (Mn, 3x1.20); Sb (3,33.00)
Daughters of 552ES+
2.43e4
100
%
0
Y
136.16
542.68
y"5
801.13
b2-18
207.97
y"1
146.93
y"4
504.07
a3-18
343.88
PB
259.14
b3-18
372.03
b4-18
484.73
a2-18
180.81
a4-17
457.32
y"6
714.32
b7-18
839.09
PPB-18
339.02
376.15
YL
276.76
380.98
306.01
x"6
741.48
a7-18
810.64
a6-18
650.33
802.08
a8-18
910.28
943.66
1016.40
1035.92
1110.13
200
300
400
500
600
700
800
900
1000
1100
Da/e

Appendix F

(A) Effect of cysteine→ alanine replacement(s) on the reactivity of the thiol functions in *r*lucD.

Protein	Thiol groups modified by DTNB[a]	DPIP reduction[b]	
		– FAD	+ FAD
*r*lucD	2 (fast) 1 (slow)	slow	rate declines with time of preincubation with DPIP
C51A *r*lucD	1 (fast) 1 (slow)	same as *r*lucD	rate fast and not influenced by DPIP
C158A *r*lucD	2 (fast)	faster than *r*lucD	rate declines as in *r*lucD
C51A/C158A *r*lucD	1 (fast)	faster than *r*lucD	rate fast and not influenced by DPIP

[a] Titration of *r*lucD in 200 mM potassium phosphate, pH 8.0 with DTNB. The values shown are the probable number of residues per mole of protein; (i) fast: reaction time ≤ 10 sec.); (ii) slow: reaction time ≈ 2-3 minutes.

[b] NADPH dependent reduction of DPIP was monitored in the absence and in the presence of FAD (see Figure 39, pg 108). The terms slow and fast are used to provide a qualitative assessment of the rates relative to that in the parent *r*lucD.

(B) Dissociation constants of complexes of FAD and *r*IucD preparations.

Protein preparation	K_d (μM)
*r*IucD	15.4
C51A *r*IucD	27.0
C158A *r*IucD	34.4
C51A/C158A *r*IucD	n.d.

The desired *r*IucD preparations (15 μM) in 200 mM potassium phosphate, pH 7.0, were treated with FAD (70 μM). The mixture was subjected to ultrafiltration with the aid of a centricon (Amicon corp.) using a 30 kDa cut off membrane. The concentration of FAD in the filtrate provided the basis for the estimation of the relative concentrations of the cofactor that is free and that present as a complex with *r*IucD. K_d values were calculated using the expression,

$$K_d = \frac{[E][D]}{[ED]}$$

[E] = concentration of free *r*IucD enzyme

[D] = concentration of FAD that remains unbound to the protein

[ED] = concentration of *r*IucD•FAD complex

Note: These values are preliminary observations.

(C) K_M and k_{cat} values of *r*lucD for NADPH, FAD, and L-lysine

Substrate	K_M (μM)	k_{cat} (sec^{-1})
L-lysine[1]	33 & 160	0.1 - 0.2
NADPH	68	
FAD	5.8	

[1] K_M values for L-lysine were taken from Thariath, A.M., 1993 (reference 57).

7.0

REFERENCES

1. Neilands, J.B. (1994) Siderophores as biological defferation agents and the regulation of their synthesis by iron, in *The Development of Iron Chelators for Clinical Use*, (R.J. Bergeron, and G.M. Brittenham, Eds.) CRC Press, Boca Raton, Florida, pp. 151-168.

2. Neilands, J.B. (1981) Iron absorption and transport in microorganisms, *Ann. Rev. Nutr.* **1**, 27-46.

3. Neilands, J.B. (1984) Methodology of siderophore in *Structure and Bonding*, Springer-Verlag Publications, Berlin **58**, 1-24.

4. Neilands, J. B., Konopka, K., Schwyn, B., Coy, M., Francis, R. T., Paw, B. H., Bagg, A. (1997) Comparative biochemistry of microbial iron assimilation, in *Iron transport in microbes, plants, and animals*, (J. B. Neilands, D. Van der Helm, and G. Winkelmann Eds.) Springer Verlag New York, pp. 3-33.

5. Neilands, J.B. (1952) A crystalline organo-iron pigment from a rust fungus (*Ustilago sphaerogena*), *J. Am. Chem. Soc.* **74**, 4846-4847.

6. Raymond, K. N., Muller, G., Matzanke, B.F. (1984) Complexation of iron by siderophores, a review of their solution and structural chemistry and biological function, in *Topics in current chemistry*, (F. L. Boschke, Ed.) **123**, Springer Verlag, Berlin Heidelberg pp. 49-102.

7. Gibson, F., & Magrath, D. T. (1969) The isolation and characterisation of a hydroxamic acid (Aerobactin) formed by *Aerobacter aerogenes* 62.1, *Biochim. Biophys. Acta* **192**, pp. 175-184.

8 de Lorenzo, V., Binderif, A., Paw, B.H. and Neilands, J.B. (1986) Aerobactin biosynthesis and transport genes of plasmid ColV-K30 in *Escherichia coli*, *J. Bacteriol.* **165**, 570-578.

9. de Lorenzo, V. and Neilands, J.B. (1986) Characterization of iucA and iucC genes of the aerobactin system of plasmid ColV-K30 in *Escherichia coli*, *J. Bacteriol.* **167**, 350-355.

10. Gross, R., Engelbrecht, F., & Braun, V. (1984) Genetic and biochemical characterisation of the aerobactin synthesis operon on pColV, *Mol. Gen. Genet.* **196**, 74-80.

11. Gross, R., Engelbrecht, F., & Braun, V. (1985) Identification of the genes and their polypeptide products responsible for aerobactin synthesis by pColV plasmids, *Mol. Gen. Genet.* **201**, 204-212.

12. Murray, G.J., Clark, G.E.D., Parniak, M.A. and Viswanatha, T. (1977) Effects of metabolites on N^6-hydroxylysine formation in ell-free extract of *Aerobacter aerogenes* 62-1, *Can. J. Biochem.* **55**, 625-629.

13. Viswanatha, T., Szczepan, E. W. & Murray, G. J. (1987) Biosynthesis of aerobactin: Enzymological and mechanistic studies, in *Iron Transport in Microbes, Plants and Animals* (J. B. Neilands, D. Van der Helm, and G. Winkelmann, Eds.), Springer-Verlag, New York, pp 117-132.

14. Parniak, M.A., Jackson, G.E.D., Murray, G.J., and Viswanatha, T. (1979) Studies on the formation of N^6-hydroxylysine in cell free extract of *Aerobacter aerogenes* 62-1, *Biochim. Biophys. Acta* **569**, 99-108.

15 Jackson, G. E. D., Parniak, M. A., Murray, G. J., Viswanatha, T. (1984) Stimulation by glutamine of the formation of N^6-hydroxylysine in a cell free extract from *Aerobacter aerogenes* 62-1, *J. Cell. Biochem.* **24**, 395-403.

16. Szczepan, E.W., Jackson, G.E.D., Grundy, B.J., and Viswanatha, T. (1989) Interrelationship between pyruvate metabolism and aerobactin production in a cell-free system of *Aerobacter aerogenes*, *FEMS Microbiology Letters* **34**, 27-30.

17. Goh, C.J., Szczepan, E.W., Wright, G., Menhart, N., Honek, J.F. and Viswanatha, T. (1989) Investigation of lysine:N-hydroxylation in the biosynthesis of siderophore aerobactin, *Bioorg. Chem.* **17**, 13-27.

18. Goh, C. J., Szczepan, E. W., Menhart, N., & Viswanatha, T. (1989) Studies on lysine:N^6-hydroxylation by cell-free systems of *Aerobacter aerogenes* 62-1, *Biochim. Biophys. Acta* **990**, 240-245.

19. Thariath, A. M., Socha, D., Valvano, M. A. & Viswanatha, T. (1993) Construction and biochemical characterization of recombinant cytoplasmic forms of the IucD protein (lysine:N^6-hydroxylase) encoded by the pColV-K30 aerobactin gene cluster, *J. Bacteriol.* **175**, 589-596.

20. Thariath, A. M., Fatum, K. L., Valvano, M. A. & Viswanatha, T. (1993) Physico-chemical characterization of a recombinant cytoplasmic form of lysine:N^6-hydroxylase, *Biochim. Biophys. Acta* **1203**, 27-35.

21. Hamilton, G. A. (1974) Chemical models and mechanisms for oxygenases in *Molecular mechanism of oxygen activation*, (O. Hayaishi, Ed.) Academic Press, New York, pp.405-451.

22. Berends, W., Posthuma, J., Sassenkach, J., and Mager, H. (1966) On the mechanism of some flavin photosensitized reactions, in *Flavins and Flavoproteins* (E. C. Slater, Ed.) Elsevier, New York, pp.22-36.

23. Hamilton, G. A. (1971) The proton in biological redox reactions in *Progress in bioorganic chemistry*, Vol. 1, (E. T. Kaiser and T.J. Kezdy, Eds.) Wiley-Interscience, New York, pp 83-158.

24. Dmitrienko, G. I., Snieckus, V. and Viswanatha. T. (1977) On the mechanism of oxygen activation by tetrahydropterin and dihydroflavin-dependent monooxygenases, *Bioorganic Chemistry* **6**, 421-429.

25. Ball, S. and Bruice, T. C. (1979) 4a-Hydroperoxyflavin N-oxidation of tertiary amines, *J. Am. Chem. Soc.* **101**, 4017-4019.

26. Ball, S. and Bruice, T. C. (1980) Oxidation of amines by 4a-hydroperoxyflavin, *J. Am. Chem. Soc.* **102**, 6498-6503.

27. Entsch, B. and Ballou, D.P. (1989) Purification, properties and oxygen reactivity of p-hydroxybenzoate hydroxylase from *Pseudomonas aerogenes*, *Biochem. Biophys. Acta* **999**, 313-322.

28. Schopfer, L.M., Wessiak., A. and Massey, V. (1991) Interpretation of the spectra observed during oxidation of p-hydroxybenzoate hydroxylase reconstituted with modified flavins, *J. Biol. Chem.* **266**, 13080-13085.

29. Detmar, K. and Massey, V. (1985) Effect of substrate and pH on the oxidative half reaction of phenol hydroxylase, *J. Biol. Chem.* **260**, 5998-6005.

30. Taylor, M.G., and Massey, V. (1990) Decay of the 4a-hydroxy-FAD intermediate of phenol hydroxylase, *J. Biol. Chem.* **265**, 13687-13694.

31. Taylor, M.G., and Massey, V. (1991) Kinetic and isotopic studies of the oxidative half reaction of phenol hydroxylase, *J. Biol. Chem.* **266**, 8291-8301.

32. Maeda-Yorita, K. and Massey, V. (1993) On the reaction mechanism of phenol hydroxylase, *J. Biol. Chem.* **268**, 4134-4144.

33. Schopfer, L.M. and Massey, V. (1980) Kinetic and mechanistic studies on the oxidation of the mellilotate hydroxylase • 2-OH-cinnamate complex by molecular oxygen, *J. Biol. Chem.* **255**, 5355-5363.

34. Hastings, J. W., Balny, C., LePeuch, C. and Douzou, P. (1973) Spectral properties of an oxygenated luciferase - flavin intermediate isolated by low temperature chromatography, *Proc. Natl. Acad. Sci. U.S.A.* **70**, 3468-3472.

35. Brissette, P., Ballou, D. P. and Massey, V. (1987) The oxidative half reaction of 2-methyl-3-hydroxypyridine-5-carboxylic acid oxygenase from *Pseudomonas sp. MA-1* in *Flavins and flavoproteins*, (D. E. Edmondson and D. B. McCormick, Eds.) Walter de Gruyter and Co., Berlin, pp. 573-576.

36. Arunachalum, U., Massey, V. and Vaidyanathan, C. S. (1992) *p*-Hydroxyphenylacetate-3-hydroxylase, *J. Biol. Chem.* **267**, 25848-25855.

37. Arunachalum, U., Massey, V. (1994) Studies on the oxidative half reaction of *p*-Hydroxyphenylacetate-3-hydroxylase, *J. Biol. Chem.* **269**, 11795-11801.

38. Ryerson, C. C., Ballou, D. P. and Walsh, C. (1982) Mechanistic studies of cyclohexanone oxygenase, *Biochemistry*, **21**, 2644-2655.

39. Wierenga, R. K., de Jong, R. J., Kalk, K. H., Hol, W. G. J. & Drenth, J. (1979) Crystal structure of p-hydroxybenzoate hydroxylase, *J. Mol. Biol.* **131**, 55-73.

40. Schreuder, H. A., van der Laan, J. M., Hol, W. G. J. & Drenth, J. (1988) Crystal structure of *p*-hydroxybenzoate hydroxylase complexed with its reaction product 3,4-dihydroxybenzoate, *J. Mol. Biol.* **199**, 637-648.

41. Schreuder, H. A., Prick, P. A. J., Wierenga, R. K., Vriend, G., Wilson, K. S., Hol, W. G. J. & Drenth, J. (1989) Crystal structure of *p*-hydroxybenzoate hydroxylase substrate complex refined at 1.9 Å resolution and comparison with 2.3 Å crystal structure of the product complex, *J. Mol. Biol.* **208**, 679-696.

42. Schreuder, H. A., van der Laan, J. M., Swarte, M. B. A., Kalk, K. H., Hol, W. G. J. & Drenth, J. (1992) Crystal structure of the reduces form of p-hydroxybenzoate hydroxylase refined at 2.3 Å resolution, *Proteins:Struct. Funct. Genet.* **14**, 178-190.

43. Schreuder, H. A., van der Laan, J. M., Hol, W. G. J. & Drenth, J. (1990) The structure of *p*-hydroxybenzoate hydroxylase in *Chemistry and Biochemistry of Flavoenzymes, Volume II* (F. Muller, Ed.) CRC Press Inc., Boca Raton, Florida, pp. 31-60.

44. Weirenga, R.K., Terpstra, P. and Hol, W.G.J. (1986) Prediction of the occurrence of the ADP-binding βαβ-fold in proteins using an amino acid sequence fingerprint, *J. Mol. Biol.* **187**, 101-107.

45. Shoun, H. (1990) *p*-Hydroxybenzoate hydroxylase from *Pseudomonas desmolytica*: relative molecular mass, amino acid composition and reactivity of the sulfhydryl groups, *Agric. Biol. Chem.* **54**, 329-336.

46. Husain, M. & Massey, V. (1979) Kinetic studies on the reaction of *p*-hydroxybenzoate hydroxylase, *J. Biol. Chem.* **254**, 6657-6666.

47. White-Stevens, R. H., Kamin, H. & Gibson, Q.H. (1972) Studies on a flavoprotein salicylate hydroxylase, *J. Biol. Chem.* **247**, 2371-2381.

48. Entsch, B., Ballou, D. P. & Massey, V. (1976) Flavin-oxygen derivatives involved in hydroxylation by *p*-hydroxybenzoate hydroxylase, *J. Biol. Chem.* **251**, 2550-2563.

49. Entsch, B., Palfey, B. A., Ballou, D. P. & Massey, V. (1991) Catalytic function of tyrosine residues in *p*-hydroxybenzoate hydroxylase as determined by the study of site directed mutants, *J. Biol. Chem.* **266**, 17341-17349.

50. Palfey, B. A., Entsch, B., Ballou, D. P. & Massey, V. (1991) Changes in the catalytic properties of *p*-hydroxybenzoate hydroxylase caused by the mutation Asn300Asp, *Biochemistry* **33**, 1545-1554.

51. Van Berkel, W. J. H. & Muller, F. (1989) The temperature and pH dependence of some properties of *p*-hydroxybenzoate hydroxylase from *Pseudomonas fluorescens*, *Eur. J. Biochem.* **179**, 307-314.

52. Eschrich, K., van der Bolt, F. J. T., de Kok, A. & van Berkel, W. J. H. (1993) Role of Tyr201 and Tyr385 in substrate activation of p-hydroxybenzoate hydroxylase from *Pseudomonas fluorescens*, *Eur. J. Biochem.* **216**, 137-146.

53. Lah, M. S., Palfey, B. A., Schreuder, H. A. & Ludwig, M. L. (1994) Crystal structures of mutant *Pseudomonas aeroginosa* p-hydroxybenzoate hydroxylase: the Tyr201Phe, Tyr385Phe and Asn300Asp variants, *Biochemistry* **33**, 1555-1564.

54. Gatti, D. L., Palfey, B. A., Lah, M. S., Entsch, B., Massey, V., Ballou, D. P. & Ludwig, M. L. (1994) The mobile flavin of 4-OH benzoate hydroxylase, *Science* **266**, 110-114.

55. Van der Bolt, F. J. T., Veervort, J. & Van Berkel, W. J. H. (1996) Flavin motion in *p*-hydroxybenzoate hydroxylase, *Eur. J. Biochem.* **237**, 592-600.

56. Cohen, S.N., Chang, A.C.Y. and Hsu, L. (1972) Non-chromosomal antibiotic resistance in bacteria: Genetic transformation of *Escherichia coli* by R-factor DNA, *Proc. Natl. Acad. Sci.* **69**, 2110-2114.

57. Thariath, A.M. (1993) Recombinant forms of lysine:N6-hydroxylase: physico-chemical characterization and mechanism, Ph.D. thesis, University of Waterloo.

58. Sambrook, J., Fritsch, E. F. & Maniatis, T. (1989) *Molecular Cloning: a laboratory manual*, 2nd edn, Cold Spring Harbor Press, Cold Spring Harbor, NY.

59. QuickChange™ Site Directed Mutagenesis Kit , Instruction Manual, Catalog #200518, Revision #125001 (1995) Stratagene Cloning Systems, La Jolla, Ca.

60. Laemmli, U.K. (1970) Cleavage of structural proteins during the assembly of the head of bacteriophage T4, *Nature* **227**, 680-685.

61. Siuzdak, G. (1994) The emergence of mass spectrometry in biochemical research, *Proc. Natl. Acad. Sci. USA* **91**, 11290-11297.

62. Marrone, L., Beecroft, M. and Viswanatha, T. (1996) Lysine:N^6-hydroxylase: cofactor interactions, *Bioorganic Chemistry* **24**, 304-317.

63. Tomlinson, G., Cruickshank, W. H. and Viswanatha, T. (1971) Sensitivity of substituted hydroxylamines to determination by iodine oxidation, *Anal. Biochem.* **44**, 670-679.

64. Linweaver, H. & Burk, D. (1954) The determination of enzyme dissociation constants, *J. Am. Chem. Soc.* **56**, 658-666.

65. Hildebrandt, A.G., Roots, L., Tjoe, M. & Heinemeyer, G. (1978) Hydrogen peroxide in hepatic microsomes, *Methods in Enzymology* **52**, 342-350.

66. Ellman, G. L. (1959) Tissue sulfhydryl groups, *Arch. Biochem. Biophys.* **82**, 70-77.

67. Riddles, P. W., Blakely, R. L. & Zerner, B. (1979) Ellman's reagent: 5,5′-dithiobis (2-nitrobenzoic acid)--a reexamination, *Anal. Biochem.* **94**, 75-81.

68. Gurd, F. R. N. (1972) Carboxymethylation, *Methods in Enzymology* **25**, 424-438.

69. Spande, T. F., Witkop, B., Degani, Y. & Patchornik, A. (1970) Selective cleavage and modification of peptides and proteins, *Adv. Protein Chem.* **24**, 96-246.

70. Schwert, G. W. and Takenata, Y. (1955) A spectrophotometric determination of trypsin and chymotrypsin, *Biochim. Biophys. Acta* **16**, 570-575.

71. Martin, B., Svendsen, I. and Ottesen, M. (1977) Use of carboxypeptidase Y for carboxyterminal sequence determination in proteins, *Carlsberg Res. Commun.* **42**, 99-102.

72. Desnuelle, P. (1960) Chymotrypsin in *The Enzymes*, Vol. 4, 2nd edition, (P. D. Boyer, H. Lardy and K. Myrback Eds.) Academic Press, New York, pp 93-118.

73. Schoellmann, G. and Shaw, E. (1963) Direct evidence for the presence of histidine in the active center of chymotrypsin, *Biochemistry* **2**, 252-255.

74. Hummel, B. C. W. (1959) A modified spectrophotometric determination of chymotrypsin, trypsin and thrombin, *Can. J. Biochem.and Physiol.* **37**, 1393-1399.

75. Breddam, K. (1984) Chemically modified carboxypeptidase Y with increased amidase activity, *Carlsberg Res. Commun.* **40**, 535-554.

76. Herrero, M., de Lorenzo, V. & Neilands, J. B. (1988) Nucleotide sequence of the iucD gene of the pColV-K30 aerobactin operon and topology of its product: studies with *phoA* and *lacZ* gene fusions, *J. Bacteriol.* **170**, 56-64.

77. Thariath, A. M., Valvano, M. A., & Viswanatha, T. (1994) Biochemical and genetic studies on lysine:N^6-hydroxylase involved in aerobactin synthesis, in *The Development of Iron Chelators for Clinical Use*, (R. J. Bergeron and G. M. Brittenham, Eds.) CRC Press, Boca Raton, Florida, pp169-186.

78. Detmer, K., and Massey, V. (1984) Effect of monovalent anions on the mechanism of phenol hydroxylase, *J. Biol. Chem.* **259**, 11265-11272.

79. Neujahr, H. Y., and Gaal, A. (1983) Effect of anions chaotropes and phenol on the attachment of flavin adenine dinucleotide to phenol hydroxylase, *Biochemistry* **22**, 580-584.

80. Neujahr, H. Y. (1990) Phenol hydroxylase in *Chemistry and Biochemistry of Flavoproteins* (F. Müller, Ed.) CRC Press, Boca Raton, Forida, pp. 65-86.

81. Steennis, P. J., Cordes, M. M., Hilkens, J. G. H., and Müller, F. (1973) On the interaction of *p*-hydroxybenzoate hydroxylase from *Pseudomonas fluorescens* with halogen ions, *FEBS Lett.* **36**, 177-180.

82. Sehl, L.C. and Castellino, F.J. (1990) Thermodynamic properties of the binding of α-ω-amino acids to the isolated kringle 4 region of human plasminogen as determined by high sensitivity titration calorimetry, *J. Biol. Chem.* **265**, 5482-5486.

83. Mares-Guia, M. and Shaw, E. (1965) Studies on the active center on trypsin, *J. Biol. Chem.* **240**, 1579-1585.

84. Neurath, H. and Schwert, G.W. (1950) The mode of action of the crystalline pancreatic proteolytic enzymes, *Chem. Rev.* **46**, 69-153.

85. Hadler, H. I., Erwin, M. J., and Lardy, H. A. (1963) The conjugation of cysteine during its oxidation by 2,6-dichloroindophenol, *J. Am. Chem. Soc.* **85**, 458-461.

86. Hadler, H. I., and Erwin, M. J. (1963) The conjugation of thiols by 2,6-dichloroindophenol, *Biochemistry* **2**, 954-957.

87. Hadler, H. I., Alt, S. K., and Falcone, A. B. (1966) Conjugation of 2,6-dichloroindophenol with mitochondrial thiol groups, *J. Biol. Chem.* **241**, 2886-2890.

88. Massey, V. (1994) Activation of molecular oxygen by flavins and flavoproteins, *J. Biol. Chem.* **269**, 22459-22462.

89. Kamin, H. (1971) in *Third international symposium on Flavins and Flavoproteins* (Kamin, H., Ed.) p. 472, University Park Press.

90. Leberman, R., and Soper, R. K. (1995) Effect of high salt concentrations on water structure, *Nature* **378**, 364-366.

91. Albalat, R., Valls, M., Fibia, J., Atrian, S. and Gonzàlez-Duarte (1995) Involvement of the C-terminal tail in the activity of *Drosophila* alcohol dehydrogenase, *Eur. J. Biochem.* **233**, 498-505.

92 Kraut, J. (1988) How do enzymes work?, *Science* **242**, 533-540.

93. Warshall, A., Papazyan, A., and Kollman, P.A. (1995) On low barrier hydrogen bonds and enzyme catalysis, *Science*, **269**, 102-104.

94 Vervoort, J., and Rietjens, I.M.C.M. (1996) Unifying concepts in flavin-dependent catalysis, *Biochem. Soc. Trans.* **24**, 127-130.

95. Vervoort, J., Rietjens, I.M.C.M., Van Berkel, W.J.H., and Veeger, C. (1992) Frontier orbital study on the 4-hydroxybenzoate-3-hydroxylase-dependent activity with benzoate derivatives, *Eur. J. Biochem.* **206**, 479-484.

96. Mizusaki, K., Sugahara, Y., Tsunematsu, H., and Makisumi, S. (1986) The conformation of lysyl side chain of substrates at the active center of trypsin, *J. Biochem.* **100**, 21-25.

97. Emery, T.F. (1966) Initial steps in the biosynthesis of ferrichrome. Incorporation of δ-*N*-hydroxyornithine and δ-*N*-acetyl-δ-*N*-hydroxyornithine, *Biochemistry* **5**, 3694-3701.

98. Atkin, C.L., and Neilands, J.B. (1968) Rhodotorulic acid a diketopiperazine dihydroxamic acid with growth-factor activity. I. Isolation and characterization, *Biochemistry* **7**, 3734-3739.

99. Akers, H.A., Llinas, M., and Neilands, J.B. (1972) Protonated amino acid precursor studies on rhodotorulic acid. Biosynthesis in deuterium oxide media, *Biochemistry* **11**, 2283-2291.

100. Stevens, R.L., and Emery, T.F. (1966) The biosynthesis of hadacidin, *Biochemistry* **5**, 74-81.

101. Tateson, J.E. (1970) Early steps in the biosynthesis of mycobactins P and S, *Biochem. J.* **118**, 747-753.

102. Snow, G.A. (1970) Mycobactin: iron chelating growth factors from mycobacteria, *Bacteriol. Rev.* **34**, 99-125.

103. MacDonald, J.C. (1965) Biosynthesis of pulcherriminic acid, *Biochem. J.* **96**, 533-538.

104. Uffen, R.L., and Canale-Parola, E. (1972) Synthesis of pulcherriminic acid by *Bacillus subtilis*, *J. Bacteriol.* **111**, 86-93.

105. Lipmann, F. (1973) Non-ribosomal polypeptide synthesis of polyenzyme templates, *Acc. Chem. Res.* **6**, 361-367.

106. Lipmann, F. (1982) On the biosynthesis of the cyclic antibiotics, gramicidin S and tyrocidine and linear gramicidin, in *Peptide Antibiotics: Biosynthesis and Function* (H. Kleinkauf, and H. von Döhren, Eds.) Walter de Gruyter & Co., Berlin, pp.23-45.

107. Jencks, W.P. (1987) Economics of enzyme catalysis, in *Cold Spring Harbor Symposia on Quantitative Biology*, Vol. LII, Cold Spring Harbor Laboratory, pp. 65-73.

108. Karle, J.M., and Karle, I.L. (1972) Correlation of reaction rate acceleration with rotational restriction. Crystal-structure analysis of compounds with trialkyl lock, *J. Am. Chem. Soc.* **94**, 9182-9189.

109. Milstein, S., and Cohen, L.A. (1972) Stereo-population control. I. Rate enhancement in the lactonization of *o*-hydroxyhydrocinnamic acids, *J. Am. Chem. Soc.* **94**, 9158-9165.

110. Jencks, W.P. (1958) The reaction of hydroxylamines with activated acyl groups. I. Formation of *o*-acylhydroxylamine, *J. Am. Chem. Soc.* **80**, 4581-4584.

111. Jencks, W.P. (1958)The reaction of hydroxylamines with activated acyl groups. II. Mechanism of the reaction, *J. Am. Chem. Soc.* **80**, 4585-4588.

112. Jencks, W.P. and Carriuolo, J. (1960) Reactivity of nucleophilic reagents towards esters, *J. Am. Chem. Soc.* **82**, 1778-1786.

113. Edwards, J.O., and Pearson, R.G. (1962) The factors determining nucleophilic reactivities, *J. Am. Chem. Soc.* **84**, 16-24.

114. Aubort, J.D., and Hudson, R.F. (1970) Enhanced reactivities of nucleophiles: orbital symmetry and the so-called "α-effect", *Chem. Commun.* 937-938.

115. Tomlinson, G., Gaudin, J.E., and Viswanatha, T. (1973) Reaction of hydroxylamine derivatives with cinnamoylimidazole, *Can. J. Biochem.* **51**, 764-771.

116. Massey, V. (1958) The identity of diaphorase and lipoic dehydrogenase, *Biochem. Biophys. Acta* **30**, 205-206.

117. Veeger, C, and Massey, V. (1962) The reaction mechanism of lipoamide dehydrogenase. II. modification by trace metals, *Biochim. Biophys. Acta* **64**, 83-100.

118. Della Corte, E., and Stirpe, F. (1972) The regulation of rat liver xanthine dehydrogenase, *Biochem. J.* **126**, 739-745.

119. Neujahr, H. Y., and Gaal, A. (1975) Phenol hydroxylase from yeast sulfhydryl groups in phenol hydroxylase from *Trichosporon cutaneum*, *Eur. J. Biochem.* **58**, 351-357.

120. Carlberg, I., and Mannervik, B. (1986) Reduction of 2,4,6-trinitrobenzene sulfonate by glutathione reductase and the effect of $NADP^+$ on the electron transfer, *J. Biol. Chem.* **261**, 1629-1635.

121. Appaji Rao, N., Nishikimi, M., and Yagi, K. (1972) Reactivity of D-amino acid oxidase with artificial electron acceptors, *Biochim. Biophys. Acta* **276**, 350-362.

122. Lundblad, R. L. (1991) *Chemical Reagents for Protein Modification*, 2nd ed. CRC Press Inc., Boca Raton, Florida.

123. Gillam, S. & Smith, M. (1979) Site specific mutagenesis using synthetic oligodeoxyribonucleotide primers: optimum conditions and minimum oligodeoxyribonucleotide length, *Gene* **8**, 81-97.

124. Schimmel, P. (1990) Hazards and their exploitation in the applications of molecular biology to structure-function relationships, *Biochemistry* **29**, 9495-9502.

125. Niyogi, S. K., Foote, R. S., Mural, R. J., Larimer, F. W., Mitra, S., Soper, T.S., Machanoff, R. & Hartman, F. C. (1986) Nonessentiality of histidine 291 of *Rhodospirillum rubrum* ribulose-bisphosphate carboxylase/oxygenase as determined by site-directed mutagenesis, *J. Biol. Chem.* **261**, 10087-10092.

126. Robey, E. A. & Schachman, H. K. (1984) Site-specific mutagenesis of aspartate transcarbamoylase, *J. Biol. Chem.* **259**, 11180-11183.

127. Sarkar, H. K., Menick, D. R., Viitanen, P. V., Poonian, M. S. & Kaback, H. R. (1986) Site-specific mutagenesis of cysteine 148 to serine in the lac permease of *Escherichia coli*, *J. Biol. Chem.* **261**, 8914-8918.

128. Profy, A. T. & Schimmel, P. (1986) A sulfhydryl presumed essential is not required for catalysis by an aminoacyl-tRNA synthetase, *J. Biol. Chem.* **261**, 15474-15479.

129. Fieschi, R., Nivière, V. & Fontecave, M. (1996) Cys5 and Cys214 of NAD(P)H:flavin oxidoreductase from *Escherichia coli* are located in the active site, *Eur. J. Biochem.* **237**, 870-875.

130. Harmoon, J.T., Neilsen, T.B., and Kempner, E.S. (1985) Molecular weight determinations from radiation inactivation, in *Methods in Enzymology*, **117**, pp65-94.

131. Kempner, E.S. (1988) Molecular size determination of enzymes by radiation inactivation, *Adv. Enzymol.*, **61**, 107-147.